Electrode Position, Channel Interaction, and Speech Perception in Cochlear Implant Listeners

Lindsay A. DeVries

A dissertation

submitted in partial fulfillment of the

requirements for the degree of

Doctor of Philosophy

University of Washington

2018

Reading Committee:

Julie G. Arenberg, Chair

Lynne Werner

Kelly Tremblay

Matthew B. Winn

Richard Wright

Program Authorized to Offer Degree:

Speech and Hearing Science

University of Washington

Abstract

Electrode Position, Channel Interaction, and Speech Perception in Cochlear Implant Listeners

Lindsay A. DeVries

Chair of the Supervisory Committee:

Julie Arenberg, Professor

Speech and Hearing Sciences

Cochlear implants (CI) are surgically implanted devices that provide sound input to individuals with severe-to-profound hearing loss. While relatively successful, speech understanding abilities are highly variable among implant listeners in both quiet and noisy environments. One source of this variability is the electrode-neuron interface, which refers to how well each electrode activates target auditory neurons. Poor electrode-neuron interfaces may increase *channel interaction*, which can distort spectral information and result in decreased speech understanding. Electrode position, bone and tissue growth, and the integrity of the auditory neurons are important factors that affect the electrode-neuron interface. Currently, it is not possible to directly measure neural integrity in CI listeners; therefore, obtaining information about electrode position is an alternative approach to assessing the electrode-neuron interface. Information about electrode position is available through computerized tomography (CT) imaging. However, CT imaging is not readily available to audiologists, thus limiting its usefulness in a clinical setting. The purpose of this dissertation work was to examine the relationship between CT-estimated

electrode position and two measures of channel interaction: an objective measure, the electrically evoked compound action potential (Experiment 1) and a behavioral measure, the psychophysical tuning curve (Experiment 2). In Experiment 3, we created novel listener strategies based on channels with poor electrode position and excessive channel interaction (based on measures from Experiment 2) in an effort to improve spectral resolution and speech understanding.

Results from Experiment 1 and 2 demonstrated that the electrically evoked compound action potential and psychophysical tuning curves, two measures of channel interaction, are correlated with CT-estimates of electrode position. In other words, those electrodes farther from the inner wall of the cochlea tended to exhibit excessive channel interaction with these measures. Results from Experiment 3 suggest that CI listeners can gain improved speech understanding when manipulating channels to compensate for poor electrode position or excessive channel interaction. Importantly, manipulating the "wrong" channels can lead to a detriment in performance. This dissertation work lays the groundwork for assessment of an important aspect of the electrode-neuron interface and the practical application of these measures to CI listener strategies.

TABLE OF CONTENTS

LIST OF FIGURES

LIST OF TABLES

ACKNOWLEDGEMENTS

I would first like to thank my parents, Linda and Larry DeVries, without which none of my dreams would have been possible. I am eternally grateful to my husband Jason, who has been by my side every step of the way and is a true partner in life.

I also want to acknowledge my mentor, Julie Arenberg, who has supported and encouraged me throughout my journey. I am proud to call you a mentor and a friend. I would also like to thank my committee, Lynne Werner, Kelly Tremblay, Matt Winn, and Richard Wright for guidance and feedback throughout the years.

I am also grateful to my sisters in science: Kate McClannahan, Homira Osman, Shae DiNino, Kelly Jahn, Elle O'Brien, Ashley Moore, Mona Oster, Susan Bolt, Melanie Fish, and Lindsey Kishline. And to Julie Braunstein, my sister in life.

Last, I'd like to thank the cochlear implant listeners who participated in my research. Without your dedication to bettering the lives of others, none of this work would exist.

DEDICATION

This dissertation is dedicated to Ray Hall, whose legacy lives on in the people who love him.

Chapter 1 : Introduction

A. Description of cochlear implants

For individuals with severe to profound hearing loss, a common treatment is cochlear implantation. According to the National Institute on Deafness and Communication Disorders, as of 2012, approximately 324,000 cochlear implants (CIs) have been implanted worldwide. CIs are relatively successful auditory protheses, with many listeners achieving substantially improved speech recognition in quiet and better quality of life; however, there is substantial variability in success with this device (e.g. Holden et al., 2013).

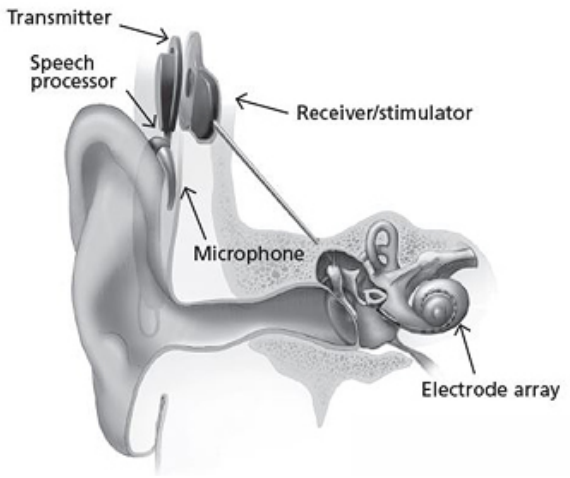

Figure 1-1: Cochlear implant illustration (NIH/NIDCD)

A CI is a surgically implanted device that electrically stimulates the auditory nerve, bypassing the impaired cochlea (inner ear). The device consists of an external speech processor and transmitter, an internal receiver/stimulator, and an electrode array that is inserted into the cochlea (Figure 1-1). The external processor contains the microphone, which picks up acoustic signals in the environment and converts them to digital signals. These signals are then transmitted to the internal receiver/stimulator, which converts the digital signals into electrical pulses. These electrical pulses are sent to the electrode array in the cochlea. Finally, the electrodes along the array stimulate different regions in the cochlea, which in turn stimulate corresponding regions of the auditory nerve. Depending on the manufacturer, there are 12-24 electrodes along the array.

B. Frequency encoding in cochlear implants

In the normal hearing ear, the basilar membrane performs a frequency analysis of incoming signals. That is, complex stimuli are separated into their frequency components along the basilar membrane. High frequency information is encoded in the base of the cochlea, and low frequencies are encoded in the apex. This arrangement is referred to as "tonotopic organization."

CIs are designed to mimic tonotopic organization by electrically stimulating auditory neurons in different regions of the cochlea. Similar to acoustic hearing, high frequency components are encoded in the basal electrodes, and low frequencies in the apical electrodes. CIs process signals by dividing their components into frequency bands, or channels. The temporal envelope, or slow changes in amplitude over time, is extracted for channel and determines the current level applied to each electrode. Temporal fine structure, or rapid changes in each frequency band, is not preserved; the loss of temporal fine structure can be detrimental in challenging listening environments. Therefore, frequency encoding in CIs is primarily through place coding, though envelope cues may be sufficient for listening in quiet environments (Xu and Pfingst, 2008). The ability for the CI listener to make use of frequency information is affected by patient-specific factors, such as neural survival, and how well the electrodes stimulate their intended neural targets.

C. The electrode-neuron interface

The quality of the electrode-neuron interface (ENI) may determine the effectiveness with which individual electrodes excite auditory nerve fibers. The ENI is affected by several peripheral factors, including: electrode position relative to the modiolus, bone and tissue growth, and the integrity of surviving auditory neurons (Bierer 2010). The quality of the ENI is suspected to affect spatial resolution, or the ability to differentiate between two channels, in CI listeners.

Poor ENIs can cause broader neural activation, which in turn increases *channel interaction*, or overlapping excitation patterns of two nearby channels. Channel interaction can distort spectral information and decrease speech perception (Abbas et al. 2004; Hughes 2008; Jones et al., 2013). Broad neural activation may be exacerbated by the clinical use of the monopolar electrode configuration, which results in broad current spread in the cochlea (e.g. Jolly et al., 1996). Investigators have used focused electrode configurations to reduce channel interaction, with improvements in speech in noise for some CI listeners (e.g. Berenstein et al., 2008; Bierer and Litvak, 2016)

The number and density of auditory neurons affects the quality of the ENI, and in turn how much channel interaction occurs. The contribution of remaining auditory neurons to speech perception is unclear; histological studies have not shown a correlation between neural survival and speech perception (e.g. Khan et al., 2005a). As neural survival is not currently measurable in CI listeners, electrode position is emerging as an alternative measure of effective CI stimulation at the ENI.

Suboptimal electrode position has been shown to increase channel interaction and contribute to poor speech understanding (e.g., Finley et al., 2008; Long et al., 2014; DeVries et al., 2016). However, effects of poor electrode placement may be moderated by patient-specific factors such as duration of deafness, age at onset of hearing loss, pre-operative speech scores, and etiology of deafness (e.g., van der Marel et al., 2015). Continued assessment of how electrode position contributes to excessive channel interaction and speech perception will increase our understanding of an important aspect of the ENI.

D. Summary

The ability for CI listeners to make use of spectral information is limited by factors related to the electrode-neuron interface. The overall goal of this dissertation work was to identify measures of channel interaction that correlate with electrode position, and to use that information to improve speech understanding with novel listener strategies.

This series of studies assessed the relationship between CT-estimated electrode position and two measures of channel interaction: an objective measure, the electrically evoked compound action potential (Experiment 1) and a behavioral measure, the psychophysical tuning curve (Experiment 2). In Experiment 3, we created novel listener strategies to limit the contribution of channels with poor electrode position and excessive channel interaction (based on measures from Experiment 2) in an effort to improve spectral resolution and speech understanding.

E. Research Questions

Experiment 1:

Can an objective measure of neural response, the electrically evoked compound action potential (ECAP), be used to identify channels with poor electrode position? We hypothesized that electrodes with excessive channel interaction, as measured by the ECAP, would be correlated with channels farther from the inner wall of the cochlea. To test our hypothesis, we measured ECAP channel interaction functions, ECAP peak amplitudes, focused behavioral thresholds, and obtained CT-estimates of electrode-to-modiolus distance and scalar location. Comparisons were made among ECAP peak amplitude, width of ECAP channel interaction functions, electrode-to-modiolus distance, scalar location, behavioral thresholds, and speech perception.

Experiment 2:

Can a behavioral measure of channel interaction, the psychophysical tuning curve (PTC), be used to identify channels with poor electrode position? We hypothesized PTCs using focused stimulation would be sensitive to local differences in the ENI, and that broader PTCs would be correlated with channels farther from the inner wall of the cochlea. To test our hypothesis, we measured PTCs using focused stimulation, focused behavioral thresholds, and obtained CT-estimates of electrode-to-modiolus distance and scalar location. Comparisons were made among PTC bandwidths, PTC tip shifts, electrode-to-modiolus distance, scalar location, behavioral thresholds, and speech perception.

Experiment 3:

Does using focused stimulation on a subset of CI channels suspected of excessive channel interaction and/or poor electrode position improve speech perception in CI listeners? We hypothesized that when using focused stimulation on a subset of electrodes with broad PTCs and greater electrode-to-modiolus distances (from Experiment 2), vowel identification and sentence recognition would improve compared to two control programs. To test our hypothesis, we created two experimental programs: 1) Tuning, based on PTCs, 2) Distance, based on electrode-to-modiolus distance, and two control programs: 1) Monopolar, and 2) Inverse, which is the mirror of the Distance program. Scores on a vowel identification and sentence recognition task were compared across programs.

Chapter 2 : Assessing the electrode-neuron interface with the electrically evoked compound action potential, electrode position, and behavioral thresholds

Published in:

DeVries L, Scheperle R and Bierer JA (2016) Assessing the Electrode-Neuron Interface with the Electrically Evoked Compound Action Potential, Electrode Position, and Behavioral Thresholds. *Journal of the Association for Research in Otolaryngology* 17(3): 237–252.

A. Introduction

Multichannel cochlear implants (CI) are successful neural prostheses that provide auditory input, allowing individuals with severe-to-profound hearing loss to perceive complex stimuli such as speech. However, perceptual abilities are highly variable across listeners, in both quiet and noisy listening environments (e.g., Holden et al. 2013; Won et al. 2007). This variability is likely influenced by the degree of auditory nerve degeneration inherent to this population (e.g., Pfingst et al. 2011), but other factors are involved as well. Evaluating the underlying sources of perceptual variability may provide valuable information for clinicians to individualize device programming, help set realistic expectations, and perhaps facilitate auditory training, ultimately leading to improved performance outcomes and quality of life for individuals with CIs.

One potential source of variability in CI perception is the electrode-neuron interface, which refers to a number of peripheral factors that can influence activation of the auditory nerve, including electrode placement, bone and tissue growth, and the integrity of the auditory neurons (Bierer 2010; Long et al., 2014). Computational modeling studies have demonstrated that current level requirements are higher and spread of excitation is broader for electrodes distant from the neurons or near a region of neural degeneration (Goldwyn et al. 2010; Kalkman et al., 2015). Broader activation can cause increased channel interaction (i.e., overlapping excitation patterns of two nearby channels), which can distort spectral information and lead to decreased pitch and speech perception (Abbas et al. 2004; Boëx 2003; Crew et al. 2012; Hughes 2008; Jones et al. 2013; Pfingst et al. 2004; Snel-Bongers et al. 2012).

Some insight into the electrode-neuron interface can be obtained via postoperative computerized tomography (CT) imaging, which provides information about electrode placement,

such as electrode-modiolus distance, scalar location, insertion depth, and wrapping factor (Holden et al. 2013; Skinner et al. 2007; Teymouri et al. 2010; Verbist et al. 2004). A portion of the variability in speech scores can be explained by electrode insertion depth and scalar location (Finley et al. 2008; Holden et al. 2013; Skinner et al. 2007), with deeper insertion and a greater number of electrodes in the SV correlated with poorer speech perception. Recently, CT data has been used to modify device programming by deactivating electrodes likely to show high levels of channel interaction (Noble et al. 2013). In that study, the programming changes led to improved outcomes on sentence recognition both in quiet and noise and improved subjective communication. However, CT imaging is costly, exposes patients to radiation, and does not provide information about the integrity of the auditory neurons.

Additional information about the electrode-neuron interface can be obtained via behavioral and electrophysiological measures, which are non-radiologic and more cost-efficient than CT imaging, and sensitive to both electrode position and neural integrity. For example, electrode-to-modiolus distance has been found to explain a portion of the variability in behavioral thresholds obtained with focused stimulation, and the remaining variability is presumed to reflect differences in neural health along the cochlear duct (Long et al. 2014). Other studies have shown that behavioral thresholds, widths of psychophysical tuning curves, and growth of loudness co-vary across the electrode array (Bierer 2007; Bierer 2010; Bierer et al. 2011; Bierer & Faulkner 2010; Cohen 2003; Hughes & Stille 2008; Landsberger et al. 2012; Litvak et al. 2007; Miller et al. 2008; Nelson et al. 2008; Bierer and Nye 2014, Pfingst & Xu 2004), consistent with localized variability in the electrode-neuron interface. Historically, behavioral measures are time-consuming and difficult to obtain, especially in pediatric listeners, although a faster threshold method has recently been validated in adults (Bierer et al. 2015).

Alternatively, the electrically evoked auditory brainstem response (EABR) has been used to measure the efficacy of individual CI channels, with EABR wave V thresholds positively correlated with focused behavioral thresholds (Bierer et al. 2011). Although the EABR is an objective measure and an option for difficult-to-test individuals, this measurement requires the placement of scalp electrodes, a sedentary subject, and a lengthy recording period (Firszt et al., 2001; Miller et al. 2008), conditions that may not be easily met in some clinics or with some patients. Further, EABR measurements are not always possible in humans due to temporal overlap with stimulus artifact (Hall 1990).

An alternative electrophysiological measurement is the electrically evoked compound action potential (ECAP) (Brown et al. 1990). In modern cochlear implant systems, the ECAP is recorded by one of the non-stimulating electrodes using a two-way telemetry system. Given the existing clinical tools to access the on-board telemetry, the ECAP is relatively easy and fast to measure, making it an appealing alternative to the more time-consuming EABR (Abbas et al. 1999; Briaire & Frijns 2005; Dillier et al. 2002; Mens 2007). As such, the ECAP has been extensively evaluated as a tool to aid clinicians with setting stimulation levels for CI processors in difficult-to-test patients (e.g., see Hughes 2013 for review).

Because the ECAP is generated by excitation of the primary auditory afferents, certain characteristics of the ECAP waveform might be a good indicator of the quality of the electrode-neuron interface across channels. Animal studies, for example, have shown that the peak amplitude of Wave I of the EABR is positively correlated with the number of surviving spiral ganglion neurons following an extended period of deafness (Smith & Simmons 1983; Hall 1990). A similar correlation has been observed with shallow slopes of the EABR wave I amplitude growth function (Miller et al. 1994). In addition, a reduced density of surviving

neurons has been shown to decrease the sensitivity of ECAP and EABR amplitudes to changes in pulse duration or interphase gap (Prado-Guiterrez et al. 2006). Ramekers et al. (2014) found that the maximum ECAP amplitude and slope were positively correlated with neural density in deafened guinea pigs; interestingly, the slope and latency of the response was dependent on variations in the interphase gap, though dependency did not extend to pulse duration. Finally, the slope of ECAP amplitude growth functions has been positively correlated with speech performance in human listeners, though the strength of this correlation is sensitive to device type, and relatively weak overall (Kim et al. 2010). It is not clear from these studies, however, if ECAP amplitude is sensitive to localized changes in neural health, and data from human listeners is limited. The available data shows that ECAP peak amplitude is variable across electrodes and CI listeners, but the source of that variability is not currently well understood.

The ECAP has also been evaluated as a tool to characterize the spatial extent of peripheral excitation, by evaluating channel interaction across electrodes, using a forward-masking paradigm (e.g., Abbas et al. 2004). Like ECAP amplitudes, the shapes of the resulting channel interaction functions (CIFs) are quite variable from channel-to-channel (e.g., Scheperle and Abbas, 2015). CIFs have been shown to strongly correlate with psychophysical tuning curves and forward masking profile widths (Cohen et al 2003; Abbas et al. 2004; Hughes & Stille 2008, 2010), suggesting that those two metrics reflect similar underlying processes. Previous studies have not, however, demonstrated a correlation between broad CIFs and poor speech perception scores, but channel interaction was only characterized for a subset of electrodes (e.g., Cohen et al. 2003; Hughes & Abbas 2006a; Hughes & Stille 2008). By measuring all available electrode CIFs in the present study, the spatial extent of excitation can be more thoroughly evaluated.

The main purpose of this study is to examine whether it is possible to differentiate between electrode position and neural status using an electrophysiological tool. Although a behavioral or electrophysiological measure that is sensitive to both factors combined might be useful, the clinical strategies to manage a poor electrode-neuron interface may prove to be very different depending on the underlying cause of the deficit. Moreover, site-specific identification of electrode position as the primary contributor to a poor electrode-neuron interface may allow for inference about the role of neural status at a given site. Additional analyses explore the relationships between speech perception and the physical, behavioral, and electrophysiological factors in this study.

In the present study, ECAP measures are compared to focused behavioral thresholds and estimates of electrode position from CT images. The underlying rationale is that radial electrode position, scalar location, and neural status may collectively influence channel-by-channel ECAP measures. The specific hypotheses are: (1) electrodes with higher sQP thresholds will be associated with smaller ECAP amplitudes and broader ECAP CIFs, and (2) electrodes with a more lateral placement and/or translocated in scalar location will be associated with smaller ECAP amplitudes and broader ECAP CIFs. Comparisons among sQP thresholds, electrode-modiolus distance, monopolar ECAP measurements, the number of electrodes located in the SV, angular insertion depth and speech perception are also made. Though the use of monopolar ECAPs (a methodological constraint, see Methods) and focused stimulation may present limitations in data interpretation, studies have shown variability in CIFs across electrodes and stimulus levels using monopolar ECAPs (e.g. Cohen et al. 2004; Hughes & Abbas 2004). Similarly, within-subject differences in the sharpness of psychophysical tuning curves have been observed with monopolar stimulation (e.g., Bierer & Faulkner 2010; Nelson et al. 2008). Based

on previous work, it is hypothesized that electrode position and sQP thresholds will be correlated with speech perception scores (Finley et al., 2008; Long et al. 2014). Further, by examining ECAP amplitudes and channel-interactions across the entire electrode array, as opposed to previous studies that evaluated a subset of electrodes (e.g., Brown et al. 1990; Hughes & Abbas 2006a), a cross-subject correlation with speech scores is predicted.

Comparing results across different aspects of the electrode-neuron interface within the same individual will be informative with regards to: 1) the viability of the ECAP as a site-specific measure of the effectiveness of electrical stimulation, 2) how the diverse measures may be interpreted and 3) in the future, how they might be used clinically. Although one purpose of exploring ECAPs is to evaluate whether an objective measure can be used as a substitute for a behavioral measure, it may be that each measure provides different information about auditory function, and that multiple measures should be combined within a test battery. More broadly, by examining the relationships between ECAP channel interaction and amplitude, focused behavioral thresholds, and CT-estimated electrode positions, this study will provide useful insight into the identification and assessment of poor electrode-neuron interfaces. The findings should help to advance efforts toward tailoring electrical stimulation for individual cochlear implant listeners, and ultimately improve cochlear implant listener perception of complex acoustic stimuli.

B. Methods

Subjects

Ten adult subjects were recruited from the University of Washington Communication Studies Participant Pool. Subjects were at least 21 years of age (M = 59.8, SD = +/- 13.9) and unilaterally implanted after 2001 with Advanced Bionics HiRes90k devices (see Table 2-1 for

demographic information). There were 7 males and 3 females in this study. Eight of the subjects were postlingually deafened and two were perilingually deafened (S40 and S44, profound hearing loss at 4 and 3 years of age, respectively). All subjects were native speakers of American English. Each participant provided written consent, and the experiments were conducted in accordance with guidelines set by the Human Subjects Division of the University of Washington. Subjects participated in 3 or 4 sessions, each lasting for 3-4 hours.

Table 2-1: Demographic table for all 10 subjects including: implanted ear, age, age at profound HL, age at implantation, etiology, and electrode array/spacing

ID	Implanted Ear	Age	Age @ Profound HL	Age at implantation	Etiology	Electrode Array/Spacing (mm)
S22	R	74	55	66	Genetic	HiFocus Helix/ 0.85
S29	L	84	47	77	Noise	HiFocus 1J/ 1.1
S38	L	50	17-18	46	Otosclerosis	HiFocus 1J/ 1.1
S40	L	52	3 (perilingual)	50	EVA	HiFocus 1J/ 1.1
S41	L	49	Birth (R), 42 (L)	43	Rubella	HiFocus 1J/ 1.1
S42	R	64	50	50	Unknown	HiFocus 1J Positioner/ 1.1
S43	R	68	50	67	Noise	Mid-Scala/ 0.85
S44	R	52	4 (perilingual)	51	Antibiotics	Mid-Scala/ 0.85
S46	R	67	14	66	Unknown	HiFocus 1J/ 1.1
S47	R	38	28	37	Unknown	Mid-Scala/ 0.85

Electrical Stimulation

All stimuli were presented using the Bionic Ear Data Collection System version 1.18.315 (Advanced Bionics, Valencia, CA). For behavioral testing, a custom Matlab (Mathworks, Inc. Natick, MA) script controlled the BEDCS software. Two types of electrode configurations were used in this study: monopolar (MP) and steered quadrupolar (sQP). MP stimulation was used for ECAP measurement because the high current requirements to achieve most comfortable level (MCL) for very brief single-pulse stimulation are often unobtainable within the compliance limits of the device with focused stimulation. MP stimulation consists of an active intracochlear electrode and a return extracochlear electrode; the large distance between the source/sink yields a broad electrical field (Litvak et al. 2007). sQP stimulation was used in the present study as sQP

thresholds were found to be equivalent to partial tripolar thresholds in another study, in which many of the same subjects participated (r = .96; for details, see Bierer et al. 2015). sQP stimulation consists of four intracochlear electrodes: the two middle electrodes serve as active electrodes, and the two outer electrodes serve as return electrodes for a fraction of the active current (an extracochlear electrode carries the remainder of the return current). Current is steered between the two middle electrodes according to the fraction, α: a value of 1 steers current to the basal electrode and 0 to the apical electrode. By convention, channel number is defined as the basal active electrode when α = 1. In the present study, this convention was maintained for electrodes 3 to 15. For electrode 2, however, it was necessary to use the same set of electrodes as channel 3 (the most apical channel possible with the 4-electrode sQP configuration) in conjunction with an α value of 0 to center the current on electrode 2. This arrangement is referred to as "channel 2," even though electrode 3 is the apical active electrode. For current focusing, the outer two electrodes in the sQP configuration receive a fraction of the return current according to σ (Bierer et al. 2015; Landsberger & Srinivasan 2009; Srinivasan et al. 2010). As with the commonly used partial tripolar configuration, higher σ results in a narrower electrical field than MP stimulation (Litvak et al. 2007). The value of σ used in the present study for sQP stimulation was 0.9 in order to retain highly focused stimulation while avoiding unreasonably high current limits and side-lobe activation.

Single-Channel Behavioral Thresholds

Stimuli were biphasic, cathodic-leading pulse trains (102 μs/ph, 0-μs interphase gap, 200.4 ms duration, 997.9 pulses per second) presented to electrodes 2 to 15 (apical to basal), using sQP stimulation. Behavioral thresholds were measured for each electrode using a two-interval, two-alternative forced choice procedure (two-down, one-up) that converges on the 70.7% correct

point on the psychometric function (Levitt 1971). Subjects were presented with two visual boxes on the computer screen (one of the boxes appeared at the same time as the sound), and asked, "Which interval contained the sound?" Subjects indicated the interval in which they thought the sound occurred using the computer mouse and were provided with feedback. Each run continued for six reversals in current level, and the average of the last four levels was taken as threshold. For the first two reversals, the signal was adjusted by 2 dB; step size decreased to 0.5 dB for the remaining four reversals. For each electrode, four runs were collected and averaged. If the four thresholds had a standard deviation greater than 2 dB, a fifth run was collected; all 5 runs were then averaged. For S44, thresholds were only collected for electrodes 4-10 due to reports of non-auditory percepts on the other electrodes. These auditory percepts included a "tingling" sensation for basal electrodes and an "uncomfortable sound quality" for apical electrodes. This subject also had non-auditory percepts clinically and electrode 11 was deactivated from her clinical map.

Electrically Evoked Compound Action Potential Measurements

ECAPs were obtained using a forward-masking, channel-interaction paradigm (Cohen et al. 2003; Abbas et al. 2004; Scheperle & Abbas 2015). Stimuli were biphasic, cathodic-leading pulses (32 μs/phase, 0 μs interphase gap) presented at a probe rate of 20 per second in the MP configuration. Stimulus level was determined behaviorally using the Advanced Bionics clinical loudness scale (Advanced Bionics, Valencia, CA), and was increased as subjects verbally identified each rating until they reached "8" ("Maximal Comfort"). The MCL was considered a rating of "7." Loudness balancing was performed at MCL by presenting the stimulus across four electrodes sequentially to assess subjective equal loudness. Electrodes differing in loudness were adjusted accordingly, and the signal was presented again on the same four electrodes. This

continued until all four were perceived as equally loud, then the next four (one overlapping with the previous set) were stimulated and the procedure repeated for all available electrodes. Both masker and probe stimuli were fixed at the loudness-balanced MCL for ECAP testing. Over a sequence of ECAP recordings, all available electrodes served as a probe channel in combination with all available electrodes as masker channels.

For each measurement series, the probe stimulus was fixed and the location of the masker stimulus varied across the electrode array. The masker pulse preceded the probe pulse by 500 μs. The recording electrode was positioned two electrodes apically relative to the probe, except when the masker and recording channel targeted the same electrode, in which case the recording electrode was moved basally by two electrodes for those conditions. For recording, gain was set to 300 and the sampling rate at 56 kHz. "After stim" was selected as the start recording option in the BEDCS software. One hundred repetitions were obtained for each masker-probe pair and averaged. The neural response was derived by subtracting averaged recordings of the masker+probe, masker alone, and system signature (i.e., no stimulation) from a probe alone stimulus condition (Brown et al. 1990; Lai & Dillier 2000; Cohen et al. 2003; Abbas et al. 2004). For the duration of the measurements, subjects were required to sit near the computer but were otherwise allowed to read, talk, eat, or sleep.

After data collection using custom Matlab software, the experimenter visually examined each derived waveform and manually set markers at the location of the first negative peak (N1; occurring at approximately 240 μs) and a later positive peak (P2; occurring at approximately 440 μs), after onset of the probe. Peak-to-peak amplitudes smaller than 0.03 mV were considered too small to discern from the noise floor and were considered as "no response" (i.e., 0 mV). Peak-to-

peak amplitudes were stored in Matlab for further analysis. For reasons mentioned above, ECAP measures were only collected for electrodes 4-10 for S44.

For each subject, CIFs were created for each probe electrode by plotting ECAP amplitude as a function of masker electrode distance from the most apical electrode, in millimeters, such that all data were plotted on the same x-axis (subjects were implanted with arrays with different electrode spacing; see Table 1). From these functions, peak amplitude and equivalent rectangular bandwidth (ERB) were calculated. Peak amplitude was quantified by selecting the maximum amplitude regardless of the masker electrode; therefore, in some cases peak amplitude occurred when the masker and the probe were on different channels. However, this occurred for only 20 CIFs (out of 129 possible), and was typically masker-probe displacements of only one electrode. Additionally, these amplitudes differed by less than .001 mV, as compared to the amplitudes for when masker and probe on the same electrode. The ERB quantifies the spatial extent of masker-probe interaction by equating the CIF to a rectangular function of equivalent amplitude. It is calculated by dividing the area under the CIF (i.e., the sum of amplitudes across all masking electrodes) by the peak ECAP amplitude (i.e., a normalized area). Note that CIFs for probes near the end of the electrode array were not fully characterized on one side due to the lack of electrodes to use as maskers. Partial functions were defined as those for which the peak amplitude decreased to 0 mV on only one side of the function. Under the assumption that excitation patterns would extend to neurons beyond the array, partial functions were completed by extrapolating the missing data points by mirroring the ECAP amplitudes from the measured data on the side with a full complement of masking electrodes. Although CIFs are often asymmetrical, we assumed that including the extrapolated data points would provide a better estimate of the spread of excitation than using partial functions.

CT Images

CT scans were performed at the University of Washington Medical Center. Briefly, ANALYZE software was used to create 3-dimensional image volumes by combining information from each subject's post-operative scan and a single body donor cochlea (for details, see Skinner et al. 2007; for verification of the method, see Teymouri et al. 2010). Pre-operative CT scans were not available for the subjects participating in the present study; therefore, a scan of the non-implanted ear was used to identify structural anatomy, and this image was co-registered with the image of the implanted ear. Micro CT and orthogonal-plane fluorescence optical sectioning (OPFOS) images from a donor cochlea were used to locate and visualize the non-bony structures. The two primary metrics from the CT imaging data that were analyzed in this study were electrode-to-modiolus distance and scalar location (similar to metrics used in Long et al. 2014). Electrode-to-modiolus distance describes the distance (mm) of an electrode from the medial wall of the cochlea. Scalar location denotes the positioning of an electrode in the fluid-filled cochlear compartments: ST, intermediate, and SV. Intermediate was used to denote those electrodes that could not be clearly determined to be in ST or SV. A third metric, angular insertion depth, was also calculated from the CT imaging data for the purpose of comparing to previous studies (i.e., Finley et al. 2008; Holden et al. 2013). Angular insertion depth is derived using the sum of the length along the electrode trajectory and the distance along the electrode array from the cochleostomy (Holden et al 2013).

Speech Testing

Speech perception testing was performed in a double-walled sound-treated booth (IAC RE-243 with an internal size of 7' by 7'). Stimuli were played through an external A/D device (SIIF USB SoundWave 7.1), amplified by a Crown D75 audio amplifier and presented through a Bose 161

speaker, placed at 0° azimuth and 1 meter from the subject's head. Custom software was used to present the stimuli (ListPlayer version 2.2.11.49; Advanced Bionics, Valencia, CA). Speech stimuli consisted of recordings of one male and one female Pacific Northwest talker uttering 10 naturally spoken vowels in the /hVd/ context (heed, hid, hayed, head, had, hod, who'd, hood, hoed, and hud). Sixteen consonants in the /aCa/ context (aba, ada, afa, aga, aja, aka, ala, ama, ana apa, asa, asha, ata, atha, ava, and aza) were also used. The speech tokens were calibrated using a B&K Type 2250 sound level meter, and presented at 60 dB-A in the sound field. During each trial, subjects were presented visually with either the vowel or consonant closed sets on a computer screen and were instructed to choose which word they heard. Within a run, each token was presented three times, and the test was scored as percent correct. Subjects were given a practice run (not included in the final averaged score), and then two test runs. If the difference between the first and second test run was greater than 10%, a third run was collected and all three runs were averaged. Results from vowel and consonant data were evaluated separately and found to be relatively similar across the variables of interest. Vowel identification was found to be significantly correlated with ECAP amplitude (T_8 = 2.84, p = .02) and sQP threshold (T_8 = -2.31, p = .05), but not for electrode-to-modiolus distance (T_8 = -1.69, p = .13) and ECAP ERB (T_8 = .42, p = .69). Consonant identification was found to be significantly correlated with ECAP amplitude (T_8 = 2.31, p = .05), sQP threshold (T_8 = -3.20, p = .01), and electrode-to-modiolus distance (T_8 = -2.48, p = .04), but not for ECAP ERB (T_8 = .23, p = .83). Scores from both vowel and consonant data were averaged to provide an overall estimate of performance across all speech sounds.

Statistical Analysis

SPSS statistical software was used to perform two multiple linear regression analyses for between-subject comparisons (IBM Corp. Released 2013. IBM SPSS Statistics for Windows). The first analysis included sQP threshold as the dependent variable, electrode-to-modiolus distance, ECAP peak amplitude and ERB as independent variables of interest, and MCL, and subject as adjustment variables. The second analysis included everything in the first except behavioral threshold, with electrode-to-modiolus distance as the dependent variable. Two regression models were needed because fewer data points were available for threshold measures (only up to 14 electrode sites were evaluated) compared to all other outcome measures (up to 16 electrode sites).

Additional analyses were conducted to evaluate the effects of scalar location on all variables of interest. *A priori*, electrodes located in the intermediate position or in SV are expected to have larger electrode-to-modiolus distances than electrodes in the ST. By design, certain array types may better facilitate insertion into the target scala (ST) (e.g., Aschendorff et al., 2007), though effect of array type is not explored here due to a small sample size. One-way ANOVAs were conducted for scalar location relative to electrode-to-modiolus distance, behavioral threshold, and ECAP measures. Adjustments using Welch's Test for unequal variances were made as appropriate and noted. Lastly, a simple linear regression analysis was conducted to evaluate mean speech performance with the variables of interest. A Bonferroni correction was applied to all multiple comparisons.

C. Results

Electrode-to-modiolus distance using CT imaging

Figure 2-1 shows the variability in electrode array positioning observed in 3D cochlear reconstructions for all subjects, arranged by electrode array type. The green area represents the reconstructed cochlea, and the red circles located within represent the individual electrodes. The red/yellow horizontal and vertical axes represent the mid modiolar axis, which is used to assign scalar location and determine insertion depth. Across subjects, electrode-to-modiolus distances ranged from 0.18-2.3 mm (M = .1.23 mm, SD = .53; for individual data, see Table 2-2). In general, the electrode trajectories in Figure 2-1 are consistent with the designs of the four types of arrays, which partially determine how far the electrodes are from the modiolus, and thus how close they are to the closest auditory neurons. The 1J electrode array (S29, S38, S40, S41 and S46) has a lateral design, whereas the 1J Helix (S22) is precurved to achieve a more medial position. The 1J with positioner (S42) pushes the array even more medially. The Mid-Scala array (S43, S44, S47) is precurved, and designed for mid-scalar placement in an effort to protect cochlear structures. However, due to a small sample size, differences between electrode array types cannot be examined further.

Table 2-2: Means and SDs for distance, threshold, ECAP measures, threshold variability and mean speech scores

ID	**Electrode-Modiolus Distance (mm) mean *(sd)***	**sQP Threshold (dB) mean *(sd)***	**sQP Threshold Variability (dB)**	**ECAP Peak Amplitude (mV) mean *(sd)***	**ERB (mm) mean *(sd)***	**Mean Speech Scores (% correct)**
S22	1.12 *(.37)*	42.72 *(6.92)*	5.49	.24 *(.12)*	5.78 *(1.51)*	74
S29	1.52 *(.23)*	47.15 *(3.32)*	3.77	.18 *(.06)*	9.20 *(3.16)*	82
S38	1.30 *(.25)*	45.16 *(3.00)*	3.29	.08 *(.02)*	4.89 *(1.67)*	46
S40	1.79 *(.22)*	54.27 *(1.30)*	2.02	.07 *(.02)*	5.22 *(2.30)*	30
S41	1.56 *(.37)*	45.14 *(.89)*	1.13	.29 *(.10)*	7.54 *(1.99)*	88
S42	.64 *(.33)*	36.96 *(4.80)*	2.03	.23 *(.13)*	5.28 *(3.04)*	95
S43	.84 *(.44)*	44.69 *(3.95)*	3.22	.07 *(.02)*	2.55 *(.01)*	60
S44	.85 *(.49)*	50.67 *(1.58)*	1.86	.11 *(.07)*	2.57 *(.40)*	73
S46	1.80 *(.32)*	51.69 *(1.53)*	.91	.06 *(.02)*	6.60 *(1.73)*	39
S47	.87 *(.46)*	38.39 *(5.91)*	4.08	.09 *(.03)*	3.11 *(.52)*	94
Summary	1.23 *(.53)*	45.43 *(6.54)*	2.85 *(1.39)*	.15 *(.11)*	5.92 *(2.86)*	67.69 *(23.24)*

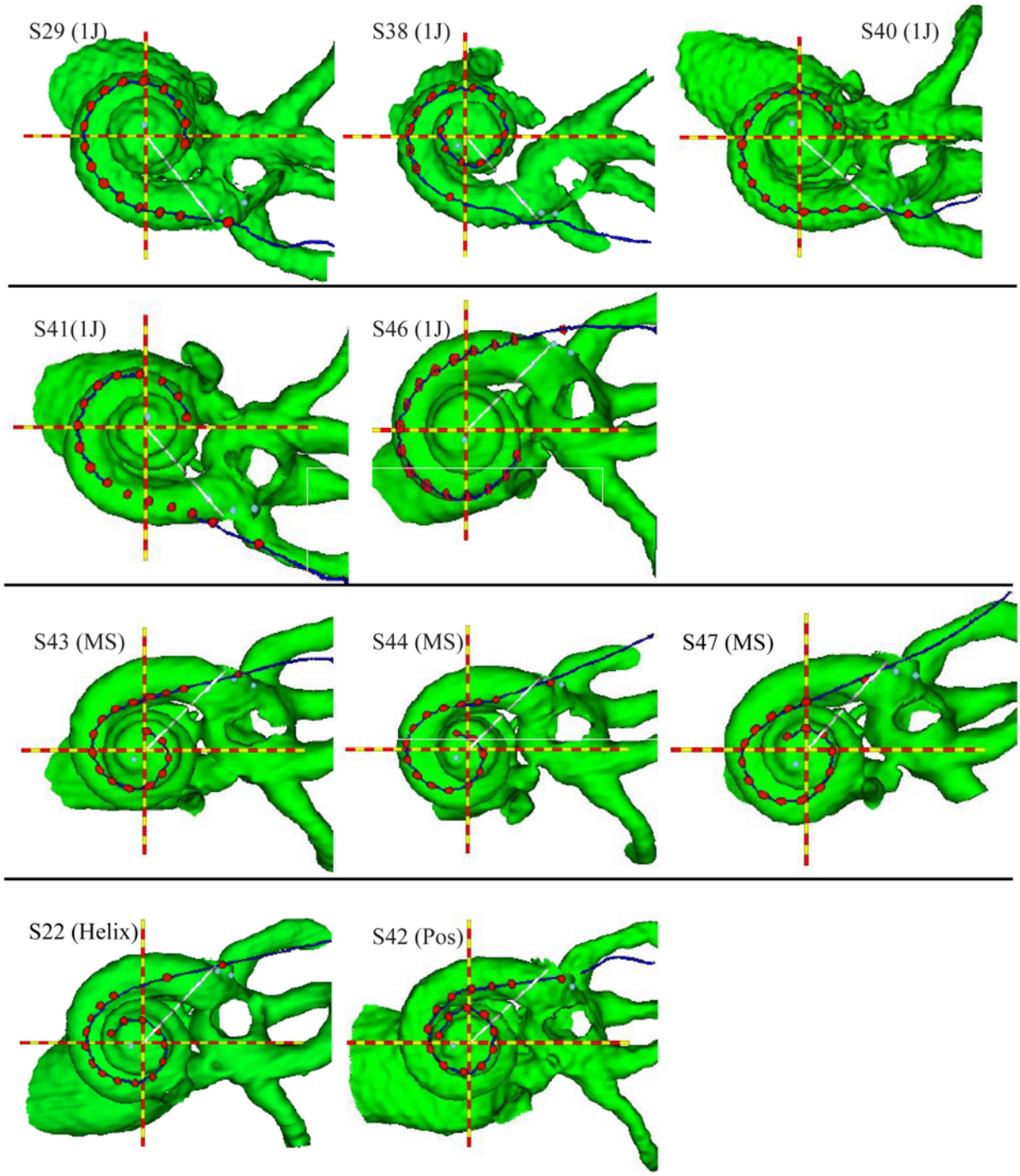

Figure 2-1: CT view of cochlea and electrode array along the midmodiolar axis(red and yellow dashed line), organized by electrode array type. The evenly spaced red dots represent electrodes; the outermost dot represents the insertion depth marker. The white line represents the 0-degree reference point from which insertion depth is measured, extending from the midmodiolar axis (see Finley et al, 2008 for more details). Rows 1-2: 1J array; Row 3: MidScala; Row 4: 1J Helix and 1J with positioner, respectively.

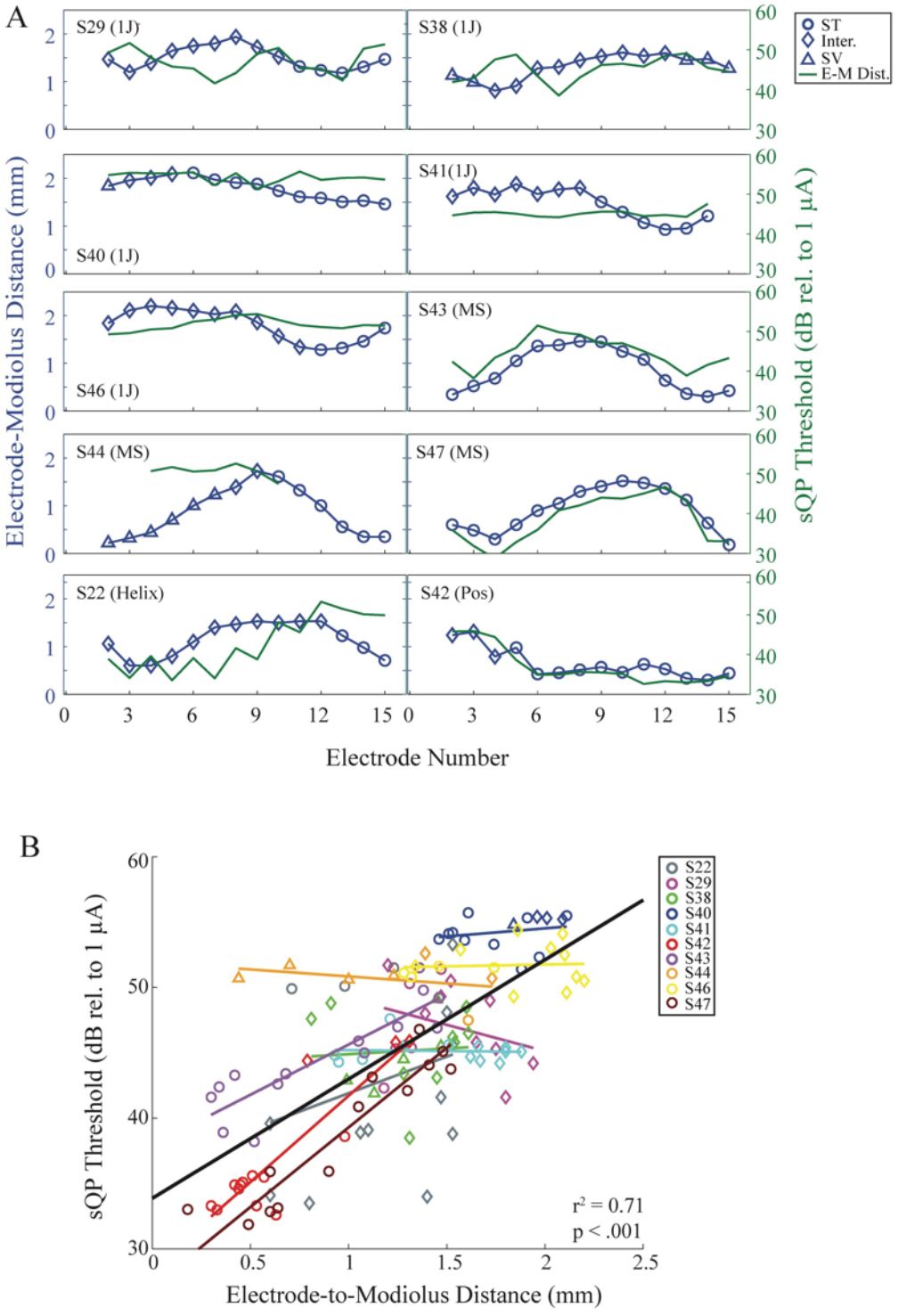

Figure 2-2: A: sQP threshold in dB (green line) and electrode position in mm (blue line) profiles for all subjects, organized by electrode array type. Scalar information is represented by symbol along the electrode position line: ST (circles), intermediate (diamonds), and SV (triangles). B: Scatter plot comparing electrode position with sQP threshold for individual subjects (colored lines; see legend) and group data (black line). The circles represent electrodes in ST, the diamonds for electrodes in the intermediate position, and the triangles for electrodes in SV.

Focused behavioral thresholds and electrode-to-modiolus distance

Figure 2-2A shows electrode-to-modiolus distance (left ordinate) and sQP threshold (right ordinate) profiles for each subject. Scalar information is indicated by symbol (see legend). sQP thresholds range from 28.8-55.7 dB rel. to 1μA (M = 45.45 dB rel. to 1μA, SD = 6.54) across subjects and electrodes (Table 1-2). Figure 2-2B illustrates the relationship between sQP threshold and electrode-to-modiolus distance, with individual subject data distinguished by color. Consistent with previous studies (Long et al., 2014; Cohen et al., 2003), a strong association between sQP thresholds and electrode-to-modiolus distance was observed; results from the multiple linear regression analysis showed a significant, positive correlation between electrode-to-modiolus distance and sQP threshold (T_{83} = 4.42 $p < .001$). Increases in electrode-to-modiolus distance trended with increases in sQP thresholds, both across subjects and to a lesser extent, across electrodes within individual subjects, although a within-subject correlation was only observed for some subjects (S42, S43, S47; $p < .01$). For the majority of participants, a correlation was not observed (S22, S29, S38, S40, S41, S44, S46).

ECAP channel interaction functions

ECAP amplitudes and the shapes of the CIFs were variable within and across subjects and electrode arrays. ECAP CIF profiles for all subjects are shown in Figure 2-3, organized by electrode array type (note the different scale on the y-axis for S29, S41, S22, and S42). It should also be noted that for S43, very few CIFs were obtained due to "no response" on electrodes 8-16. Neither ERBs nor peak amplitudes were calculated for these electrodes, and are considered missing data. For S44, no basal information was available due to non-auditory percepts, and these data are also considered missing. For electrodes with responses, the mean ECAP peak amplitude and ERB was calculated for each subject (Table 2-2; mean amplitudes also displayed

in each panel of Figure 2-3). Mean peak amplitudes ranged from 0.06-.29 mV (*M* = .15 mV, *SD* = .11), and mean ERB values ranged from 2.55 to 9.20 mm (*M* = 5.92 mm, *SD* = 2.86).

Each CIF is expected to peak when the masker is presented at the probe site; however, in some cases the peaks were offset from the probe location, as is the case for S29, S40, S46, S47, and S22. For example, for subject S29 (Figure 2-3), the peak for probe electrode 1 is located at

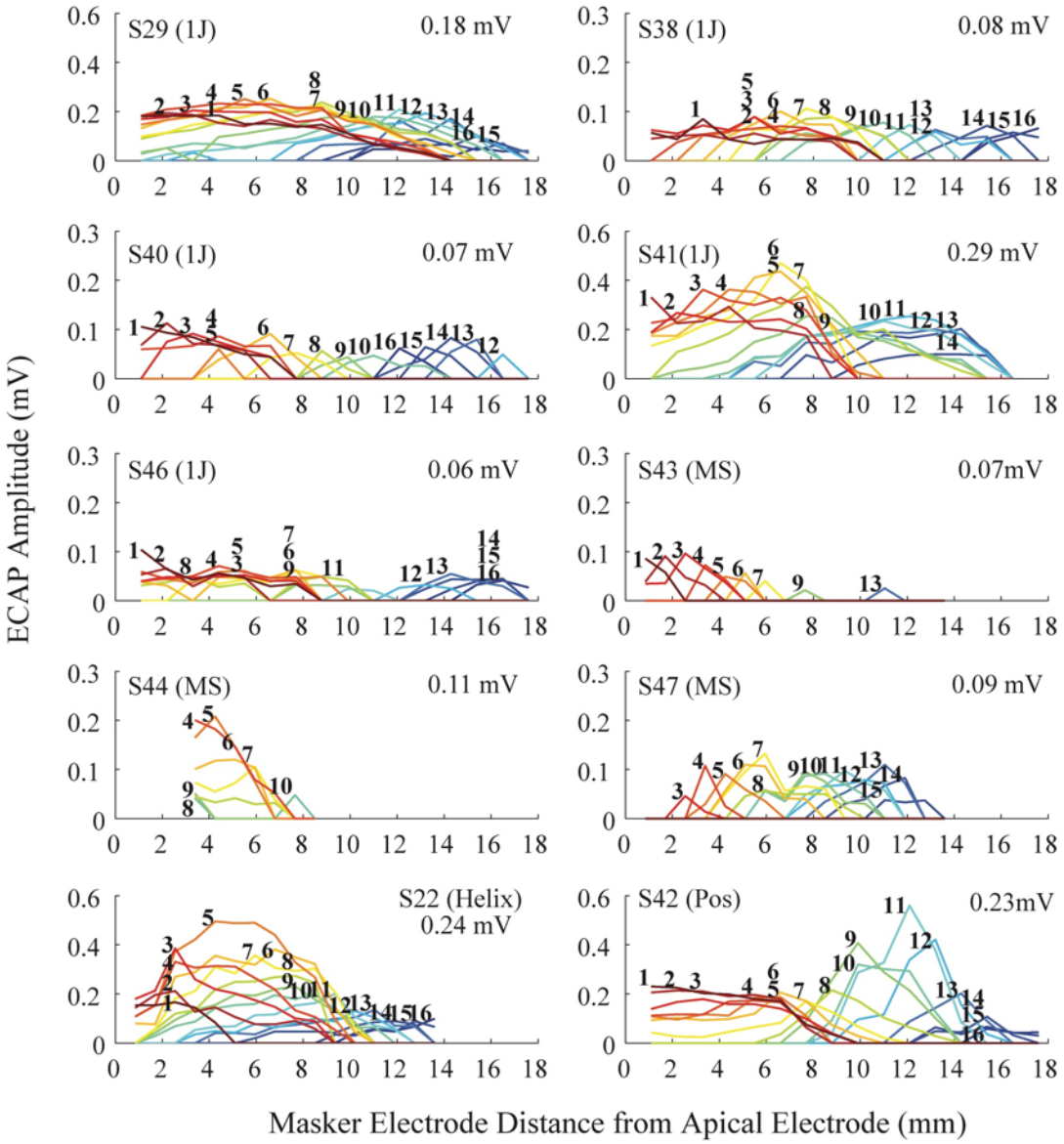

Figure 2-3: CIFs for all subjects, organized by electrode array type. The x-axis represents masker electrode (mm from the apical electrode). The y-axis represents ECAP amplitude (mV). For subjects with overall low amplitudes, the y-axis ranges from 0-0.3 mV; for the others, it ranges from 0-0.6 mV; note this is reflected in the scales on the y-axis. Mean ECAP peak amplitude (mV) is indicated at the top right of each panel. The numbered lines inside the plot are probe electrodes, labeled at the peak amplitude of the CIF.

the peak for electrode 4; however, S29s CIFs are quite broad, and little "noise" would be required to dislocate the peak to an off-masker channel. For S22, the first four electrodes share a peak location; a masker presented to electrode 2 was the most effective for all of these probe sites. For some electrodes, the CIF appears to have a secondary peak (e.g., S41, probe electrode 1). For apical probe electrodes, CIFs with dual peaks have been shown to indicate an electrode array with a tip fold over (Grolman et al., 2009), but this is not observed in the CT data for any of the subjects in the present study.

For all subjects, overlapping excitation patterns across CIFs was observed. Often, the greatest amount of overlap occurred for adjacent probes, as can be seen in Figure 2-3 for S22's first four electrodes; however, overlaps were also observed for more distant probe electrodes (e.g., S44's electrodes 4, 8, and 9). Additionally, some CIFs completely enveloped others. For instance, S22's probe 5 has a relatively large peak amplitude and a broad spread of excitation across basal electrodes that completely or partially envelops the CIFs associated with probe electrodes 1-10.

Comparisons of ECAP measures with focused thresholds and electrode-to-modiolus distances

Scatterplots between the ECAP data and sQP thresholds (left) and electrode-to-modiolus distance (right) are shown in Figure 2-4. Mean peak amplitudes are shown in the top panels, and mean ERBs are shown in the bottom panels. Results from the multiple linear regression analysis indicated a significant, negative correlation between ECAP peak amplitude and sQP threshold (T_{83} = -6.08, $p < .001$), and a significant, positive correlation between electrode-to-modiolus distance and ERB (T_{91} = 2.39, p = .02). The other two comparisons were not significant (sQP threshold and ERB: T_{83} = 1.73, p = .09 and electrode-to-modiolus distance and ECAP peak amplitude: T_{91} = -.94, p = .35). Overall, the results show that ECAP peak amplitudes are smaller

for channels with high sQP thresholds, and ECAP ERBs are broader for large electrode-to-modiolus distances.

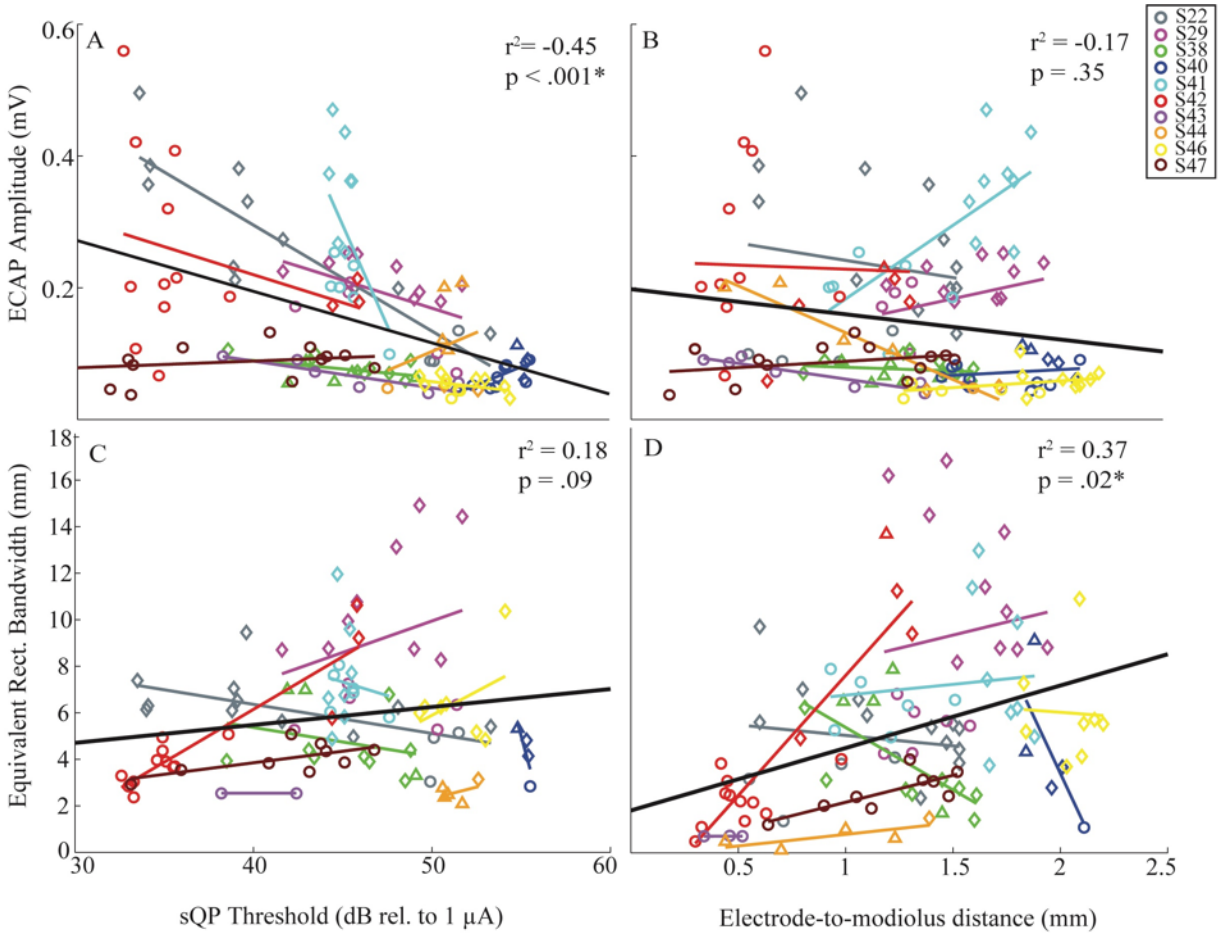

Figure 2-4: Comparisons between sQP threshold, electrode position, and the ECAP variables of interest for individual subjects and group data (black line). All p-values are from the multiple linear regression analysis. The circles represent electrodes in ST, the diamonds for electrodes in the Intermediate position, and the triangles for electrodes in SV. A: Comparison between sQP threshold and ECAP peak amplitude. B: Comparison between electrode position and ECAP peak amplitude. C: Comparison between sQP threshold and ERB. D: Comparison between electrode position and ERB.

Scalar location

Scalar location was estimated for all subjects and electrodes. 52% of all electrodes were located in the ST, which is the target location during surgical implantation. Most of the other electrodes were estimated to be in the intermediate position (37%), with the remaining electrodes in the SV (11%). Figure 2-5 presents histograms relating scalar location data to sQP threshold (A),

electrode-to-modiolus distance (B), and ECAP peak amplitude (C) and ERB (D). Results from the ANOVA show a main effect of scalar location, wherein sQP threshold was lower for electrodes in ST compared to those in an intermediate position; however, this was not significant after Bonferroni adjustment ($F(2,129) = 3.54$, $p = .03$). Electrodes located in either the intermediate position or in SV were further from the modiolus ($F(2,157) = 19.38$, $p < .001$), which was shown previously to correlate with higher thresholds. An unexpected finding was that ECAP peak amplitude was significantly smaller for electrodes in ST and the intermediate

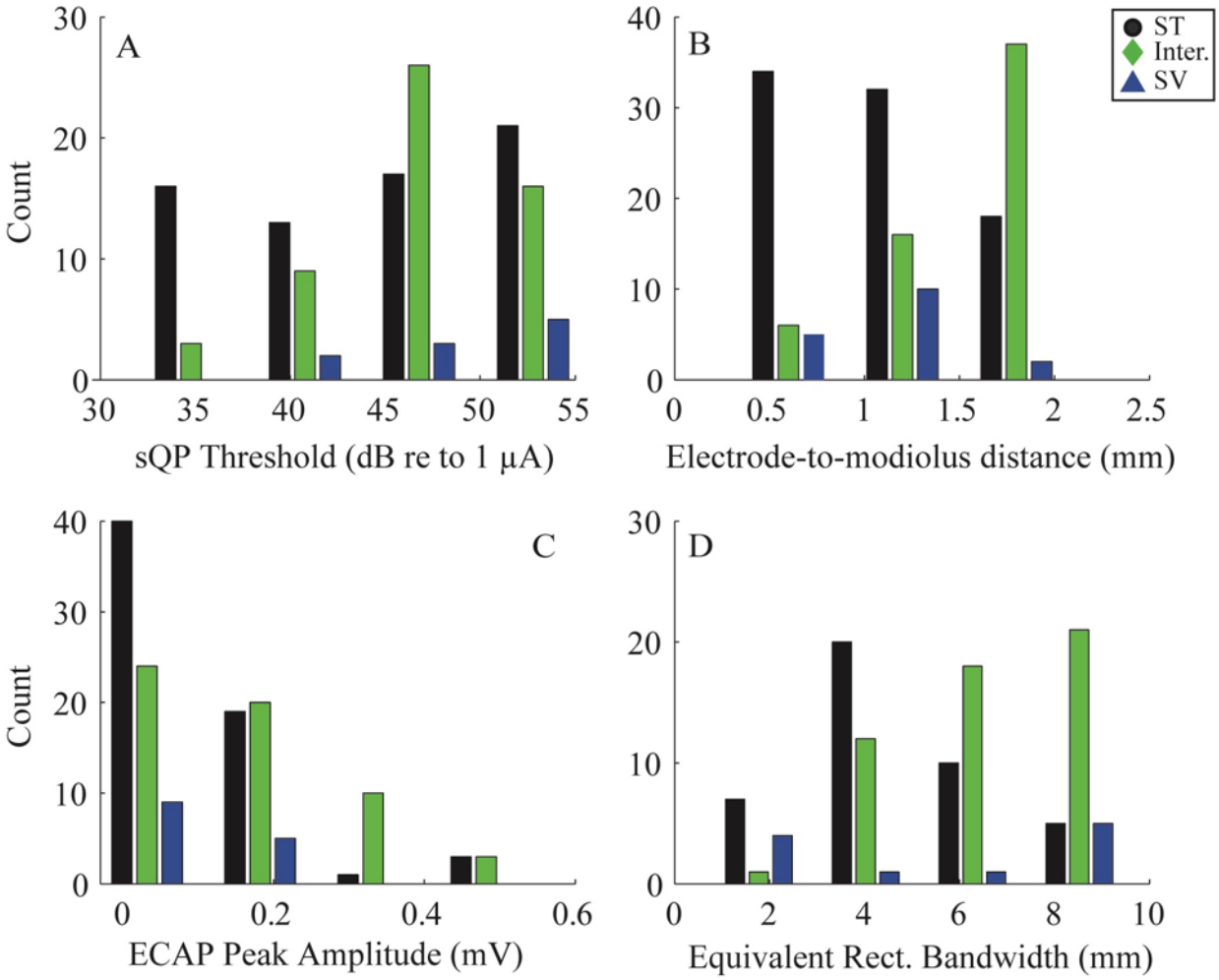

Figure 2-5: Histograms of scala counts for all variables of interest. Black, green and blue bars represent ST, intermediate, and SV, respectively. It is important to note that panels for sQP threshold and ERB have a different y-axis from the other panels, for ease of viewing the distributions. A: sQP threshold (dB rel. to 1 μA); B: electrode position (mm), C: ECAP peak amplitude (mV), and D: ECAP ERB (mm).

position, with no effect for SV ($F(2,131) = 5.97$, $p = .003$). Electrodes in ST had a narrower spread of excitation than those in the intermediate position, but electrodes in the SV did not differ from ST or those in the intermediate position ($F(2,101) = 14.00$, $p < .001$) (Figure 2-5D). It is possible that for some measures, electrodes in SV did not differ significantly from the other scalae due to the low number of SV electrodes available for analysis.

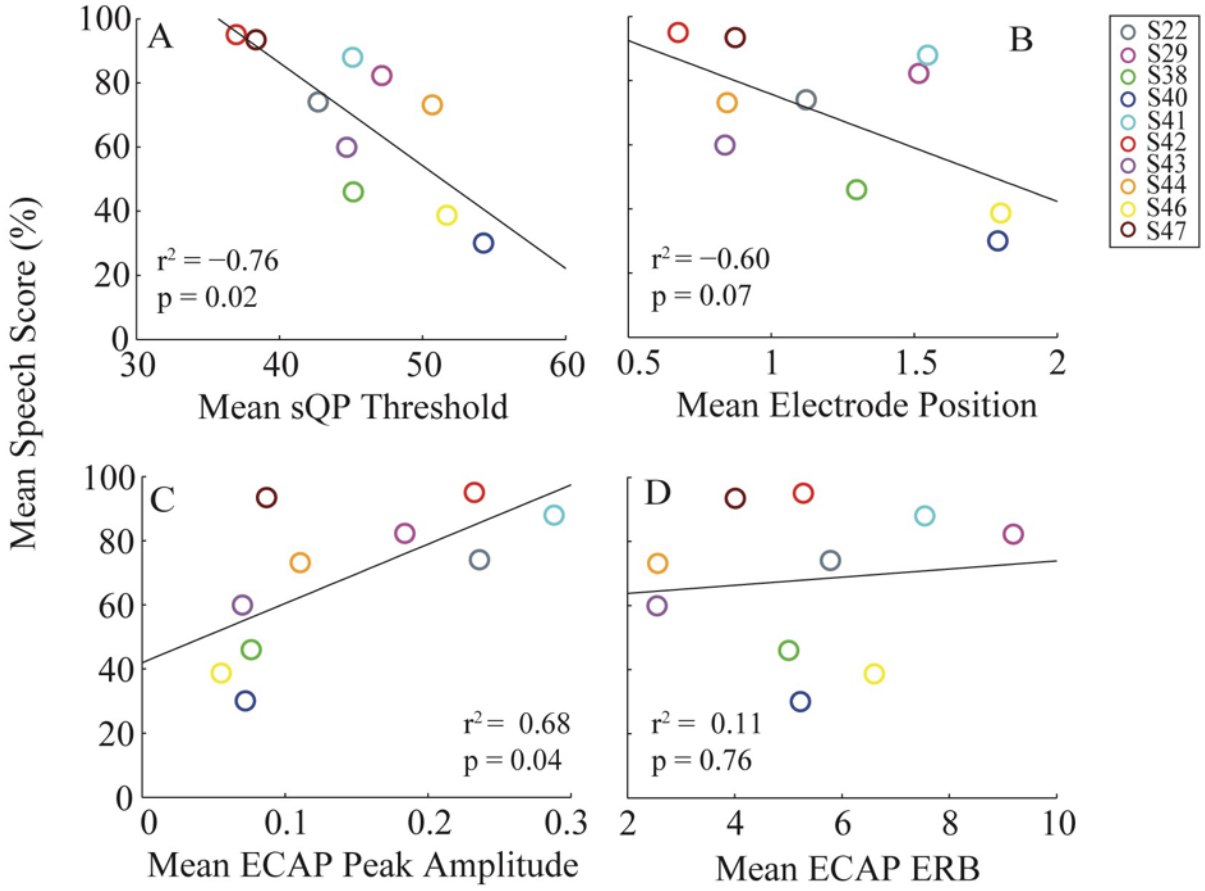

Figure 2-6: Relationships between the variables of interest and mean speech scores (from aCa and hVd stimuli). A: mean sQP threshold (dB rel. to 1 μA); B: mean ECAP peak amplitude (mV); C: mean ECAP ERB (mm), and D: mean electrode position (mm).

Speech performance

Figure 2-6 shows mean speech performance (the average of medial vowel and consonant discrimination scores) in relation to sQP threshold (A), electrode-to-modiolus distance (B),

ECAP peak amplitude (C), and ERB (D). Simple linear regression analyses reveal a positive correlation between mean speech score and ECAP peak amplitude (T_8 = 2.50, p = .04), and a negative correlation with sQP threshold (T_8 = -2.84, p = .02). However, no association was observed with ERB (T_8 = 0.31, p = .76), or electrode-to-modiolus distance (T_8 = -2.11, p = .07). Finally, results show no relationship between mean speech performance and number of electrodes in the SV, (F(4,5) = .75, p = .60), or with angular insertion depth, (F(1,8) = .15, p = .71).

D. Discussion

The present study sought to assess the relationship between the ECAP and other metrics related to the electrode-neuron interface: sQP thresholds and estimates of electrode-to-modiolus distance and scalar location using estimates from CT imaging. Results support the hypothesis that electrodes further from the modiolus are associated with higher behavioral thresholds and broader ECAP CIFs, and electrodes with lower behavioral thresholds are associated with larger ECAP amplitudes. However, channels with lower thresholds did not yield narrower ECAP CIFs, nor were electrodes far from the modiolus associated with smaller ECAP peak amplitudes. From these results and those showing that ECAP peak amplitude was predictive of speech performance, we infer that ECAP peak amplitude may be more sensitive to neural status than electrode position. Likewise, we infer that ECAP CIF width is more sensitive to electrode-to-modiolus distance and scalar location than neural status, as the ERB measure was not correlated with behavioral threshold or speech performance. Thus, ECAP peak amplitude and CIF widths appear differentially sensitive to two important aspects of the electrode-neuron interface.

Focused single channel thresholds and electrode-to-modiolus distance

Previous physical measurements in animals (e.g., Jolly & Spelman, 1996) and computational modeling studies of human cochleae (e.g., Goldwyn et al., 2010) demonstrate that voltage decreases with distance from the electrodes; therefore, electrodes that are farther from the modiolus require more current to drive neural responses. Consistent with modeling expectations and other studies (Cohen et al., 2003; Goldwyn et al., 2010; Long et al., 2014), focused thresholds (measured with sQP configuration in the present study) were highly correlated with electrode-to-modiolus distance, such that increased thresholds were indicative of greater electrode-to-modiolus distances. Despite the significant correlation, however, distance did not account for all of the variability in focused thresholds, particularly within subjects (Figure 2-2B). Long et al (2014) suggested that the remaining variability may be presumed to reflect variable neural health, though factors such as local variations in tissue impedance may play a role as well. They explored this hypothesis by correlating the RMS error of the threshold-distance model with speech perception scores, and found that subjects for whom threshold was well predicted by distance tended to have better speech perception. However, we were unable to replicate those findings with the data obtained in the present study (r^2 = .14, $F(1,8)$ = .16, p = .70).

The results presented in Fig 2-6A show a significant correlation between mean speech performance and sQP threshold. These results also differ from the Long et al study (2014), which found that mean phased array threshold was not correlated with logit-transformed speech performance on CNC words. However, they did observe that the within-subject variance (V = 34.8 dB^2) of phased array threshold was correlated with speech performance. Similarly, Bierer (2010) showed a negative correlation between channel-to-channel threshold variability (based on

the difference in standard deviation) and CNC words, such that greater variability in thresholds resulted in poorer speech performance. The present results did not replicate the correlation between either measure of threshold variability and speech performance (V = 42.8 dB^2, r^2 = .42, p = .22; $F(1,6)$ = .07, p = .80; r^2= -.12, for individual data, see Table 2-2), likely due to the small sample size.

ECAP amplitude and channel interaction

Peak Amplitude

Most previous ECAP studies have related evoked potential thresholds to behavioral threshold and comfort levels (reviewed in Miller et al. 2008; Jeon et al. 2010). To our knowledge, studies specifically evaluating the relationship between peak amplitude at a suprathreshold level (MCL) and behavioral thresholds have not been conducted. In the present study, ECAP peak amplitudes were small for electrodes with high focused behavioral thresholds (Figure 2-4A). In animal studies, the amplitude of evoked responses has been correlated with neural status, such that longer deafened animals had smaller amplitudes and fewer surviving auditory neurons (Hall 1990; Shepherd & Javel; 1997, Ramekers et al 2014; Smith & Simmons 1983).

There was no observed relationship between electrode-to-modiolus distance and ECAP peak amplitude. In this study, peak amplitudes were measured using masker and probe stimulus levels that were loudness-balanced at MCL, as opposed to a fixed stimulation level. For a fixed stimulus level, smaller ECAP amplitudes would be expected for electrodes with a more lateral placement because the stimulus decays as a function of distance. By adjusting stimulus level for each electrode (loudness balancing in this study), electrodes farther away from the modiolus were presumably stimulated with greater current than electrodes close to the modiolus; however, the stimulus reaching the neurons was comparable.

The significant correlation between ECAP peak amplitudes and speech-perception scores (Figure 2-6B) has, to our knowledge, not been observed previously. Brown et al (1990) evaluated the relationship between ECAP amplitude of a single electrode stimulated at a high level and speech-perception scores but did not observe a correlation. The different outcomes may be due to the fact that ECAP amplitudes were averaged across electrode sites in the present study, and a smaller sample size was used, among other factors. If smaller amplitudes are indicative of poor neural survival (Hall 1990; Smith & Simmons 1983), poorer speech outcomes may be reasonably expected for those listeners.

Given that ECAP peak amplitudes were not correlated with electrode-to-modiolus distance, we speculate that amplitude, evoked using stimulus levels equated for loudness, primarily reflected the number and health of the neurons contributing to the response. This speculation is further supported by the significant correlation with speech perception scores, though this result should be interpreted with caution because of the small sample size. Another element to consider is that if neural health is poor near the stimulating electrode the distribution of responding neurons will be broad and less synchronous than a more tightly bunched group of neurons. Synchrony, not just the number of activated neurons, is essential to measurable evoked potentials and at least one animal study has shown that with neural degeneration, neural synchrony is reduced (Shepherd & Javel 1997).

Channel Interaction

ECAP CIFs were sensitive to electrode position. The ERB was moderately correlated with electrode-to-modiolus distance, such that electrodes further away from the modiolus showed a greater degree of channel interaction (Figure 2-4D). Additionally, electrodes in the ST had narrower ERB widths compared to electrodes in the intermediate position. These results are

consistent with observations from previous studies that spread of the excitation pattern is primarily affected by electrode position (Cohen et al., 2003; Hughes & Abbas, 2006b; Miller et al., 2008).

Furthermore, consistent with previous studies, the present results did not show a correlation between channel interaction width (mean ERB) and mean speech performance (Brown et al. 1990; Cohen et al. 2003 Hughes & Abbas 2006a); in fact, the results across subjects were quite variable (Figure 2-6C). This suggests that previous null results were not solely due to sampling CIFs for a limited number of electrodes. Scheperle and Abbas (2015) found a similar result across subjects; however, within subjects, ECAP channel-separation indices (used as a measure of peripheral spatial selectivity) were correlated with speech perception. Though interaction width was estimated differently in the present study, the general results are similar. The evidence suggests that while CIF width may be predictive of electrode-to-modiolus distance, it does not appear to extend to speech performance across subjects; however, more data is needed to support this result.

The data suggest that although a laterally placed electrode may have a direct effect on the degree of channel interaction, channel interaction may not be the most sensitive measure of neural status. If ECAP peak amplitude is taken as an indirect measure of neural status, as suggested previously, and ECAP channel interaction width as a measure of electrode position, combining these measures may yield a comprehensive assessment of the electrode-neuron interface.

Scalar location and insertion depth

In the present study, electrode positions outside of ST were primarily located in an intermediate area, with a much smaller percentage of electrodes in the SV (about 10.6%). Finley

et al. (2008) also categorized translocations into SV, finding that the number of electrodes in SV was correlated with greater insertion depth and decreased speech perception. Holden et al (2013) also reported that across 114 subjects with either Advanced Bionics or Cochlear Corporation implants, 23.2% of all contacts were located in the SV, and that those translocations were more common for individuals with decreased speech performance (across groups). In the present study, no correlation was found between mean speech performance and the number of electrodes located in the SV; however, the sample size in this study was small compared to Holden et al. (2013), and there were very few electrodes in SV in this population.

To further compare with previous studies, angular insertion depth of the basal-most electrode was evaluated relative to mean speech performance. A correlation was not observed in the present data set, which does not replicate the findings of Finley et al (2008) or Holden et al (2013), who observed poorer speech scores associated with deeper angular insertions. However, the present results are consistent with the findings of a recent study evaluating six position-related variables; neither angular insertion depth nor electrode-to-modiolus distances were related to speech outcomes (van der Marel et al., 2015). Though these comparisons are interesting, they should be interpreted with caution, primarily due to the small sample size in the present study. Additionally, in the present study, a closed set task was used and subjects were relatively good performers, whereas in the study by Holden and colleagues (2013), open-set monosyllabic words were used and a wider range of speech perception scores was observed.

Clinical Implications

A recent study used CT imaging data and a computational model as a basis for deactivating electrodes (Noble et al., 2013). When a subset of channels that were estimated to be highly interactive were deactivated, significant improvements on both objective and subjective

tasks was observed. The results of the present study suggest that similar programming manipulations should be explored to determine if recommendations could be made based on sQP thresholds or ECAP measures. The ECAP measures may be advantageous over the behavioral and/or CT measures in that peak amplitude and channel interaction functions appear differentially sensitive to electrode position and neural status. With this combined information, perhaps clinical management strategies could be tailored to the underlying cause of a poor electrode-neuron interface. For instance, if an electrode is located far from the modiolus, current focusing may aid in increasing its effectiveness. If an electrode is located near a dead region, frequency re-allocation or channel deactivation may be the best method for optimal stimulation. Future studies are needed to examine the relationship between ECAP peak amplitude, CIF overlap and speech perception, using programs tailored in this manner.

E. Conclusions

The electrode-neuron interface likely contributes to the variability observed in speech performance in cochlear implant listeners, and thus should be explored with the aim of improving current programming techniques. Current clinical approaches are time consuming, potentially costly, or expose listeners to radiation. The ECAP may serve as an alternative to these approaches and has the benefit of measurement without the active engagement of the listener.

The present study showed a moderate association between focused behavioral thresholds and the peak amplitude of the ECAP, which may be useful if small peak amplitude is related to a degraded neural status. Large electrode-to-modiolus distance and wide ECAP ERB were also correlated, indicating that electrodes far away from the neurons are likely to have more channel interaction. Those findings suggest that the placement of the electrode array may have an effect on the degree of spread of excitation that occurs, and that ECAP CIFs may be a tool to assess

those factors. Additionally, scalar location may be an important causal influence on these relationships, with electrodes in the ST more likely to have smaller electrode-to-modiolus distances, which can lead to lower thresholds and narrower CIFs. Speech performance was also associated with focused thresholds and ECAP peak amplitude. If ECAP peak amplitude is taken as a proxy for neural health, this highlights the potential utility of this measure as a predictor of implant outcomes.

In conclusion, different aspects of ECAP measures relate to different aspects of the electrode-neuron interface, and specifically, ECAP peak amplitude may be sensitive to neural status. It is possible that examining both ECAP peak amplitude and spatial extent of channel interaction may provide a more efficient and holistic approach to evaluating the electrode-neuron interface than the current clinical methods.

Chapter 3 : Psychophysical tuning curves as a correlate of electrode position in cochlear implant listeners

Accepted as:

DeVries LA and Arenberg JG. Psychophysical Tuning Curves as a Correlate of Electrode Position in Cochlear Implant Listeners. *Journal of the Association for Research in Otolaryngology*. Forthcoming 2018.

A. Introduction

Cochlear implants (CIs) are neural prostheses that provide auditory input to people with severe-to-profound hearing loss. Outcomes are highly variable across listeners; performance on word and sentence tests ranges from 0% to 100% (Koch et al. 2004; Won et al. 2007; Holden et al. 2013). A potential source of this high variability is the electrode-neuron interface (ENI), which includes peripheral components such as: electrode position, bone and tissue growth, and the integrity of remaining spiral ganglion neurons (Bierer 2010; Pfingst et al. 2011; Long et al. 2014). Computational modeling, CT imaging, electrophysiological, and behavioral studies have demonstrated that behavioral thresholds are higher and spatial spread of excitation is broader for electrodes distant from target spiral ganglion neurons, or those that may be near degenerated neurons (Goldwyn et al. 2010; Long et al. 2014; Kalkman et al. 2015; DeVries et al. 2016). Broader spread of excitation increases channel interaction, or overlapping areas of neural activation, which may lead to poorer spectral resolution and decreased word understanding (e.g., Abbas et al. 2004; Hughes & Stille 2008; Jones et al. 2013).

Animal studies have demonstrated that long-term deafness results in smaller evoked potential responses and fewer surviving spiral ganglion neurons (Smith & Simmons 1983; Hall 1990; Shepherd & Javel 1997; Ramekers et al. 2014). Human temporal bone studies have *directly* measured spiral ganglion survival rates in both non-CI and CI listeners, with rates ranging from 4-100% survival (e.g. Hinojosa & Lindsay 1980; Linthicum et al. 1991; Khan et al. 2005b). Others have studied potential *indirect* measures of neural health in CI listeners, such as behavioral thresholds (Long et al. 2014; Zhou & Pfingst 2016). Despite this, it is not currently possible to directly assesses neural health *in vivo* in CI listeners.

Using CT imaging techniques, one can directly estimate a different component of the ENI—electrode position. CT imaging provides information including, but not limited to: electrode-to-modiolus distance, scalar location, insertion angle, and wrapping factor (Verbist et al. 2005; Skinner et al. 2007; Teymouri et al. 2011; Holden et al. 2013). By quantifying this aspect of the ENI, deductive inferences may be made about neural status local to each electrode. Thus, disambiguating different aspects of the ENI may provide important information about the functional capacity of a given implant channel, which may have a direct effect on success with the device.

While CT imaging may offer insight into the ENI, this technique has notable disadvantages, such as: high costs, exposing patients to radiation, no direct information about neural status, and limited availability. Therefore, an alternative method to measure electrode position is needed. A recent study in our laboratory compared aspects of electrode position to the electrically-evoked compound action potential (ECAP); however, in that study many participants did not have measureable ECAPs, or responses were noisy due to large stimulus artifact (DeVries et al 2016). Therefore, evaluating a more reliable measure of channel interaction, such as the psychophysical tuning curve (PTC), is warranted.

Bierer and Faulkner (2010) demonstrated that broad PTCs were correlated with higher behavioral thresholds using focused stimulation, such that channels with higher thresholds had broader spatial tuning; these findings echoed those of Nelson and colleagues (2008) with bipolar stimulation. These studies suggest that focused PTCs may capture site-specific variations in spatial tuning. However, the use of PTCs has not been explored to estimate electrode-to-modiolus distance in CI listeners. Furthermore, PTCs have not been fully characterized across the electrode array, as most studies have examined a small subset of electrodes due to the lengthy

testing time required with traditional psychophysical methods (e.g. Nelson et al. 2008; 2011). The present study used a faster method for obtaining focused PTCs based on a Békésy-like sweep procedure recently used for measuring focused thresholds in CI listeners (Bierer et al. 2015).

In broad terms, this study aims to assess: (1) the viability of using PTCs as a site-specific measure of channel interaction, (2) if measures of electrode position allow for inferences about neural status, and (3) insight into the identification and assessment of poor ENIs.

Specifically, we quantify the relationship between PTC bandwidths, focused behavioral thresholds, and electrode-to-modiolus distances. We predict that channels with broader PTC bandwidths will have: 1) larger electrode-to-modiolus distances, 2) scalar locations outside of scala tympani, and 3) higher focused thresholds. Other comparisons between focused behavioral thresholds, electrode-to-modiolus distance, scalar location, PTC tip location, and word recognition were made.

These findings may help advance understanding of the complexities of the ENI and how site-specific measures of channel interaction relate to word recognition.

B. Methods

Subjects

Thirteen adult subjects who were unilaterally implanted after 2001 with Advanced Bionics HiRes90k devices participated (Table 3-1). Subjects were at least 21 years of age (M = 62.8, SD = 15.3), and eight were males. Two subjects were pre-lingually deafened (diagnosed with severe to profound hearing loss before the age of 4), one was peri-lingually deafened (diagnosed with severe to profound hearing loss at age 4), and the remaining ten were post-lingually deafened. Two subjects were deafened in childhood (S54, age 7, and S46, age 14), but are still considered

with the post-lingually deafened subjects as they learned language before they were diagnosed with a severe-to-profound hearing loss. All subjects were fluent English speakers. Each participant provided written consent, and the experiments were conducted in accordance with guidelines set by the University of Washington Human Subjects Division.

Table 3-1: Demographic information for all 13 subjects including: ear implanted, chronological age, age diagnosed with a profound hearing loss, age at implantation, duration of deafness, etiology (if known), electrode array type and electrode spacing, and CNC word score.

ID	Ear	Age	Age @ Profound HL	Age Implanted	Duration of Deafness (years)	Etiology	Electrode Array/Spacing (mm)	CNC Word Score (%)
S22	R	77	55	66	11	Suspected Genetic	1J Helix/0.85	50
S29	L	86	47	77	30	Noise	HiFocus 1J/1.1	76
S40	L	55	4	50	46	EVA	HiFocus 1J/1.1	20
S42	R	67	50	50	0	Idiopathic	HiFocus 1J Pos./0.9	93
S43	R	71	50	67	17	Noise	Mid-Scala/0.85	78
S46	R	66	14	62	48	Unknown	HiFocus 1J/1.1	30
S47	R	68	28	37	9	Unknown	Mid-Scala/0.85	83
S49	R	44	1.5	43	41.5	Suspected Genetic	Mid-Scala/0.85	30
S53	R	54	1	44	43	Meningitis	1J Helix/0.85	84
S54	L	26	7	23	16	Suspected EVA	Mid-Scala/0.85	72
S55	R	63	41	49	8	Suspected Genetic	HiFocus 1J/1.1	92
S56	L	72	30	58	28	Idiopathic	HiFocus 1J Pos./0.9	76
S57	R	67	63	65	2	Idiopathic	Mid-Scala/0.85	62

CT imaging

CT scans were performed at the University of Washington Medical Center within the last three years. CT scans were analyzed at Washington University in St. Louis, MO. Briefly, ANALYZE software was used to create 3-dimensional image volumes by combining information from each subject's post-operative scan and a single body donor cochlea (for details, see Skinner et al. 2007; for verification of the method, see Teymouri et al. 2011). Pre-operative CT scans were not available for the subjects participating in the present study; therefore, a scan of the non-implanted ear was used to identify structural anatomy, and this image was co-registered with the image of the implanted ear. Micro CT and orthogonal-plane fluorescence optical sectioning

(OPFOS) images from a donor cochlea were used to locate and visualize the non-bony structures. The two CT-estimated metrics used in this study were electrode-to-modiolus distance and scalar location. Electrode-to-modiolus distance refers to the lateral distance (mm) of an electrode from the medial wall of the cochlea. Scalar location denotes the positioning of an electrode in the fluid-filled cochlear compartments: scala tympani (ST), intermediate, and scala vestibuli (SV). Intermediate refers to those electrodes that could not be clearly determined to be in ST or SV.

Electrical stimulation

All stimuli were presented using the Bionic Ear Data Collection System version 1.18.315 (Advanced Bionics, Valencia, CA). For behavioral testing, a custom Matlab (Mathworks, Inc. Natick, MA) script controlled the BEDCS software. Two types of electrode configurations were used in this study: monopolar (MP) and steered quadrupolar (sQP). MP stimulation consists of an active intracochlear electrode and a return extracochlear electrode; the large distance between the source/sink yields a broad electrical field. sQP stimulation was used in the present study as it has been found to be equivalent to partial tripolar in another study, in which many of the same subjects participated (Bierer et al. 2015). sQP stimulation consists of four intracochlear electrodes: the two middle electrodes serve as active electrodes, and the two outer electrodes serve as return electrodes for a fraction of the active current (an extracochlear electrode carries the remainder of the return current). Current is steered between the two middle electrodes according to the fraction, α: a value of 1 steers current to the basal electrode and 0 to the apical electrode. By convention, channel number is defined as the basal active electrode when $\alpha = 1$. In the present study, this convention was maintained for electrodes 3 to 15. For electrode 2, however, it was necessary to use the same set of electrodes as channel 3 (the most apical channel

possible with the 4-electrode sQP configuration) in conjunction with an α value of 0 to center the current on electrode 2. This arrangement is referred to as "channel 2," even though electrode 2 is the apical active electrode. For current focusing, the outer two electrodes in the sQP configuration receive a fraction of the return current according to σ (Landsberger & Srinivasan 2009; Srinivasan et al. 2010; Bierer et al. 2015). As with the commonly used partial tripolar configuration, higher σ results in a narrower electrical field than MP stimulation (Litvak et al. 2007). A value of $\sigma = 0.5$ was used in the present study for masker stimulation to retain sufficiently focused stimulation while avoiding unreasonably high current limits and side-lobe activation. For the shorter duration probe stimulation, an σ value of 0 (monopolar) was used to ensure the probe stimulus was salient to the listener. MP stimulation was used for probe stimuli, rather than sQP stimulation, because the high current requirements to achieve most comfortable level (MCL) for a very brief pulse train were often unobtainable within the compliance limits of the device with sQP; further, some subjects could not perceive the probe stimulus using the more focused sQP stimulation. A fixed probe level measured in percent dynamic range was used to facilitate direct comparisons of PTCs across electrodes and subjects (McKay 2012).

Most comfortable listening levels

MCLs were measured for use in the PTC procedure, described below. MCLs for masker and probe stimuli were determined using the Advanced Bionics clinical loudness scale (Advanced Bionics, Valencia, CA). To determine MCL, current level was increased manually until subjects reported a loudness rating of "6," or "most comfortable." The level was changed in 2 dB steps until a loudness rating of 4 was reached; thereafter the level was changed in 0.5 or 0.1 dB steps, depending on subject response. Device compliance limits were not reached for any subject. MCLs served as the maximum stimulus level for all psychophysical procedures.

Single-channel behavioral thresholds

Single-channel thresholds were measured for electrodes 2—15 using the sweep threshold procedure (Bierer et al., 2015). Stimuli were biphasic, cathodic-leading pulses trains (102 μs/ph, 0-μs interphase gap, 200.4 ms duration, 997.9 pulses per second) using sQP stimulation with σ = 0.9; highly focused thresholds were measured to capture local variability for later comparison with PTC measures. Pulse trains were presented starting at 6 dB below the MCL, with α-value increasing from 0 to 1 in 0.1 steps from electrode 2-15 for a *forward* sweep (apical to basal), and from 15-2 (basal to apical), for a *backward* sweep (based on Sek et al. 2005; for details, see Bierer et al. 2015). A forward and backward sweep was run for each set of stimuli and averaged to estimate thresholds. Device compliance limits were not reached for any subject during threshold measurement. Sweep thresholds served as the minimum stimulus levels for all psychophysical procedures.

Sweep psychophysical tuning curves

Single-channel behavioral thresholds were measured for masker and probe stimuli using sQP stimulation and the threshold sweep procedure (Bierer et al. 2015). Stimuli were biphasic, cathodic-leading pulse trains (102 μs/ph, 0-μs interphase gap, 997.9 pulses per second), presented to electrodes 2—15 (apical to basal), for both masker (200.4 ms duration) and probe (20 ms duration) stimuli. Masker stimuli were presented with sQP stimulation using an σ = 0.5; probe stimuli used σ = 0. These thresholds determined the lower limit of stimulation, and the MCLs determined the upper limit.

PTCs were obtained for all available electrodes within a forward-masking paradigm using a modified threshold sweep procedure (Figure 3-1a; Bierer et al. 2015). This procedure is similar to the sweep threshold procedure (see Single-channel behavioral thresholds section),

though in this case the masker was swept across the electrode array, varying in level, while the probe remained fixed in level and location. Each PTC sweep took approximately 6 minutes, with a total of 24 minutes per electrode for a complete PTC. Probe stimuli were presented at 30% probe dynamic range when possible; for some subjects, the level was increased to 40-50% dynamic range due to some subject's inability to do the task with the probe at a softer level. Probe levels were set as a percentage of the probe dynamic range to ensure that the stimuli were consistently soft and equally loud across all probe electrodes (McKay 2012). Masker levels were normalized to the percentage of the masker dynamic range, which reduces variability and allows for ease of comparison across all probe electrodes and subjects.

The listener was presented with a box on the computer screen and instructed to hold down the space bar when they heard the target sound (probe) and release the space bar when they no longer heard it. This procedure was repeated until all available electrodes served as probes. Two subjects, S40 and S49 had difficulty with the sweep PTC procedure; they were unable to hear the probe in the presence of the masker, even at higher levels and at longer masker-probe intervals. In those cases, a two-interval, two-alternative, forced choice (2IFC) procedure, identical to that used by Bierer and Faulkner (2010) was used for all electrodes to explore the central hypothesis. A recent study by Bierer and colleagues (2015) did not find any systematic differences between 2IFC thresholds and the threshold sweep procedure, which allows for significantly faster collection of psychophysical data.

PTC quantification

PTCs were characterized as a function of masker level, normalized to the masker-alone dynamic range. The equivalent rectangular bandwidth (ERB_{DR}) was used to quantify the spatial extent of masker-probe interaction by equating the PTC to a rectangular function of equivalent minimum

masker level (Figure 3-1b). It was calculated by dividing the area above the PTC by the minimum masker level (PTC tip). This is a commonly used method in psychoacoustics, which avoids selection of a fixed masker level from which a PTC bandwidth is often derived. PTCs with probes near the end of the electrode array (typically electrodes 2 and 15) were not fully characterized on one side due to the lack of electrodes to use as maskers. Partial tuning curves were defined as those for which the tip of the PTC was determined to be at the end of the electrode array. Under the assumption that neural excitation would extend to neurons beyond the array, partial tuning curves were completed by mirroring the masker levels from the measured data on the side with a full complement of masker electrodes.

PTC tip shifts were quantified to examine the relationship between suspected areas of poor neural health and electrode position. For each subject, two runs of PTC sweeps were collected. One run consists of a forward and backward sweep. The difference between PTC sets was calculated and averaged to assess within-subject variability between sweep sets. This resulted in an individual criterion cut-off for what was considered a tip shift. For example, if there was a 15% mean difference between PTC sets, a greater than 15% difference between the masker level at the probe and the tip (the minimum masker level), was considered to be a tip shift. Table 2 shows the tip shift criterion used, standard deviation between PTC sets, and number of tip shifts for each subject. There were 39 tip shifts out of the 182 PTCs. There were eight PTCs with tips shifted by more than one electrode. There were 19 apical and 20 basal tip shifts in this dataset. The tip shifts were collapsed across electrodes and are reported as “tip shift” or “no tip shift” and analyzed as a binary variable.

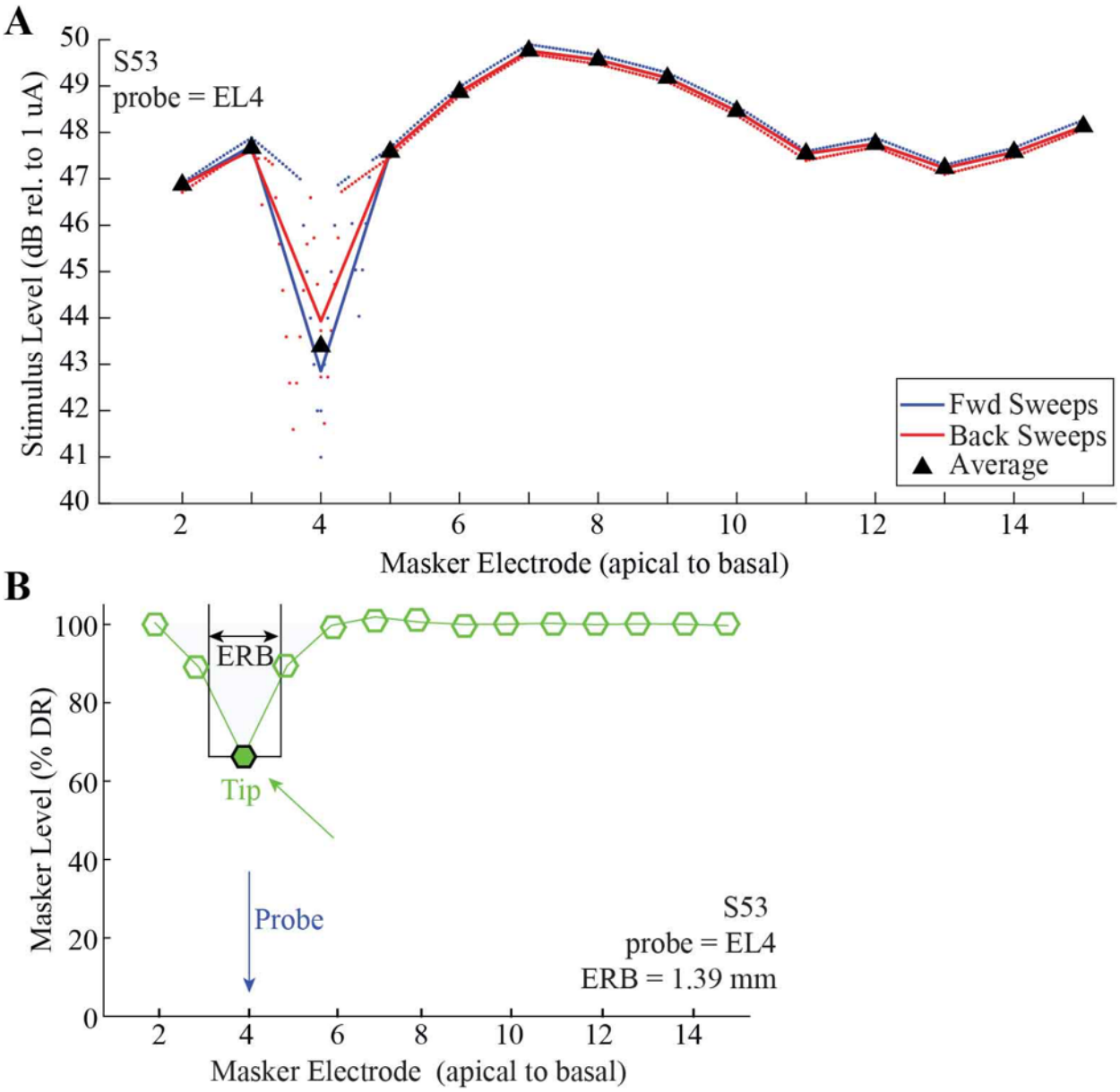

Figure 3-1: A: Example of one forward (blue) and one reverse (red) sweep for S53, probe 4. The x-axis is masker electrode (apical to basal), and the y-axis is stimulus level (dB rel. to 1 μA). The black triangles represent the mean masker level for each of the cardinal electrodes. B: Example PTC for S53, probe 4. The x-axis is masker electrode (apical to basal), and the y-axis is masker level (percent dynamic range). The PTC ERB_{DR} is labeled (black rectangle), and the PTC ERB_{DR} value is marked inside the plot. The PTC tip (filled green circle) and probe electrode (blue arrow) are also labeled.

Table 3-2: Individual mean difference (% masker DR) and standard deviation between two sets of PTC sweeps. For S40 and S49, the values were calculated by comparing each run from the 2IFC procedure. The mean differences are used as criterion for whether a PTC tip shift occurred.

ID	Mean Diff (%DR)	SD (+/-)	# of Tip Shifts
S22	12.3	0.09	5
S29	12.5	0.12	4
S40	11.5	.08	4
S42	19.5	0.25	4
S43	18.1	0.15	3
S46	17.9	0.16	4
S47	12.6	0.09	1
S49	11.9	.08	4
S53	14.8	0.18	2
S54	13.7	0.11	2
S55	8.9	0.08	4
S56	9.3	0.08	1
S57	13.5	0.11	1

Word recognition

Scores on a word recognition task were obtained to evaluate clinical performance in the context of sQP threshold, electrode-to-modiolus distance, and PTC ERB_{DR}. Performance on the Consonant-Nucleus-Consonant (CNC) words were obtained from each subject's clinical audiologist. Per audiologist report, the CNC words were presented at 60 dB-SPL in the sound field using the subject's everyday speech processor program. For subjects S46 and S49, the only scores available from the audiologist were in the bimodal condition; therefore, they were tested in the laboratory in the CI-only condition at 60 dB-SPL in the sound field using the subject's everyday speech processor program. All scores were from within the last two years and are reported in Table 1.

Statistical analysis

SPSS statistical software was used to perform linear mixed effects analyses for between-subjects comparisons (IBM Corp. Released 2015. IBM SPSS Statistics for Windows). The first analysis assessed whether PTC ERB_{DR}s measured with the 2IFC procedure (used for S40 and S49) significantly differed from those subjects who used the modified threshold sweep procedure. This analysis showed no significant effect of psychophysical task on PTC ERB_{DR}s ($F(20.3) = .18$, $P = .68$); therefore PTC ERB_{DR}s from both tasks were compiled in all following statistical models.

The first model included sQP threshold as the dependent variable, electrode-to-modiolus distance as the independent variable of interest, and duration of deafness as a covariate. The second analysis included PTC ERB_{DR} as the dependent variable, with sQP threshold, and electrode-to-modiolus distance as fixed factors, and duration of deafness as a covariate. Duration of deafness was added as a continuous covariate in these models due to the presence of two pre- (S49, S53) and one peri-lingually (S40) deafened subject in this dataset; these three subjects have similar durations of deafness (41.5, 43, and 46 years, respectively). Additional linear mixed effect analyses were conducted to evaluate the effects of scalar location (dependent ordinal variable) on sQP threshold, electrode-to-modiolus distance, and PTC ERB_{DR}. For all mixed effects models, electrode was added as the repeated factor, and subjects were entered as a random factor, so that each subject had their own intercept and by-subject random slopes for the effects of interest (Baayen et al. 2008). A Bonferroni correction was applied to all multiple comparisons and is noted where appropriate.

A Generalized Estimating Equations (GEE) procedure was performed to evaluate the presence of a tip shift (dependent binary variable) on sQP threshold, electrode-to-modiolus distance, and PTC ERB_{DR} (independent continuous variables). The GEE procedure extends the generalized linear model to allow for a repeated measures analysis on a binary dependent variable (IBM Corp. Released 2015. IBM SPSS Statistics for Windows); reported results are from a Wald's test.

A multiple linear regression analysis was performed to evaluate the relationship between clinical CNC scores and mean electrode-to-modiolus distance, mean sQP threshold, and mean PTC ERB_{DR}.

C. Results

Electrode-to-modiolus distance using CT imaging

Figure 3-2 highlights the variability in electrode array positioning observed in 3D cochlear reconstructions for all subjects, arranged by electrode array type. In general, the electrode trajectories in Figure 3-2 are consistent with the designs of the four types of arrays, which partially determine how far the electrodes are from the modiolus, and thus how close they are to target auditory neurons. The 1J electrode array (S29, S40, S46 and S55) has a lateral design, whereas the 1J Helix (S22, S53) is pre-curved to achieve a more medial position.

The 1J with positioner (S42, S56), by design, pushes the electrode array even more medially.

The Mid-Scala array (S43, S49, S47, S54, S57) is pre-curved, and designed for mid-scalar placement to protect cochlear structures.

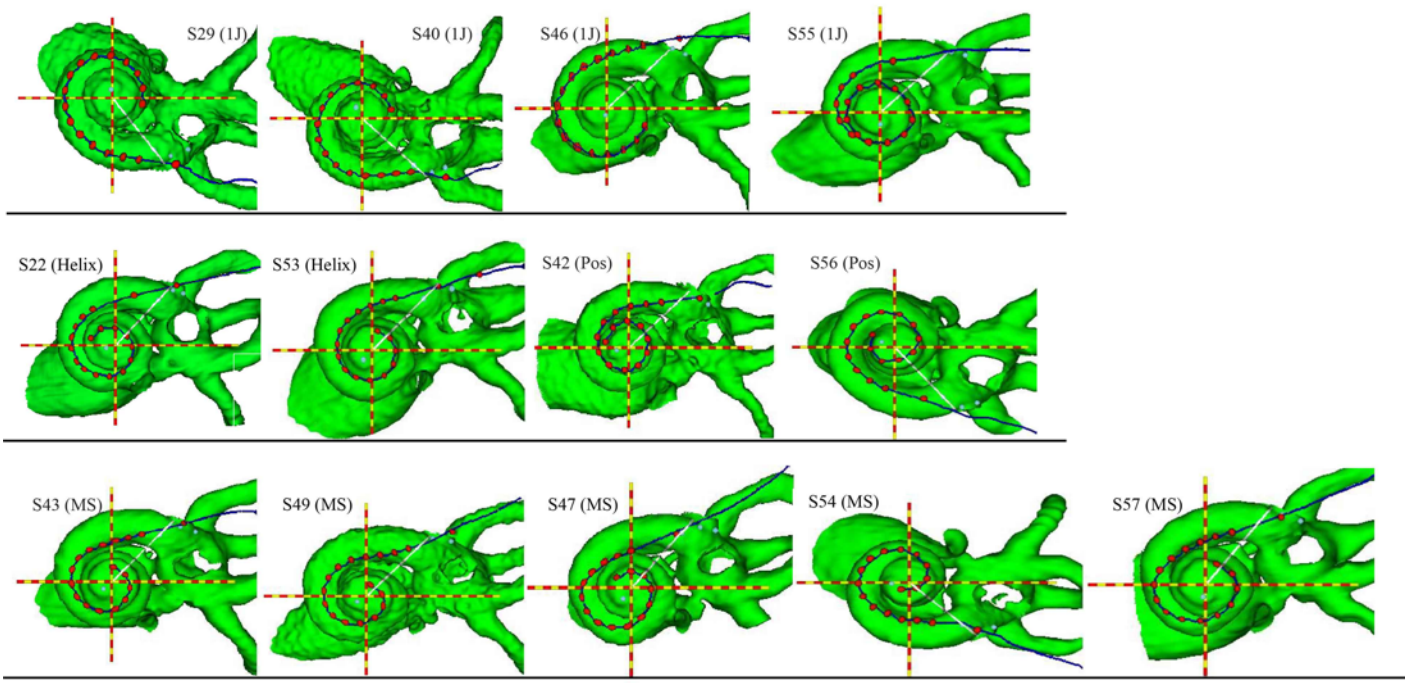

Figure 3-2: CT view of cochlea and electrode array along the midmodiolar axis(red and yellow dashed line), for all subjects, organized by electrode array type. The evenly spaced red dots represent electrodes; the outermost dot represents the insertion depth marker. The white line represents the 0-degree reference point from which insertion depth is measured, extending from the midmodiolar axis. Row 1: 1J; Row 2: 1J Helix and 1J with positioner; Row 2: MidScala electrode array.

Focused behavioral thresholds and electrode-to-modiolus distance

Figure 3-3a shows electrode-to-modiolus distance (left ordinate) and sQP threshold (right ordinate) profiles for each subject. Scalar location is indicated by symbol (see legend). sQP thresholds ranged from 28.8-55.7 dB rel. to 1μA (M = 45.67 dB rel. to 1μA, SD = 6.12) across all subjects and electrodes (Table 3-3). Electrode-to-modiolus distance, or the lateral distance in millimeters from the modiolus, ranged from 0.18-2.2 mm (M = 1.06 mm, SD = .52; see Table 3-3). Figure 3-3b illustrates the relationship between sQP threshold and electrode-to-modiolus distance, with individual subject data distinguished by color and shape; the line of best fit for all subjects is plotted (solid black). Figure 3-3c shows the line of best fit for individual subjects, as well as the group line of best fit (solid black). Consistent with previous studies (Long et al., 2014; Cohen et al., 2003), a strong association between sQP thresholds and electrode-to-modiolus distance was observed. Results from the linear mixed effects analysis show a significant, predictive relationship between electrode-to-modiolus distance and sQP threshold ($F(1,170.5) = 57.33$ $P < .001$); in other words, across subjects, electrodes with higher behavioral thresholds tended to be further from the modiolus. It is worth noting that for the six subjects where this relationship was observed (S42, S43, S47, S49, S53, S57), four have the Mid-Scala electrode array; the other two subjects have a 1J with positioner and a 1J Helix array. For subjects with the 1J array (S29, S40, S46, S55), which tends to sit laterally to the modiolus, electrode-to-modiolus distance did not predict sQP threshold, likely due to low variability in electrode position in this data set. Due to the small sample size for each electrode array, statistical differences between array types cannot be further examined.

While duration of deafness significantly contributed to this relationship ($F(11.6) = 15.4$ $P < .001$), duration of deafness did not dictate whether a correlation between sQP threshold and

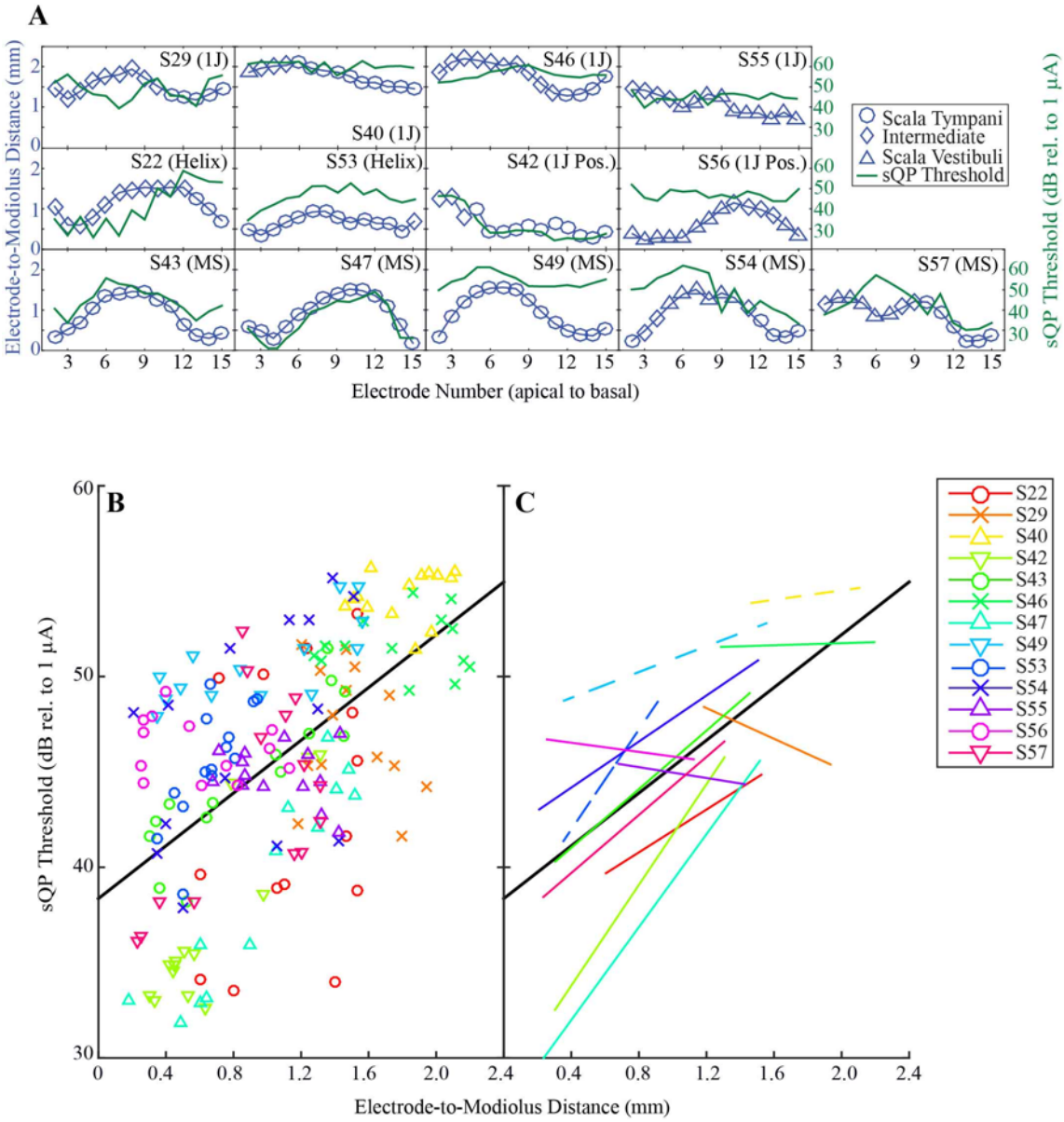

Figure 3-3: A: sQP threshold in dB rel. to 1 μA (green line) and electrode-to-modiolus distance in mm (blue line) for all subjects, organized by electrode array type. Scalar information is represented by symbols along the electrode-to-modiolus distance line: ST (circles), Intermediate (diamonds), and SV (triangles). B: Scatter plot comparing electrode-to-modiolus distance with sQP threshold for individual subjects (distinguished by color) and the line of best fit for all subjects (solid black line). C: The line of best fit for individual subjects for the data in panel B (lines distinguished by color), and for all subjects (solid black line).

electrode-to-modiolus distance *existed*. Those subjects with longer durations of deafness tended to have higher thresholds overall, but this did not preclude a significant, positive correlation with electrode distance; the line of best fit was simply shifted up the y-axis for these subjects.

Table 3-3: Means and standard deviations for electrode-to-modiolus distance, sQP threshold, and tuning equivalent rectangular bandwidth (ERB); data shown are for electrodes 2—15. Threshold-distance RMS error, number of tip shifts, and %DR used for PTCs are also listed. The summary line indicates means and standard deviations across subjects.

ID	EMD (mm) mean *(sd)*	Focused Thres. (dB) mean *(sd)*	Tuning ERB (mm)	Threshold-Distance RMS Error	%DR for PTCs
S22	1.12 *(.37)*	42.72 *(6.92)*	2.14 *(1.14)*	6.22	30
S29	1.52 *(.23)*	47.15 *(3.32)*	3.70 *(1.37)*	3.31	40
S40	1.79 *(.22)*	54.27 *(1.30)*	5.40 *(2.40)*	1.32	50 (2IFC)
S42	.64 *(.33)*	36.96 *(4.80)*	3.07 *(1.73)*	2.3	30
S43	.84 *(.44)*	44.69 *(3.95)*	3.09 *(1.48)*	1.9	40
S46	1.80 *(.34)*	50.67 *(1.58)*	5.51 *(2.23)*	1.59	30
S47	.87 *(.46)*	38.39 *(5.91)*	2.61 *(.76)*	2.08	30
S49	.94 *(.47)*	50.70 *(2.15)*	2.85 *(1.02)*	1.49	40 (2IFC)
S53	.66 *(.17)*	45.41 *(3.01)*	2.30 *(.96)*	2.09	30
S54	.89 *(.46)*	47.14 *(5.77)*	3.16 *(1.43)*	5.27	50
S55	1.06 *(.26)*	44.88 *(1.47)*	5.81 *(1.74)*	1.48	40
S56	.62 *(.33)*	46.26 *(1.53)*	4.51 *(2.62)*	1.53	30
S57	.90 *(.39)*	43.39 *(4.32)*	2.89 *(1.27)*	4.58	30
Summary	1.06 *(.52)*	45.68 *(6.13)*	3.62 *(2.01)*	N/A	N/A

Psychophysical tuning curve characteristics

There was wide variability observed in the PTCs within and across subjects. Across subjects, PTC ERB_{DR}s ranged from 0.70-10.40 mm, with a mean of 3.62 mm (*SD* = 2.01; Table 3-3). There was a total of 39 tip shifts out of 182 PTCs; S22 had the greatest number of tip shifts at five (see Table 3-2). There was no apparent effect of apical or basal-ward tip shifts in the data. Figure 3-4 shows all 14 PTCs across the electrode array for three example subjects S56 (A), S57 (B), and S53(C). PTCs are plotted as masker level (% dynamic range) as a function of masker electrode (apical to basal). The mean PTC ERB_{DR} for these subjects is marked on each panel. There was a high degree of overlap, or presumed channel interaction, between PTCs within a given subject. This is particularly evident for S56 (Figure 3-4a), where most PTCs are overlapping, and some PTC tips (such as electrode 3) are shifted quite far basally, and some apically (electrode 5). S57 (Figure 3-4b) had quite deep PTCs, with few tip shifts; however, a high degree of PTC overlap is observed across the electrode array. S53 (Figure 3-4c) had

shallower PTCs apically, and deeper PTCs basally; there are more easily observable PTC tips and less channel interaction overall. Interestingly, though the PTC characteristics of these example subjects differ, their clinical performance is very similar (Table 3-1).

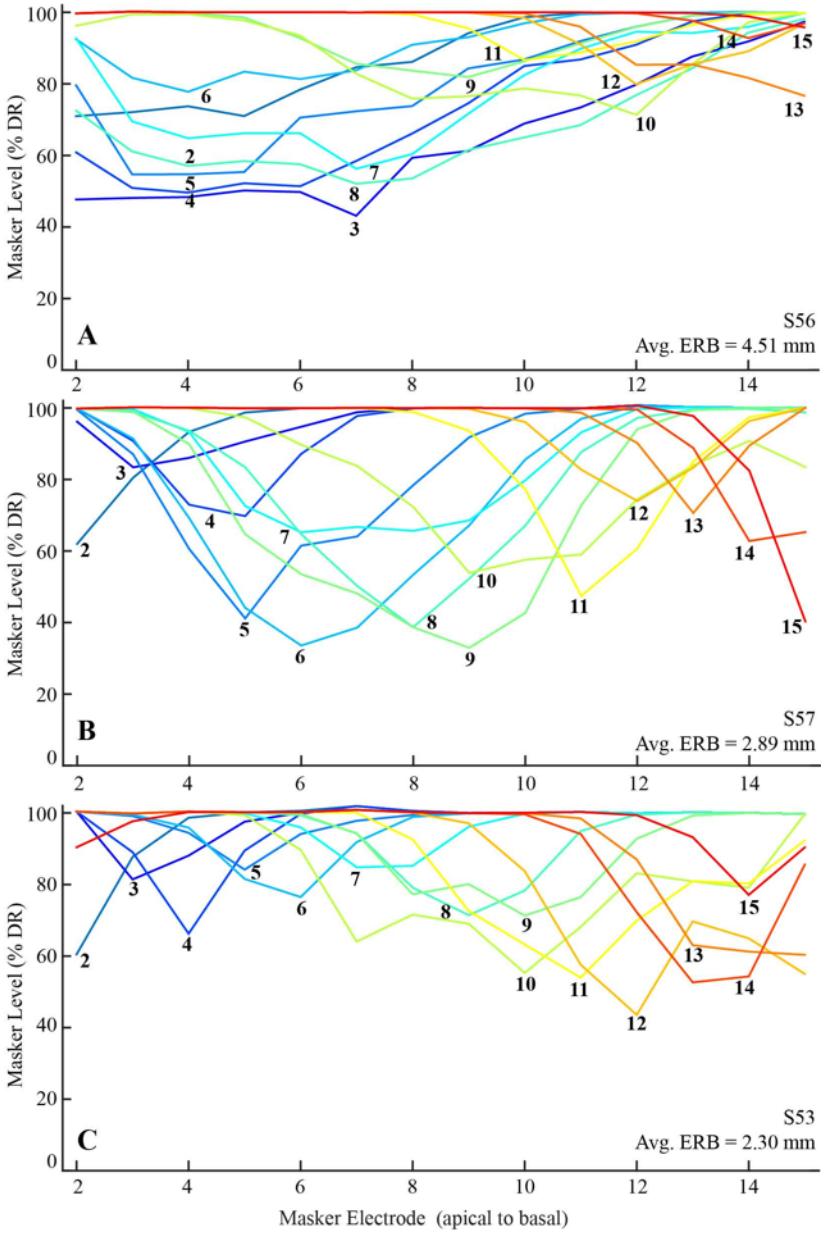

Figure 3-4: PTCs across the electrode array for 3 example subjects (S56, S53, and S57). The x-axis denotes the masker electrode (apical to basal). The y-axis represents the masker level in percent dynamic range. The numbered lines inside the plot are probe electrodes, labeled at the tip of the PTC. The mean PTC ERB_{DR} in mm is marked inside each plot.

Comparisons between focused thresholds, electrode-to-modiolus distances, and tuning curve bandwidths

Scatterplots of PTC ERB_{DR}s and electrode-to-modiolus distance (Figure 3-5a), and sQP thresholds (Figure 3-5c) are shown for all subjects, with individual data distinguished by color and shape. Figures 3-5b and 3-5d show the lines of best fit for individual subjects and the group (solid black line). Table 3-4 shows results for within-subject correlations for these comparisons. Results from the linear mixed effects analysis show PTC ERB_{DR}s are predictive of electrode-to-modiolus distance ($F(1,163.87) = 9.30$, $P = .003$). Although there was a trend toward higher sQP thresholds for broader PTC ERB_{DR}s, there was no statistically significant effect ($F(1,177.83) = 3.14$ $P = .08$). There was no effect of duration of deafness ($F(1,13.96) = .02$, $P = .89$). These results indicate that PTC ERB_{DR}s are broader for electrodes further from the modiolus, but that PTC ERB_{DR}s were not a reliable predictor of focused behavioral thresholds in these subjects.

Table 3-4: Individual Pearson's r and p-values for the correlations between PTC ERB_{DR}s and sQP thresholds (dB rel. to 1 μA), in the left two columns, labeled Threshold-ERB_{DR}, and between PTC ERB_{DR}s and electrode-to-modiolus distance (EMD; mm) in the right two columns, labeled as EMD-ERB_{DR} in the left two columns and electrode-to-modiolus distance in the right two columns (EMD; mm).

ID	*r* (Threshold-ERB_{DR})	*p* (Threshold-ERB_{DR})	*r* (EMD-ERB_{DR})	*p* (EMD-ERB_{DR})
S22	-.06	.83	.53	.05*
S29	-.45	.11	.81	.0004*
S40	-.18	.53	.47	.09
S42	.62	.02*	.70	.006*
S43	.53	.053	.66	.01*
S46	.20	.48	.17	.56
S47	.49	.08	.55	.04*
S49	.26	.36	.18	.55
S53	.51	.06	.19	.51
S54	.70	.006*	.21	.48
S55	.05	.87	.28	.34
S56	.26	.36	-.27	.35
S57	.69	.006*	.60	.02*

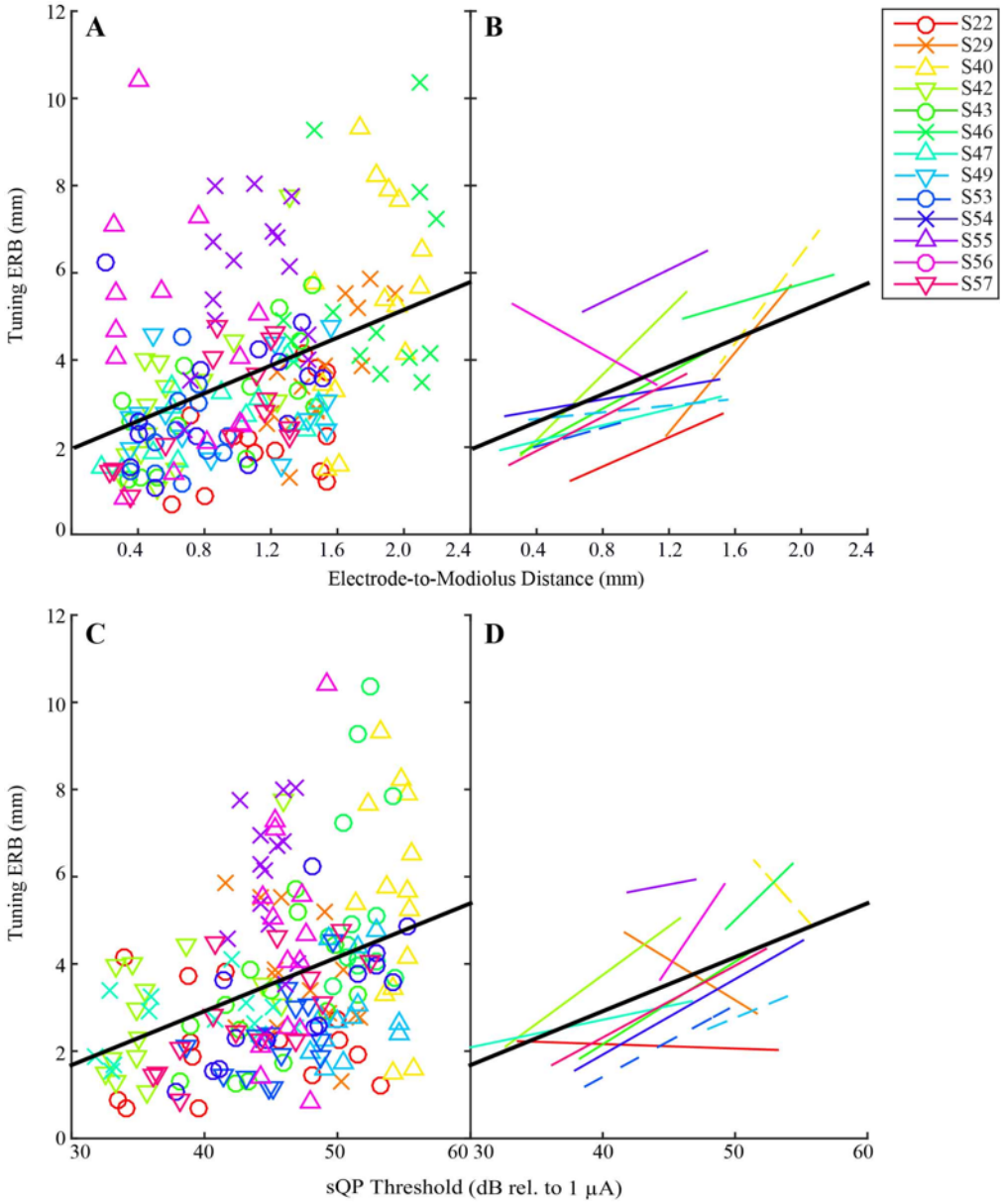

Figure 3-5: Comparisons between sQP threshold, electrode position, and PTC ERB_{DRS} for individual subjects.A: Electrode-to-modiolus distance and PTC ERB_{DR} individual data and group best fit line. B: Electrode-to-modiolus distance and PTC individual and group best fit lines C: sQP threshold and PTC ERB_{DR} individual data and group best fit line. D: sQP threshold and PTC ERB_{DR} individual and group best fit lines.

Scalar location

CT-estimated scalar location was assessed for all subjects and electrodes. Of 182 electrodes, 54.4% were in ST, the target scalar location during surgical implantation. Most of the other electrodes were estimated to be in the intermediate position (28%), with the remaining electrodes

in the SV (17.6%). Figure 3-6 presents box plots of the distribution of scalar location for: sQP threshold (A), electrode-to-modiolus distance (B), and PTC ERB_{DR} (C). Results from the linear mixed effects analysis show a main effect of scalar location for sQP threshold ($F(1.174.7) = 7.59$, $P = .001$) , electrode-to-modiolus distance ($F(1.177.31) = 18.93$, $P < .0001$), and PTC ERB_{DR} ($F(1,170.09) = 7.0$, $P < .01$).

After Bonferroni adjustment, results show that sQP thresholds were higher for electrodes in SV as compared to ST ($P < .0001$) and as compared to electrodes in the intermediate position ($P = .05$). There were no significant differences in sQP threshold between intermediate electrodes and those in ST ($P = .11$). As expected, electrodes located in either SV ($P = .003$) or the intermediate position ($P < .001$) had greater electrode-to-modiolus distances as compared to ST; there were no significant differences between electrodes in SV and the intermediate position ($P = .58$). As sQP threshold and electrode-to-modiolus distance was shown to be correlated in this study and others (Long et al 2014; DeVries et al 2016), these results indicate that for electrodes in SV, high sQP thresholds may be primarily driven by electrode position. PTC ERB_{DR}s were significantly broader for electrodes in SV ($P < .01$) as compared to ST but did not reach statistical significance when compared to electrodes in the intermediate position ($P = .06$). There were no significant differences in PTC ERB_{DR}s between intermediate electrodes and those in ST ($P = .19$).

It is important to interpret these analyses with caution. While the linear mixed effects analysis accounts for uneven sample sizes, the boxplots show that the distributions of the variables of interest tend to overlap substantially in many cases (particularly with sQP threshold). This may signify that the statistically significant effects observed are small in magnitude.

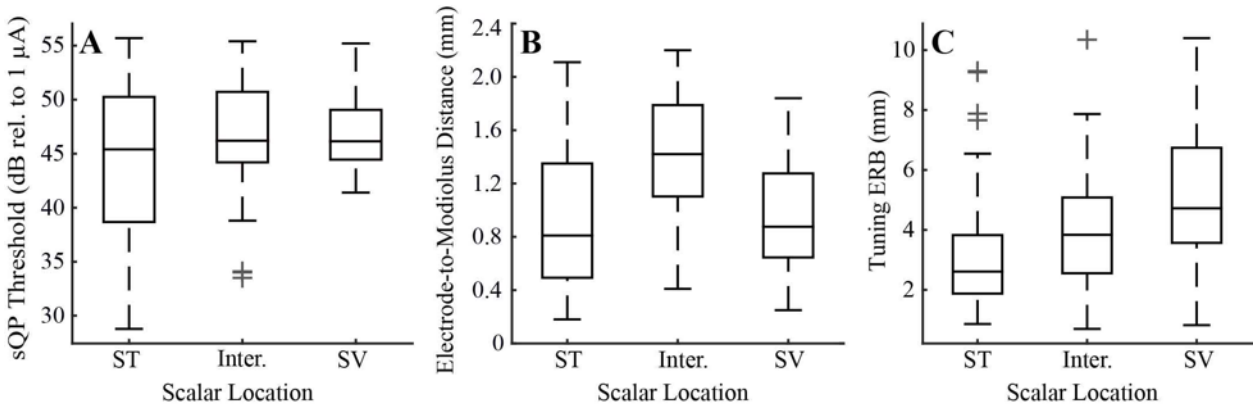

Figure 3-6: Box-and-whisker plots for the distribution of scalar location relative to: A: sQP threshold (dB rel. to 1 µA), B: electrode position (mm), and D: PTC ERB_{DR} (mm). Scalar location is labeled as: scala tympani (ST), intermediate, and scala vestibuli (SV).

Effect of PTC tip shifts

Results from the GEE procedure (see Statistical analysis) show no effect of tip shift for sQP threshold ($\chi^2 = 2.33$, $P = .13$; Figure 3-7a) or PTC ERB_{DR} ($\chi^2 = .50$, $P = .48$; Figure 3-7a). Interestingly, there was a significant effect of tip shift for electrode-to-modiolus distance ($\chi^2 = 7.35$, $P = .007$; Figure 3-7b), wherein electrodes with PTC tip shifts were likely to be positioned more lateral to the modiolus.

Further analyses were conducted to ascertain whether the number of within-subject tip shifts were correlated with high sQP thresholds *not* predicted by electrode-to-modiolus distance (quantified as greater than +1 SD above the mean). In other words, we examined whether high sQP thresholds *not* accounted for by electrode position were correlated with more tip shifts, and thus possibly indicative of poor neural health. However, a linear regression showed that tip shifts were not correlated with sQP thresholds +1 SD from the best fit line ($F(1,11) = 1.68$, $P = .22$).

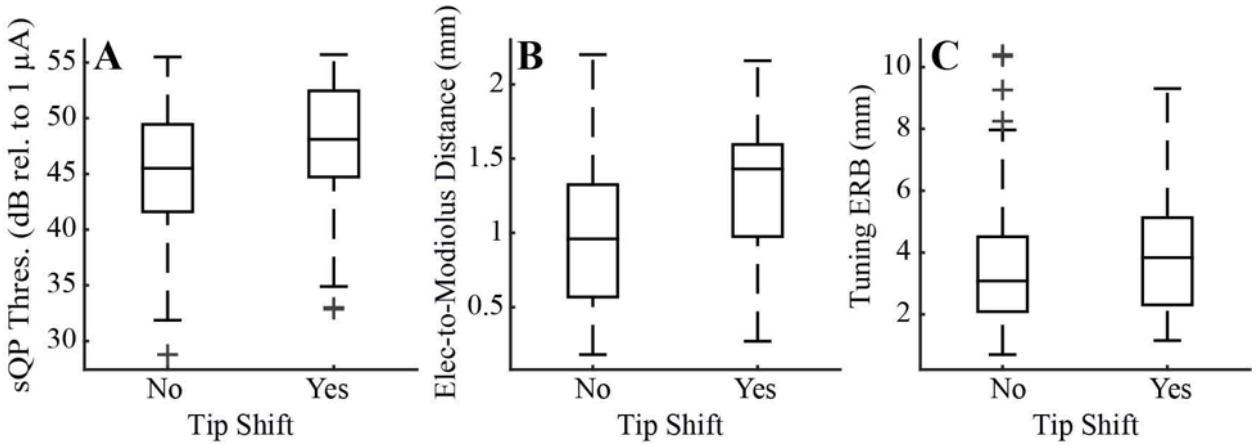

Figure 3-7: Box-and-whisker plots for the distribution of PTC tip shifts relative to A: sQP threshold (dB rel. to 1 µA), B: electrode position (mm), and D: PTC ERB$_{DR}$ (mm). Tip shifts are coded as either absent ("no") or present ("yes") or for all 182 PTCs in this data set.

Word recognition

Figure 3-8 shows mean performance on the CNC word test (% correct) in relation to mean sQP threshold (3-8a), mean electrode-to-modiolus distance (3-8b) and mean PTC ERB$_{DR}$ (3-8c). This set of predictors accounted for a significant amount of variance in CNC word scores (R^2 = .72, $F(3,9) = 7.56$, P = .008, $R^2_{adjusted}$ = .62). The model shows no significant effect of mean PTC ERB$_{DR}$ (T_{19} = 1.65, R = -.26, P = .13) or mean electrode-to-modiolus distance (T_{19} = -1.76, R = -.66, P = .11). sQP thresholds had a unique positive effect on CNC word scores (T_{19} = -2.86, R = -.76, P = .02), wherein subjects with higher mean sQP thresholds across the array tended to have lower CNC word scores.

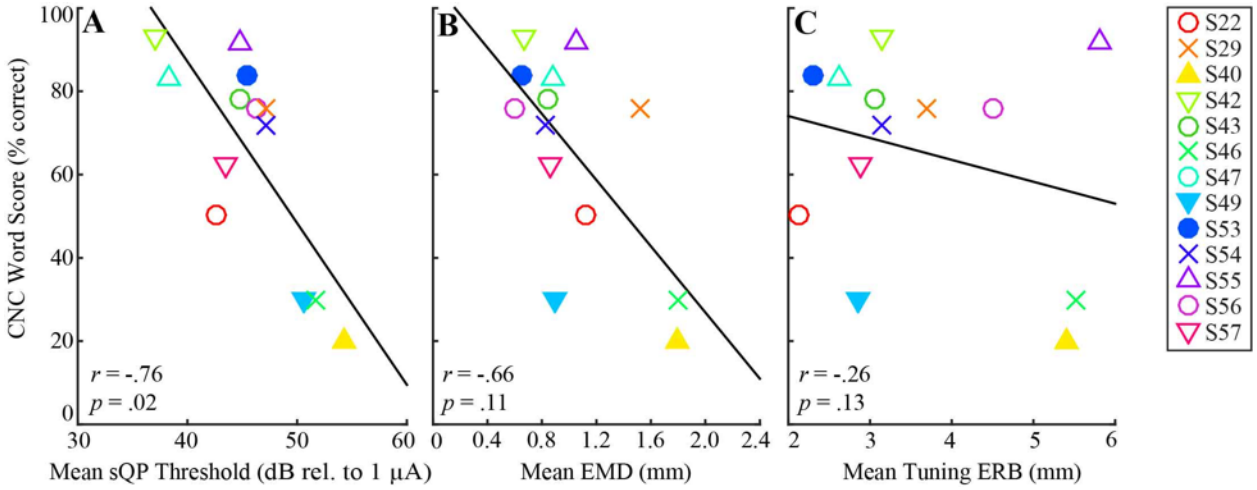

Figure 3-8: Correlations between the variables of interest and clinical CNC word scores(% correct). A: mean sQP threshold (dB rel. to 1 μA); B: electrode-to-modiolus distance (mm); and C: mean PTC ERB_{DR} (mm). The pre-/peri-lingually deafened subjects (S40, S49, and S53) are represented by filled in symbols, for ease of viewing.

D. Discussion

The present study assessed the relationship between PTC ERB_{DR}s, sQP behavioral thresholds and CT-estimated electrode position. Results support the hypothesis that electrodes farther from the modiolus tend to have: higher behavioral thresholds, broader PTC ERB_{DR}s, are translocated to SV, and a higher number of PTC tip shifts across the electrode array. There was no statistically significant relationship between sQP thresholds and PTC ERB_{DR}s or tip shifts. Mean sQP thresholds were predictive of word recognition, whereas mean PTC ERB_{DR}s and mean electrode-to-modiolus distances were not, indicating that sQP thresholds may capture an additional aspect of the electrode-neuron interface important for speech perception.

Focused single-channel behavioral thresholds and electrode-to-modiolus distance

Consistent with other studies, sQP thresholds were predictive of electrode-to-modiolus distance, such that electrodes with higher thresholds had larger electrode-to-modiolus distances (Cohen et al. 2001; Cohen 2009b; Long et al. 2014; DeVries et al. 2016). As duration of deafness increased, sQP thresholds tended to be higher, but this did not preclude a significant relationship with electrode-to-modiolus distance in some subjects. These findings are supported by

histological data (Kawano et al., 1998), computational modeling (Briaire & Frijns et al., 2006; Frijns et al., 1995; 1996; Goldwyn et al., 2010), and EABR thresholds in animals (Shepherd et al. 1993).

Figures 3-3b-c demonstrate that electrode-to-modiolus distance does not account for all the variability in sQP thresholds. It may be presumed that sQP thresholds not predicted by electrode-to-modiolus distance reflect areas with poor neural survival, though bone and tissue growth and tissue impedance may affect this relationship as well.

PTC bandwidths, electrode-to-modiolus distance, and focused single-channel behavioral thresholds

Electrodes with broader PTC ERB_{DR}s were predictive of electrodes located farther from the modiolus, consistent with previous studies that used electrophysiological (Brown et al. 1990; Cohen et al. 2003; Hughes and Abbas 2006b; DeVries et al. 2016) and modeling techniques (Briaire & Frijns et al. 2006). PTC ERB_{DR}s were *not* correlated with sQP thresholds, though results trended toward significance in the expected direction. This result is consistent with a recent study in our laboratory that used the electrically-evoked compound action potential (DeVries et al. 2016).

sQP thresholds likely capture the effects of electrode-to-modiolus distance *and* other factors such as neural status, which may explain the lack of relationship between sQP thresholds and PTC ERB_{DR}s. It is also possible that ERB_{DR}s are unable to capture this relationship. Other studies have used slopes or fixed widths to quantify PTCs (e.g. Nelson et al. 2008); comparisons between these methods will be made in a future study. We also used a monopolar probe and pTP masker, resulting in a lower degree of current focusing compared to another study that found a strong correlation between highly focused PTCs and behavioral thresholds (Bierer & Faulkner

2010). Finally, the use of %DR to set probe levels does not guarantee that the probes were equally loud for the listener, though PTC widths have been shown to be insensitive to probe level (Nelson et al. 2008; 2011). It may be this methodological "noise" in the PTC measure weakened the correlations between PTC ERB_{DR}s, sQP thresholds, and electrode-to-modiolus distance for some subjects.

Effects of scalar location

Electrodes translocated from ST to SV had higher sQP thresholds, greater electrode-to-modiolus distances, and broader PTC ERB_{DR}s (Figure 3-6), consistent with a recent study (DeVries et al. 2016). These results are reflective of the physical distance between electrodes located in ST and those in SV (Teymouri et al. 2011), which likely leads to increased current requirements and broader spread of excitation.

Shepherd and colleagues (1993) evaluated EABR thresholds in implanted adult cats at different scalar locations *within* ST. EABR thresholds were reduced when moving from lateral electrode placements to peripheral dendrite and spiral ganglion cell body positions. Frijns and colleagues (1995; 1996) extended this work using a computational model examining the same ST positions as the Shepherd study, with comparable results. These findings have also been observed in a guinea pig model (Snyder et al. 2004).

Some studies have found that a greater number of electrodes located in SV correlates with poorer CNC word recognition (Finley et al. 2008; Holden et al. 2013); however, we were unable to replicate that finding with these data. ($T_{12} = 1.07$, $P = .31$).

These results support the contention that ST is the ideal scalar location for electrode array insertion, although behavioral and electrophysiological variability is noted even *within* ST. Given previously observed relationships between scalar location and word recognition (Holden

et al. 2013), this underlines the importance of surgical technique and electrode array design to optimize implant insertions.

PTC tip shifts and electrode-to-modiolus distances

There were 39 tip shifts out of a possible 182 PTCs, with no evidence of a predominance of apical or basalward shifts, as seen by others (Nelson et al. 2008). PTC tip shifts were analyzed across subjects and electrodes in relation to sQP threshold, electrode-to-modiolus distance, and PTC ERB_{DR} (Figure 3-7).

There was no significant relationship between PTC tip shifts and sQP threshold or PTC ERB_{DR}s. This is inconsistent with other studies that have found electrodes with tip shifts tend to have broader PTCs (Nelson et al. 2008; Bierer and Faulkner 2010). It is possible we did not replicate this result due to the very small number of tip shifts larger than one electrode contact observed in this study; it may be that more dramatic tip shifts are needed to observe these relationships.

Electrodes farther from the modiolus tended to have more tip shifts; this is perhaps unexpected, as tip shifts are traditionally viewed as indicative of neural status. Bierer et al. (2010) measured forward-masked PTCs in the inferior colliculus of guinea pigs, and found PTC tips shifted toward the apex where the guinea pig cochlea tapers, causing the apical electrodes to be much closer to the modiolus. In the present study, it is possible that asymmetrical current spread occurred for electrodes further from the modiolus, due to the increase in current required to reach auditory neurons. This spread may have caused a small shift in the tip of the PTC, which was the predominant type of tip shift observed in this data set.

Word recognition

We observed a significant, negative correlation between mean sQP threshold and CNC word recognition in these subjects (Figure 3-8a), but no correlation with mean electrode-to-modiolus distance (Figure 3-8b) or mean PTC ERB_{DR} (Figure 3-8c).

Poorer word recognition in subjects with higher mean focused thresholds is consistent with a recent study in our laboratory (DeVries et al. 2016). However, this result has not been observed by others using bipolar (Pfingst et al. 2004) and phased array stimulation (Long et al. 2014). In the Long study, high within-subject variance for focused thresholds was negatively correlated with the logit-transformed CNC word scores, similar to the findings of Pfingst et al. 2004. We were unable to replicate these results using the within-subject variance of sQP thresholds and raw (T_{12} = .70, P = .50) and logit-transformed (T_{12} = .55, P = .59) CNC scores. Long also found that higher RMS error from the threshold-distance correlation was predictive of poorer logit-transformed CNC word recognition scores; subjects with thresholds *well-predicted* by electrode-to-modiolus distance tended to perform better with their implant. The present study did not replicate these results for either raw (T_{12} = .13, P = .90) or logit-transformed (T_{12} = -.07, P = .95) CNC word scores, similar to a recent study in our laboratory (DeVries et al. 2016).

Bierer (2007) used the standard deviation of the absolute value of the difference between focused thresholds of adjacent channels, finding a relationship between higher threshold variability and lower CNC word scores. Pfingst et al. (2004) found the same result using the mean of the difference between thresholds. We were unable to replicate the results using the unsigned difference of the standard deviation (T_{12} = .86, P = .41) or the mean of the difference between thresholds (T_{12} = -1.34, P = .21).

Zhou et al. (2017) found that steeper multipulse integration (MPI) functions measured with bipolar stimulation were correlated with lower speech reception thresholds. MPI measures have been shown to predict spiral ganglion neural density in implanted guinea pigs (Zhou et al. 2015), thus pointing to an possible relationship between behavioral threshold-related measurements and neural survival.

Given that the present study was unable to replicate results from some of the above studies, it is likely due to a limitation within this dataset, possibly due to insufficient variability in CNC word scores.

The finding that there is no relationship between mean electrode-to-modiolus distance and word recognition is consistent with recent studies (Long et al. 2014; Holden et al. 2013; van der Marel et al. 2015; DeVries et al. 2016), though Aschendorff (2007) did observe that perimodiolar insertions tended to result in better speech outcomes. van der Marel and colleagues (2015) examined six electrode position-related factors and did not find any correlations with word recognition, but did find that duration of deafness and preoperative word scores correlated with speech outcomes, as others have found (Blamey et al. 2013).

There was no correlation between PTC ERB_{DR} and word recognition, consistent with other studies (Cohen et al., 2003; Anderson et al. 2011; Nelson et al. 2011), though the Anderson study did find a positive correlation between the inverse of the PTC bandwidth and sentence recognition. This is also consistent with previous studies that used the ECAP (Brown et al., 1990; Cohen et al. 2003; Hughes and Abbas 2006a), and one that measured ECAP ERB_{DR}s in all available electrodes (DeVries et al. 2016). Constraints introduced by the speech processor may make it difficult to compare spatial spread measured via direct stimulation to speech recognition, as suggested by others (Nelson et al. 2008; 2011; Anderson et al. 2011).

Duration of deafness was negatively correlated with CNC word scores (T_{12} = -2.68, P = .02). It is possible that pooling the pre/peri- and post-lingually deafened subjects weakened the correlations between the variables of interest and CNC word scores. However, one pre-lingually deafened subject (S53) scored 84% on CNC words, and a post-lingually deafened subject (S46) is a much poorer performer (Figure 3-8). Central mechanisms and plasticity resulting from deprivation during auditory development are not well understood in humans. It has been suggested that variability in central plasticity may contribute to a variability in performance into adulthood (Lazard et al. 2012).

While PTC ERB_{DR}s were correlated with electrode-to-modiolus distance, they were not predictive of word recognition. The fact that position-related factors did not correlate with word recognition, but duration of deafness and mean focused thresholds did, suggests that additional factors at the ENI are stronger contributors to word recognition.

E. Conclusions

The widely-documented variability in CI listener outcomes is likely due, in part, to the status of the electrode-neuron interface. Quantifying and disambiguating factors that contribute to poor electrode-neuron interfaces may be useful for optimization of programming techniques for these listeners. The ability to evaluate the electrode-neuron interface in the clinical environment is limited due to resources, time, and costs. Therefore, identifying measurements that may help to bypass these limitations is of the utmost importance.

This study demonstrated that a measure of spatial spread of excitation, or channel interaction, was correlated with electrode-to-modiolus distance, but not with behavioral thresholds. Scalar location appears to influence behavioral thresholds, degree of channel

interaction, and electrode-to-modiolus distance, indicating that proper placement of the electrode array may have an influence on psychophysical and objective measurements.

Behavioral thresholds were the only variable that was predictive of word recognition. This may indicate that while spatial measures of channel interaction reflect an important aspect of the electrode-neuron interface, and may prove useful for device programming, performance with the implant is not fully captured by electrode position or degree of channel interaction.

Finally, these results suggest that electrode array placement influences spatial spread of excitation, and that PTCs may be a useful behavioral measure to disambiguate electrode-neuron interface factors for some CI listeners. Future studies will use PTCs and electrode position to create experimental programs that account for electrodes with high degrees of channel interaction and determine if performance can be meaningfully improved when incorporating this information.

Chapter 4 : Current Focusing to Reduce Channel Interaction for Distant Electrodes in Cochlear Implant Programs

Submitted as:

DeVries LA and Arenberg JG. Cochlear Implant Programming Using Current Focusing to Reduce Channel Interaction for Distant Electrodes. *Trends in Hearing*, Manuscript submitted for publication.

A. Introduction

Outcomes are highly variable among cochlear implant (CI) listeners, potentially due to variations in perceptual acuity across stimulation sites (e.g. Won et al., 2007; Holden et al., 2013). Studies in CI listeners have demonstrated across-site variation in spatial spread of excitation (Abbas et al., 2004; Nelson and Donaldson, 2008; Bierer and Faulkner, 2010; Jones et al., 2013; DeVries et al., 2016; Zhou) et al., 2017), electrode discrimination (Zwolan et al., 1997; Throckmorton and Collins, 1999), and behavioral thresholds (Pfingst et al., 2004; Bierer, 2007; Long et al., 2014; DeVries et al., 2016). This variation may be partially attributable to the electrode-neuron interface (ENI), which refers to peripheral factors such as: spiral ganglion neuron density, electrode position, bone growth, and other factors (e.g. Bierer, 2010). Channels with suspected poor ENIs may cause a high degree of *channel interaction*, which occurs when the neural excitation patterns of adjacent channels overlap. Increased channel interaction can distort spectral information and lead to decreased pitch and speech perception (e.g. Jones et al., 2013), emphasizing the importance of identifying aspects of the ENI that contribute to increased channel interaction.

Human temporal bone studies have shown non-uniform distributions of spiral ganglion neural density in CI listeners and individuals with hearing loss (Linthicum et al., 1991; Nadol, 1997; Khan et al., 2005b). Animal studies have also demonstrated that long-term deafness results in smaller evoked potential responses and fewer surviving spiral ganglion neurons (Smith and Simmons 1983; Hall 1990; Shepherd and Javel 1997). However, histological studies have not shown a correlation between neural survival and speech perception in CI listeners (e.g. Khan et al., 2005a). While it is not yet possible to directly measure neural survival *in vivo* in humans,

several investigators are studying indirect measures of neural health (Zhou & Pfingst, 2016; Long et al., 2014; DeVries et al., 2016).

Another major component of the ENI, electrode position, can be *directly* assessed using computerized tomography (CT) imaging techniques. CT imaging can provide estimates of electrode-to-modiolus distance, scalar location, insertion angle, and wrapping factor (Verbist et al. 2005; Skinner et al. 2007; Teymouri et al. 2011; Holden et al. 2013). Suboptimal electrode positions lead to increased channel interaction and higher focused thresholds in humans (Cohen et al., 2001; Kawano et al., 1998; Long et al., 2014; DeVries et al., 2016), in animals using electrophysiological measures (Jolly and Spelman, 1996; Shepherd et al., 1993), and in computational modeling studies (Briaire and Frijns et al., 2006; Cohen et al., 2009a; Frijns et al., 1995; Goldwyn et al., 2010; Kalkman et al., 2014). Electrode arrays with poor placement often result in poorer performance on speech perception tasks, though results are mixed (Skinner et al., 2002; Finley et al., 2008; DeVries et al., 2016). While useful, this technique is limited in terms of clinical application. Post-operative CT scans are not often available to clinicians, incur high costs, and expose patients to radiation. Therefore, assessing alternative methods to measure electrode position is warranted.

A recent study evaluated the electrically evoked compound action potential (ECAP) as a possible objective measure of CT-estimated electrode-to-modiolus distance in CI listeners (DeVries et al., 2016). ECAP spread of excitation was moderately predictive of electrode-to-modiolus distance in most subjects, similar to a study by Cohen and colleagues (2003) using radiographs. However, the ECAP can be unreliable as some subjects do not have measurable responses, and responses can be small and contain large stimulus artifact.

In the present study, a potentially more reliable measure of channel interaction was used: the psychophysical tuning curve (PTC). Broad PTCs have been correlated with higher behavioral thresholds using focused stimulation, identifying suspected areas of excessive channel interaction (Nelson et al., 2008, Bierer and Faulkner, 2010). Recently, we measured PTCs using focused stimulation for all electrodes in 13 subjects, using a Bekesy-like, sweep procedure used for measuring thresholds in CI listeners (Bierer, et al., 2015; DeVries and Arenberg, in press); most of the same subjects participated in the present study. In that study, PTC bandwidths were predictive of CT-estimated electrode-to-modiolus distance, but not focused behavioral thresholds, across subjects.

Hypothetically, the predictive relationship between PTC bandwidths and CT-estimated electrode-to-modiolus distance may be exploited to create new listener programs to reduce channel interaction. As PTCs likely capture aspects of the ENI other than electrode position, it is useful to compare performance with CT-based and PTC-based programs. For instance, broad PTCs *not* correlated with electrode-to-modiolus distance may indicate areas of poor neural health, providing useful information beyond what CT-estimates can offer.

One approach to improve speech perception has been to deactivate electrodes to reduce channel interaction (Noble et al., 2013; 2014; 2016; Bierer & Litvak, 2016) or improve a psychophysical percept (Henshall & McKay 2001; Garadat et al., 2012; Zhou & Pfingst, 2012; Saleh et al., 2013; Vickers et al., 2016), with mixed results. In the Noble studies, computational modeling and CT-estimates were used to deactivate electrodes modeled to have excessive channel interaction. After one-month experience with the experimental program, there were significant improvements on sentence recognition and increased subjective quality of communication. However, deactivating electrodes with poor electrode position may sacrifice the

opportunity to improve spectral resolution by limiting the stimulation of viable neurons in that region. Using focused stimulation for these channels may serve to compensate for increased distance from the target neurons while minimizing channel interaction due to the narrower current spread.

Several studies have used focused stimulation across the electrode array to reduce channel interaction and improve speech perception (Berenstein et al., 2008; Srinivasan et al., 2013; Bierer and Litvak, 2016). Across studies, results are mixed, but with notable improvements in speech perception in noise. While encouraging, focused stimulation has some practical limitations for clinical use. This stimulation may have higher current level requirements, which could lead to greater power consumption and issues with voltage compliance limits (Bierer and Litvak, 2016). Side-lobe activation can also occur when using a high degree of focusing, which can increase channel interaction in unpredictable ways (Litvak et al., 2007). However, if only a *subset* of channels estimated to have poor electrode position uses focused stimulation, some of these limitations may be ameliorated. To date, channel selection strategies using behavioral data and focused stimulation are limited and have not incorporated electrode position.

The aim of the present study is to 1) assess the within-subject relationship between CT-estimated electrode-to-modiolus distance and PTC bandwidths, and 2) determine whether using this information to create individualized programs improves speech perception in an acute setting. Two test programs were created that use focused stimulation on a subset of channels, selected based on: 1) far electrode-to-modiolus distance from CT-estimates (Distance), and 2) broad tuning from PTC bandwidths (Tuning). Two control programs were also created: 1) channels *not* focused in the Distance program were focused (Inverse-Control), and 2) broad stimulation for all channels (Monopolar-Control). The Inverse-Control program evaluates how

focusing electrodes *close* to the modiolus affects speech perception; focusing all electrodes would not allow us to evaluate perceptual detriments when focusing *only* ostensibly "good" channels. The Monopolar-Control program evaluates how the test programs compare stimulation similar to what CI listeners hear every day. We expect the Inverse-Control program will be detrimental to speech perception, as areas with excessive channel interaction may still be uncontrolled, or there may not be sufficient spiral ganglion neurons activated because of current focusing and neural sparsity, as suggested by Bierer and Litvak (2016). We further hypothesize subjects will have higher scores with the Tuning and Distance programs, as compared to the controls. Subjects were tested on closed-set medial vowel identification, a spectrally challenging task, and open-set sentence recognition, which may reflect more real-world conditions. Subjects also completed a sound quality questionnaire to assess subjective program preferences. The results of this study may provide an important link between site-specific peripheral measures of the ENI and the practical application of these measures to CI listener programs.

B. Methods

Subjects

Thirteen adult subjects who were unilaterally implanted after 2001 with Advanced Bionics HiRes90k devices participated (Table 4-1). Twelve of these subjects participated in the previously mentioned DeVries and Arenberg study (in press). Subjects were at least 21 years of age (M = 66.2, SD = 10.65), and there were eight males in the study. Two subjects were pre-lingually deafened (S49, S53), one was peri-lingually deafened (S40), and the remaining 10 were post-lingually deafened. One of the post-lingual subjects was deafened in childhood (S46, age 14), but is still considered with the post-lingually deafened subjects as they learned language before they were diagnosed with a severe-to-profound hearing loss. All subjects were fluent English speakers. Each participant provided written consent, and the experiments were

conducted in accordance with guidelines set by the University of Washington Human Subjects Division.

Table 4-1: Demographic information for all 13 subjects including: ear implanted, chronological age, age diagnosed with a profound hearing loss, age at implantation, duration of deafness, etiology (if known), electrode array type and electrode spacing, and clinical CNC word score.

ID	Ear	Age	Age @ Profound HL	Age Implanted	Duration (years)	Etiology	Electrode Array/Spacing (mm)
S22	R	77	55	66	11	Suspected Genetic	1J Helix/0.85
S29	L	86	47	77	30	Noise	HiFocus 1J/1.1
S40	L	55	4	50	46	EVA	HiFocus 1J/1.1
S42	R	67	50	50	0	Idiopathic	HiFocus 1J Positioner/0.9
S43	R	71	50	67	17	Noise	Mid-Scala/0.85
S46	R	66	14	62	48	Unknown	HiFocus 1J/1.1
S47	R	68	28	37	9	Unknown	Mid-Scala/0.85
S49	R	44	1.5	43	41.5	Suspected Genetic	Mid-Scala/0.85
S53	R	54	1	44	43	Meningitis	1J Helix/0.85
S52	R	70	60	60	10	Idiopathic	HiFocus 1J/1.1
S55	R	63	41	49	8	Suspected Genetic	HiFocus 1J/1.1
S56	L	72	30	58	28	Idiopathic	HiFocus 1J Pos./0.9
S57	R	67	63	65	2	Idiopathic	Mid-Scala/0.85

CT imaging

CT scans were performed at the University of Washington Medical Center within the last three years. Briefly, ANALYZE software was used to create 3-dimensional image volumes by combining information from each subject's post-operative scan and a single body donor cochlea (Figure 4-1; for details, see Skinner et al., 2007; for verification of the method, see Teymouri et al., 2011). Pre-operative CT scans were not available for the subjects participating in the present study; therefore, a scan of the non-implanted ear was used to identify structural anatomy, and this image was co-registered with the image of the implanted ear. Micro CT and orthogonal-plane fluorescence optical sectioning (OPFOS) images from a donor cochlea were used to locate and visualize the non-bony structures. The CT-estimated metric used in this study was electrode-to-modiolus distance, which refers to the lateral distance (mm) of an electrode from the medial wall of the cochlea.

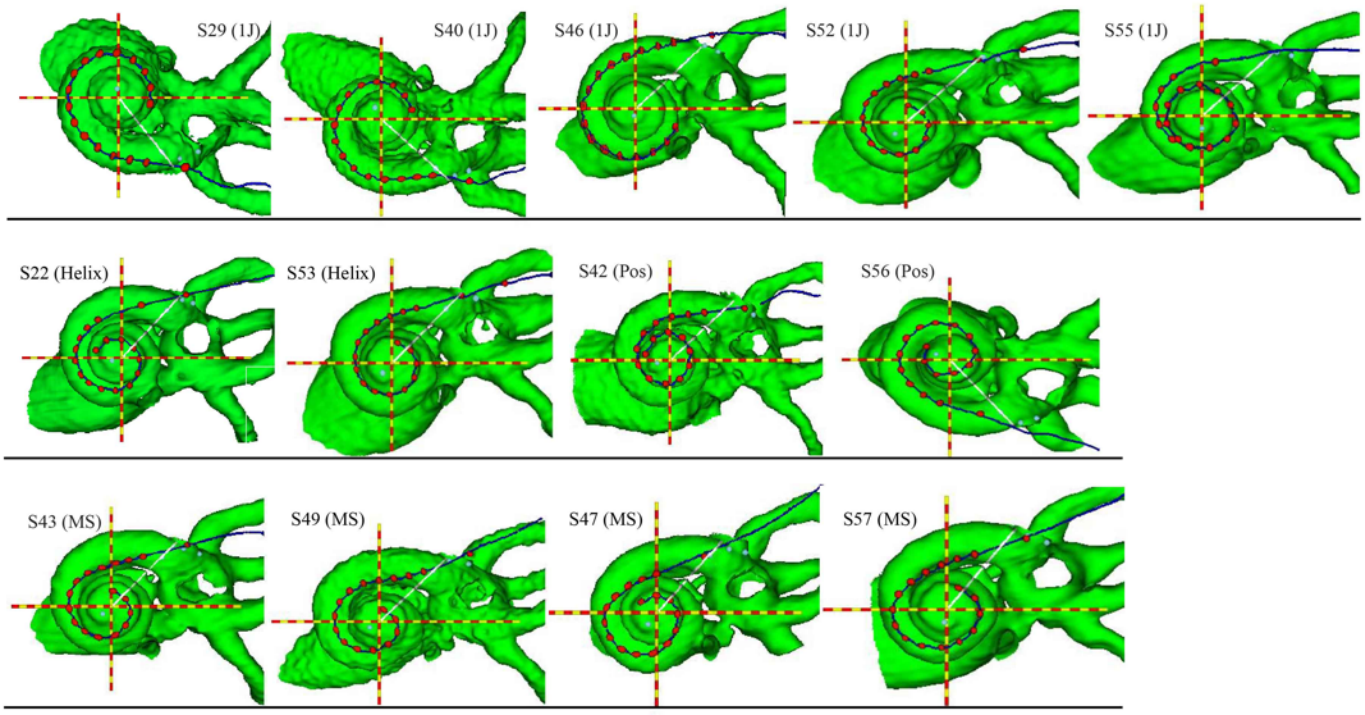

Figure 4-1: CT view of cochlea and electrode array along the midmodiolar axis (red and yellow dashed line), for all subjects, organized by electrode array type. The evenly spaced red dots represent electrodes; the outermost dot represents the insertion depth marker. The white line represents the 0-degree reference point from which insertion depth is measured, extending from the midmodiolar axis. Row 1: 1J; Row 2: 1J Helix and 1J with positioner; Row 3: MidScala electrode array. Adapted from DeVries and Arenberg (in press).

Electrode configurations

All stimuli were presented using the Bionic Ear Data Collection System version 1.18.315 (Advanced Bionics, Valencia, CA). For psychophysical testing, a custom Matlab (Mathworks, Inc. Natick, MA) program controlled the BEDCS software. Three types of electrode configurations were used in this study: monopolar (MP), steered quadrupolar (sQP), and partial tripolar (pTP).

The MP configuration consists of an active intracochlear electrode and a return extracochlear electrode; the large distance between the source/sink yields a broad electrical field (e.g., Litvak et al. 2007). The sQP configuration consists of four intracochlear electrodes: the two middle electrodes serve as active electrodes, and the two outer electrodes serve as return electrodes for a fraction of the active current (an extracochlear electrode carries the remainder of

the return current). Current is steered between the two middle electrodes according to the fraction, α: a value of 1 steers current to the basal electrode and 0 to the apical electrode. By convention, channel number is defined as the basal active electrode when α = 1. In the present study, this convention was maintained for electrodes 3 to 15. For electrode 2, however, it was necessary to use the same set of electrodes as channel 3 (the most apical channel possible with the 4-electrode sQP configuration) in conjunction with an α value of 0 to center the current on electrode 2. This arrangement is referred to as "channel 2," even though electrode 2 is the apical active electrode. The pTP configuration is a variant of the traditional tripolar (TP) configuration. In the TP configuration, there is one intracochlear active electrode, with the return current divided equally between each of the two adjacent, flanking electrodes. The pTP configuration is similar, but only a fraction of the return current is delivered to the flanking electrodes; the remainder flows to the extracochlear ground.

For pTP and sQP configurations, the fraction of the return current varies according to "σ" (Landsberger and Srinivasan 2009; Srinivasan et al., 2010; Bierer et al., 2015). A higher σ results in a narrower electrical field than the MP configuration; for instance, σ = 0 is considered MP, and σ = 1 is considered TP, the highest possible focusing (Litvak et al. 2007). In the present study, sQP stimulation, as opposed to pTP, was used for some psychophysical procedures as sQP allows some data to be collected significantly faster, described below. sQP thresholds were found to be equivalent to pTP in another study, in which many of the same subjects participated (Bierer et al., 2015).

Most comfortable listening levels

Most comfortable listening levels (MCL) were measured for use in the PTC procedure, described below. MCLs for masker and probe stimuli were determined using the Advanced Bionics clinical

loudness scale (Advanced Bionics, Valencia, CA). To determine MCL, current level was increased manually until subjects reported a loudness rating of "6," or "most comfortable." The level was changed in 2 dB steps until a loudness rating of 4 was reached; thereafter the level was changed in 0.5 or 0.1 dB steps, depending on subject response. Four sets of MCLs were measured: 1) PTC masker stimuli, 2) MP thresholds for PTC probe stimuli, 4) MP thresholds for programming procedures, and 5) pTP thresholds for programming procedures. These levels served as the maximum stimulus level for all psychophysical and programming procedures.

Single-channel behavioral thresholds

Single-channel thresholds were measured for electrodes 2—15 using a sweep threshold procedure (Bierer et al., 2015). Pulse trains were presented with α-value increasing from 0 to 1 in 0.1 steps from electrode 2-15 for a *forward* sweep (apical to basal), and from 15-2 (basal to apical), for a *backward* sweep (based on Sek et al., 2005; for details, see Bierer et al., 2015). A forward and backward sweep was run for each set of stimuli and averaged. Four sets of sweep thresholds were measured for the same stimuli as the MCLs. These levels served as the minimum stimulus level for all psychophysical and programming procedures.

Sweep psychophysical tuning curves

Psychophysical tuning curves (PTCs) were obtained for all available electrodes within a forward-masking paradigm, with a varying masker and fixed probe, using a modified threshold sweep procedure (Bierer et al., 2015). This procedure is similar to the sweep threshold procedure (see Single-Channel Behavioral Thresholds section), though in this case the masker was swept across the electrode array, varying in level, while the probe remained fixed in level and location. Figure 4-2 shows PTCs for S53 on all available electrodes; PTCs are plotted as masker level (% dynamic range) as a function of masker electrode (apical to basal). S53 had shallower, narrower

PTCs apically, indicating minimal presumed channel interaction. Basally, PTCs appeared deeper and broader, indicative of excessive channel interaction in this region.

PTCs were quantified as a function of masker level, normalized to the masker-alone dynamic range. The equivalent rectangular bandwidth (ERB_{DR}) was used to quantify the spatial extent of masker-probe interaction by equating the PTC to a rectangular function of equivalent minimum masker threshold. For detailed methodology, see DeVries and Arenberg, in press.

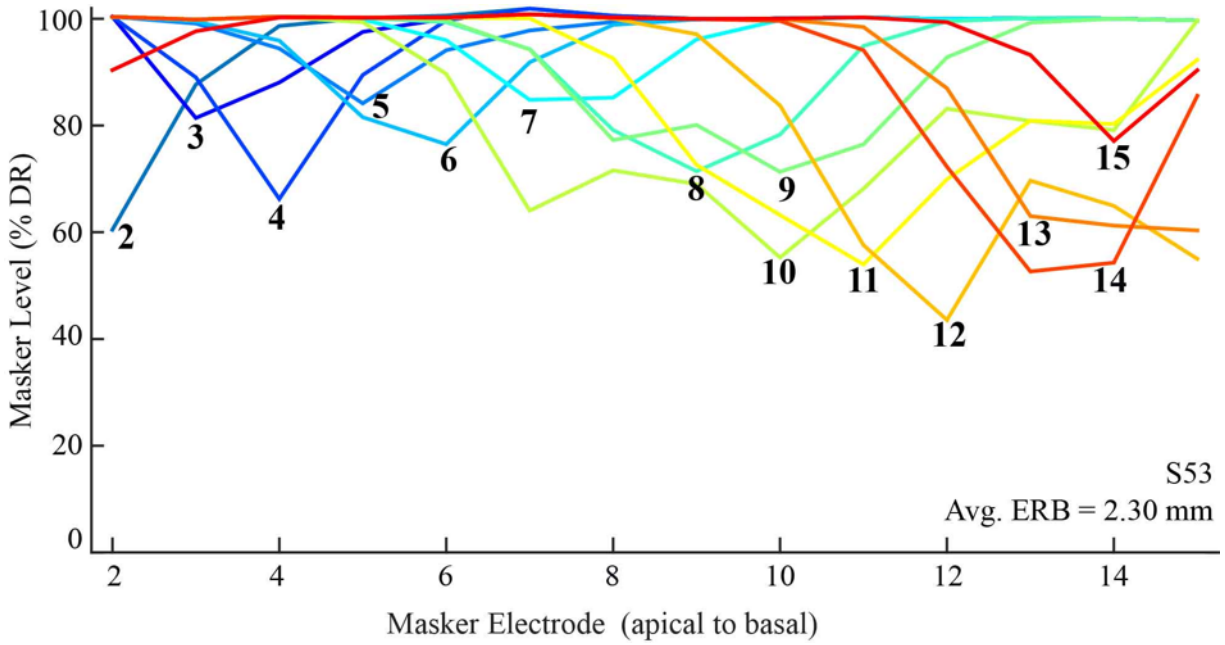

Figure 4-2: PTCs across the electrode array for an example subject (S53). The x-axis denotes the masker electrode (apical to basal). The y-axis represents the masker threshold in percent dynamic range. The numbered lines inside the plot are probe electrodes, labeled at the tip of the PTC. The mean PTC ERB_{DR} in mm is marked inside the plot. Adapted from DeVries and Arenberg (in press).

Channel selection and programs

Channels selected for focused stimulation were based on the median values of CT-estimated electrode-to-modiolus distance and PTC ERB_{DR}s (Figure 4-3A). Those electrodes more distant, or with broader tuning than the within-subject median were programmed with the pTP configuration, and all other channels with the MP configuration (Figure 4-3B). This simple criterion was chosen so that each subject had a relatively equal number of channels using

focused stimulation (typically 6-8), and as a straightforward starting point for exploring focusing a subset of channels based on CT-estimates and PTCs.

Four programs were created: 1) "Tuning," based on PTC ERB_{DRS}, 2) "Distance," based on CT-estimated electrode-to-modiolus distance, 3) "Inverse-Control" wherein the channels *not* focused in the Distance program are focused, and 4) "Monopolar-Control," an all-channel monopolar program.

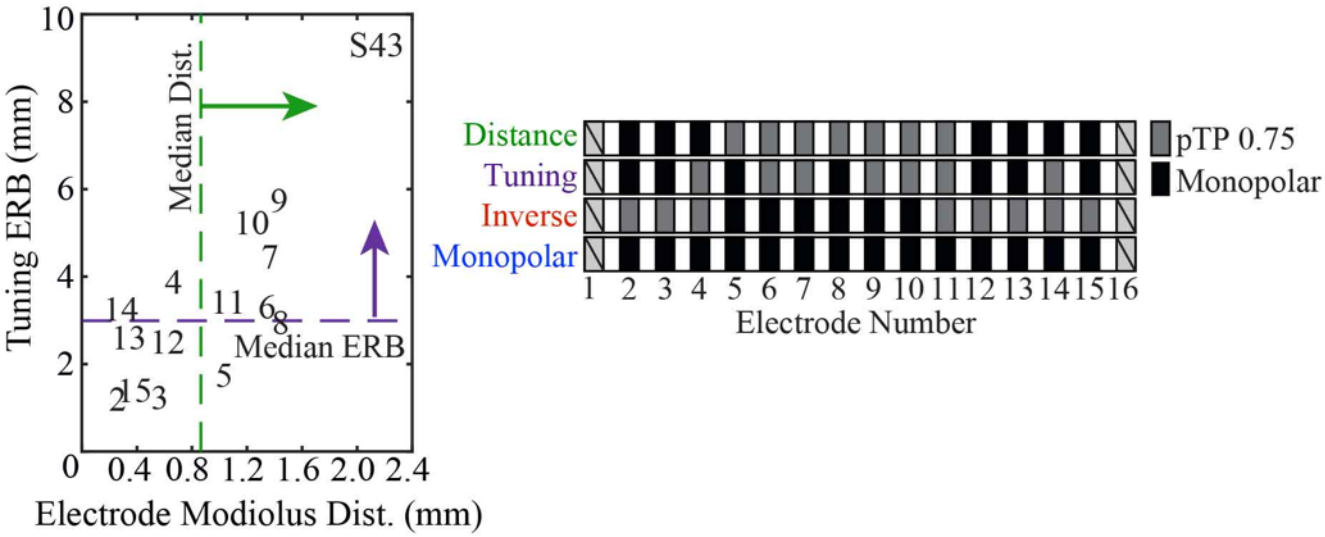

Figure 4-3: Left: Tuning curve ERB_{DR} as a function of electrode-to-modiolus distance (mm) for S43. The numbers inside the figure indicate channels. The green dashed line is set at the median electrode-to-modiolus distance and the purple dashed line is set to the median PTC ERB_{DR}. Right: Electrode configuration schemes for "Distance", "Tuning", "Inverse-Control" and "Monopolar-Control" programs. Gray boxes are channels that use pTP stimulation, and black boxes are channels that use monopolar stimulation for each program. Channels 1 and 16 are not used due to the nature of sQP stimulation.

Programming Procedures

All programs were created for each subject using BEPS+ software version 1.18.26.24691 (Advanced Bionics Corp., Valencia, CA, USA). Table 4-2 provides subject-specific programming details. The pTP configuration was used for programming procedures as sQP is not available in BEPS+. pTP with $\sigma = .75$ was used for electrode focusing, to avoid reaching

compliance limits. For S49, σ = .62 was used as σ = .75 caused abnormal auditory percepts ("vibrating"). For all subjects, electrodes that were not focused used MP stimulation.

Programs were created on a Harmony research processor dedicated for use in the laboratory. All behavioral MCLs and thresholds were converted into charge units for use in BEPS+. All four 14-channel programs used electrodes 2 through 15; electrodes 1 and 16 were excluded as they could not serve as active electrodes when using focused stimulation. Program settings such as Clear Voice and frequency filter settings were maintained, and current steering was deactivated. The input dynamic range was set to 60 dB SPL and the gain was set to zero. Pulse width and rate were equal within-subject and across programs, based on the auto pulse width obtained using the program with the most focused channels.

Thresholds and MCLs were entered from the previously conducted psychophysical procedures (see above sections). MCL levels were loudness balanced in sets of four electrodes beginning with electrode 2. The subject was instructed to inform the researcher if the sounds were equally loud. Adjustments were made until all channels were perceived as equally loud.

After balancing M-levels, the volume was reduced on the speech processor, the M-levels were globally reduced by 10 steps, and the microphone was activated through BEPS+. The M-levels were slowly increased until the subject indicated the overall loudness was "Most Comfortable," or a "6" on the clinical loudness scale. M-levels were then individually adjusted according to subjective reports of loudness and clarity. The Ling sounds were presented, and M-levels were adjusted to ensure the subject had access to important consonant and vowel cues that span the speech spectrum. The subject was finally instructed to indicate if the programs sounded equally loud. Once complete, all four programs were converted to Aux Only and loaded onto the processor for testing through direct audio input.

Table 4-2: Signal-to-noise ratios (SNR) used for both medial vowel identification and sentence recognition tasks, number of channels focused in each program (except for Monopolar-Control), the degree of focusing (σ) used, pulse width, and pulse rate for all programs.

ID	SNR (hvD)	SNR (IEEE/HINT*)	# of Channels Focused	σ value	Pulse Width	Pulse Rate
S22	+7	+7	7	.75	33.2	1075
S29	Quiet	Quiet	8 (CT), 7 (PTC), 6 (Inv)	.75	55.7	641
S40	Quiet	+16*	7	.75	50.3	710
S42	+6	+11	7	.75	28.7	1170
S43	+11	+15	7	.75	26.9	1326
S46	Quiet	Quiet*	7	.75	89.8	398
S47	+6	+13	7	.75	28.7	1243
S49	Quiet	Quiet*	7	.62	50.3	181
S53	+6	+10	7	.75	18	1989
S52	+11	+17	7	.75	18	1989
S55	+9	+5	7	.75	57.5	621
S56	+10	+17	7	.75	75.4	473
S57	+10	+9	7	.75	44.9	795

Speech perception testing

Using ListPlayer software (Advanced Bionics, Valencia, CA) and direct audio input, subjects listened to randomized, closed-set AZ-Bio sentences (Spahr et al., 2012) in quiet for 15 minutes before beginning testing with each program; subjects were able to see the sentences on the computer screen, if desired. Stimuli were presented using at 60 dB-A, with Auditech 4-Talker Babble presented at a signal-to-noise ratio (SNR) that reflects 50% performance with the Monopolar-Control program (referred to as "SNR 50"). The SNR was adjusted for each subject, wherein performance between 40-60% was accepted; therefore, the noise level was different for each subject. S29, S40, S46, and S49 were unable to reach 40-60% performance in quiet, so all of their testing was performed in quiet. The Monopolar-Control program was always tested first (as this program was used to obtain the SNR 50 noise level); the remaining three programs were randomized and tested. Subjects were blinded to the programs that were tested and did not see their scores following testing.

Vowel stimuli consisted of one female, Pacific Northwest talker, uttering 10 naturally spoken vowels (/i/, /ɪ/, /eɪ/, /ɛ/, /æ/, /ɑ/, /u/, /ʊ/, /o/, /ʌ/) in the /hVd/ context (DiNino et al., 2016). Subjects used a computer mouse to select from the vowels presented on the computer screen. Subjects were given one practice run in quiet and two test runs at SNR 50. Each run consisted of three repetitions of each vowel token. If the two test runs differed by 10% or more, a third run was conducted, and all three runs were averaged.

IEEE sentences were used for sentence recognition testing (IEEE, 1969). The IEEE sentences consist of 72 lists of 10 sentences each. These sentences are low-context, phonetically balanced, and represent various speech sounds at the same frequency used in everyday English. As this was an open set task, the subject verbally repeated what they heard, and the researcher scored each response manually. Subjects were given one practice run in quiet and two test runs at SNR 50. If the two test runs differed by 10% or more, a third run was conducted, and all three runs were averaged.

Two subjects, S40 and S49, were unable to reach 40-60% scores with the IEEE sentences in quiet, likely due to the open-set and somewhat low context nature of the task. Therefore, the Hearing in Noise test (HINT; Nilsson et al., 1994) was used as these sentences tend to be easier for listeners. The HINT consists of 25 phonemically balanced lists of 10 sentences each. S40 and S49 could perform the task in an open-set manner for all programs when using these materials. As with the IEEE sentences, the subject verbally repeated what they heard, and the researcher scored each subject manually. Subjects were given one practice run in quiet and two test runs at SNR 50. If the two test runs differed by 10% or more, a third run was conducted, and all three runs were averaged.

Sound quality questionnaire

Following testing with each program, subjects were asked to rate sound quality and clarity on a scale from 1 to 10, in comparison to their everyday program. A rating of "5" was considered equivalent to their everyday program, less than 5 was considered "worse", and more than 5 was considered "better." Subjects were asked to rate clarity in quiet, clarity in noise (where applicable), ease of listening, and naturalness for each program.

Statistical analysis

SPSS statistical software was used to perform within and between-subjects comparisons (IBM Corp. Released 2015. IBM SPSS Statistics for Windows). A simple linear regression was conducted to determine the within-subject relationship between PTC ERB_{DR} and electrode-to-modiolus distance. In a recent study in which the same subjects participated, PTC ERB_{DR}s measured with the 2IFC procedure in two subjects (S40 and S49) did not significantly differ from those that used the modified threshold sweep procedure (DeVries and Arenberg 2018, in press). Therefore, PTC ERB_{DR}s were compiled for all statistical analyses.

Two planned mixed-model repeated measures linear regression was performed to investigate the effect of program on medial vowel identification and sentence recognition (Model 1) and on ERB_{DR}-Distance correlation/no correlation groups (Model 2). Duration of deafness was calculated for each participant and included as a covariate due to the presence of two pre- (S49, S53) and one peri-lingually (S40) deafened subject in this dataset; these three subjects have similar durations of deafness (41.5, 43, and 46 years, respectively). "Subject" was entered as a random intercept, and "program" and "test" were entered as repeated factors (Baayen et al., 2008). A compound symmetry covariance matrix was specified for all models. A Bonferroni

correction was applied to all multiple comparisons and is noted where appropriate; all p-values reported from this procedure are adjusted for a significance level of $\alpha = .05$ (Wright, 1992).

A repeated-measures analysis of variance (RMANOVA) was conducted on all sound quality data; all results are reported with a Greenhouse-Geisser correction to account for a lack of sphericity in the data. A correlational analysis was performed to compare preference and performance across programs.

C. Results

CT-estimated electrode-to-modiolus distance

The variability in electrode array positioning is shown in 3D cochlear reconstructions for all subjects, arranged by electrode array type in Figure 4-1. Electrode-to-modiolus distances ranged from 0.66-1.80 mm (Table 3; *M* = 1.04 mm, *SD* = .52). In general, the electrode trajectories are consistent with the designs of the four types of arrays, which partially determine how far the electrodes are from the modiolus, and thus how close they are to target auditory neurons. The 1J

Table 4-3: Individual means and standard deviations for electrode-to-modiolus distance and PTC ERB_{DR}. The right two columns show individual Pearson's r and p-values for the correlation between electrode-to-modiolus distance and PTC ERB_{DR}.

ID	EMD (mm) mean *(sd)*	Tuning ERB (mm*)*	*r*	*p*
S22	1.12 *(.37)*	2.14 *(1.14)*	.53	.05*
S29	1.52 *(.23)*	3.70 *(1.37)*	.81	.0004*
S40	1.79 *(.22)*	5.40 *(2.40)*	.47	.09
S42	.64 *(.33)*	3.07 *(1.73)*	.70	.006*
S43	.84 *(.44)*	3.09 *(1.48)*	.66	.01*
S46	1.80 *(.34)*	5.51 *(2.23)*	.17	.56
S47	.87 *(.46)*	2.61 *(.76)*	.55	.04*
S49	.94 *(.47)*	2.85 *(1.02)*	.18	.55
S52	.71 *(.30)*	2.98 *(1.01)*	.54	.05*
S53	.66 *(.17)*	2.30 *(.96)*	.19	.51
S55	1.06 *(.26)*	5.81 (*1.74)*	*.28*	.34
S56	.62 *(.33)*	4.51 *(2.62)*	-.27	.35
S57	.90 *(.39)*	2.89 *(1.27)*	.60	.02*
Summary	1.04 *(.52)*	3.60 *(1.99)*	N/A	N/A

electrode array (S29, S40, S46, S52, and S55) has a lateral design, whereas the 1J Helix (S22, S53) is pre-curved to achieve a more medial position.

The 1J with positioner (S42, S56), by design, pushes the electrode array even more medially. The Mid-Scala array (S43, S49, S47, S57) is pre-curved, and designed for mid-scalar placement to preserve cochlear structures. Due to the small sample size for each electrode array, differences between array types cannot be examined further.

Within-subject comparisons between PTC bandwidths and electrode-to-modiolus distance

Across subjects, PTC ERB_{DR}s ranged from 0.70-10.40 mm (Table 3; M = 3.75 mm, SD = 1.96). PTC ERB_{DR}s and electrode-to-modiolus distance are shown for each subject (Figure 4-4), with dashed lines indicating the median PTC ERB_{DR} (purple) and median electrode-to-modiolus distance (green). For 7 out of 13 subjects, there was a significant, positive correlation between PTC ERB_{DR} and electrode-to-modiolus distance, wherein electrodes further from the modiolus tended to have broader PTC ERB_{DR}s (Figure 4-4, top row).

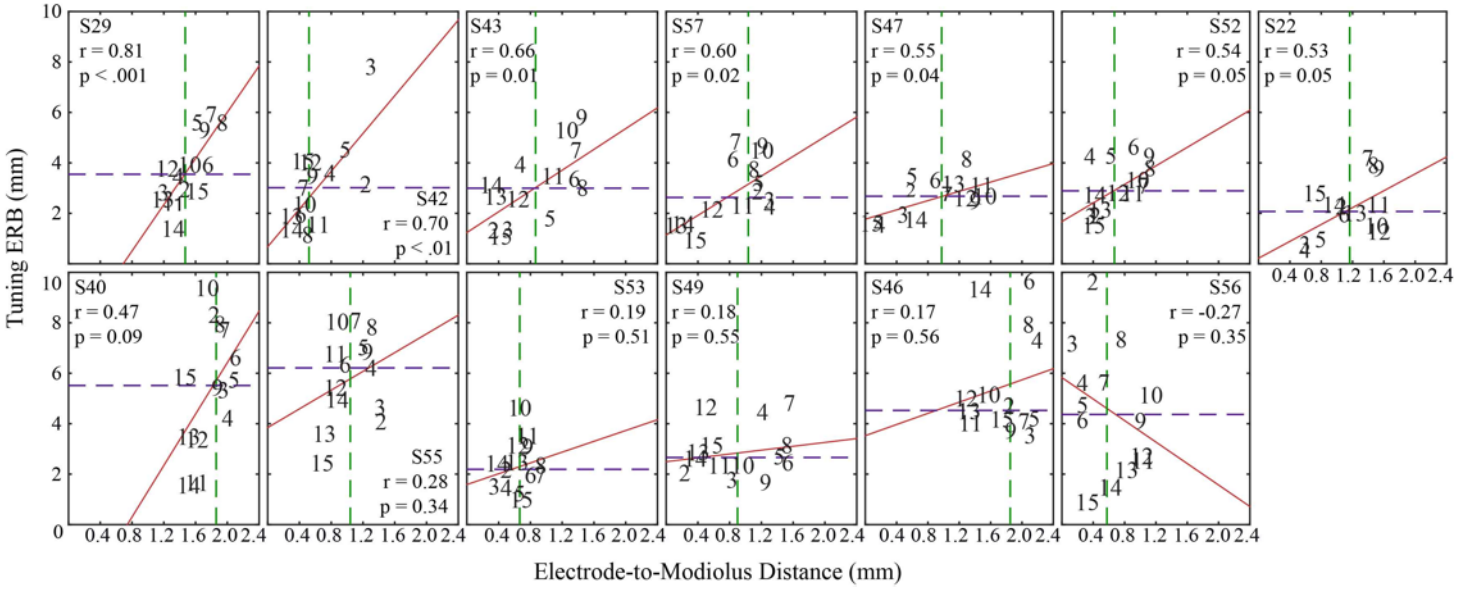

Figure 4-4: Tuning curve ERB_{DR} (mm) as a function of electrode-to-modiolus distance (mm) for 13 subjects, arranged by Pearson's r from highest to lowest. The numbers inside the figure indicate channels. The green dashed line is set at the median electrode-to-modiolus distance and the purple dashed line is set to the median PTC ERB_{DR}. The red line is the best fit line for each subject.

Speech perception performance

On average, results show that performance is similar with the Monopolar-Control program as with Distance and Tuning, and significantly poorer with the Inverse-Control program for both sentence recognition and vowel identification tasks.

Raw scores (percent correct) for all programs are presented in the top panel for medial vowel identification (Figure 4-5A), and sentence recognition in the bottom panel (Figure 4-5B). Scores relative to the Monopolar-Control program are presented for medial vowel identification (Figure 4-6A) and sentence recognition (Figure 4-6B), for ease of viewing the relative differences in performance. These figures clearly demonstrate the variability seen in individual benefit from each program.

Results from a linear mixed model analysis show a significant effect of program ($F(3,83.77) = 13.28$, $p < .0001$), across sentence recognition and medial vowel identification tests. There was no effect of duration of deafness ($F(1,28.56) = .28$, $p = .60$), and no interaction between experimental program and tests ($F(4,83.77) = .28$, $p = .89$). After Bonferroni correction, medial vowel identification scores were significantly higher for the Monopolar-Control ($p = .03$), Distance ($p < .001$) and Tuning programs ($p = .007$), as compared to the Inverse-Control program (Figures 4-6A-B). Scores for the Distance and Tuning programs were not significantly different from each other ($p = .99$), or from the Monopolar-Control program ($p = .42$ and $p = 99$, respectively).

Sentence recognition scores were significantly higher with the Distance ($p = .001$) and Tuning programs ($p = .02$), as compared to the Inverse-Control program. Scores with the Distance and Tuning programs were not significantly different from each other ($p = .99$) or from the Monopolar-Control program ($p = 99$). There were no significant differences between the

Monopolar-Control and Inverse-Control programs (p = .06), though a trend is evident. As previously mentioned, subjects S40, S46, and S49 were unable to reach 50% performance in quiet using the IEEE sentences; as a result, the HINT sentences were used for these subjects. To ensure sentence recognition results were not driven by subjects using the HINT sentences, the mixed model was re-run without those subjects. The results are similar, with the exception that the Tuning program scores are no longer significantly better than those of the Inverse-Control program (p = .22). Therefore, it is possible that subjects using the HINT test were driving the significant difference between the Tuning and Inverse-Control programs. However, it is unclear whether this is due to the use of the HINT, loss of statistical power, or some other cause. For ease of viewing, these subjects will be presented with the subjects who used the IEEE sentences, with an asterisk to denote the use of the HINT. We opted to present these subjects in the sentence recognition analysis as they represent real CI listeners who may not be able to use preferred clinical materials. These results suggest that improvements in speech perception are possible when focusing channels suspected of a high degree of channel interaction. The significantly poorer performance on the Inverse-Control program may indicate: 1) focusing the "good" channels is detrimental, or 2) refusing to focus the "bad" channels is detrimental; future studies will compare this program to an all-channel focused program, similar to Bierer and Litvak (2016). Either way, this result suggests that if a subset of channels use focusing, they must be carefully selected to avoid detriments to perception. Speech perception scores between the Distance and Tuning programs did not differ across subjects, but not all subject's PTC ERB_{DR}s were correlated with CT-estimated electrode-to-modiolus distance (see Figure 4). For subjects where this relationship was not observed, it is possible that improved performance with the Distance and Tuning programs is due to an aspect of the ENI other than electrode position.

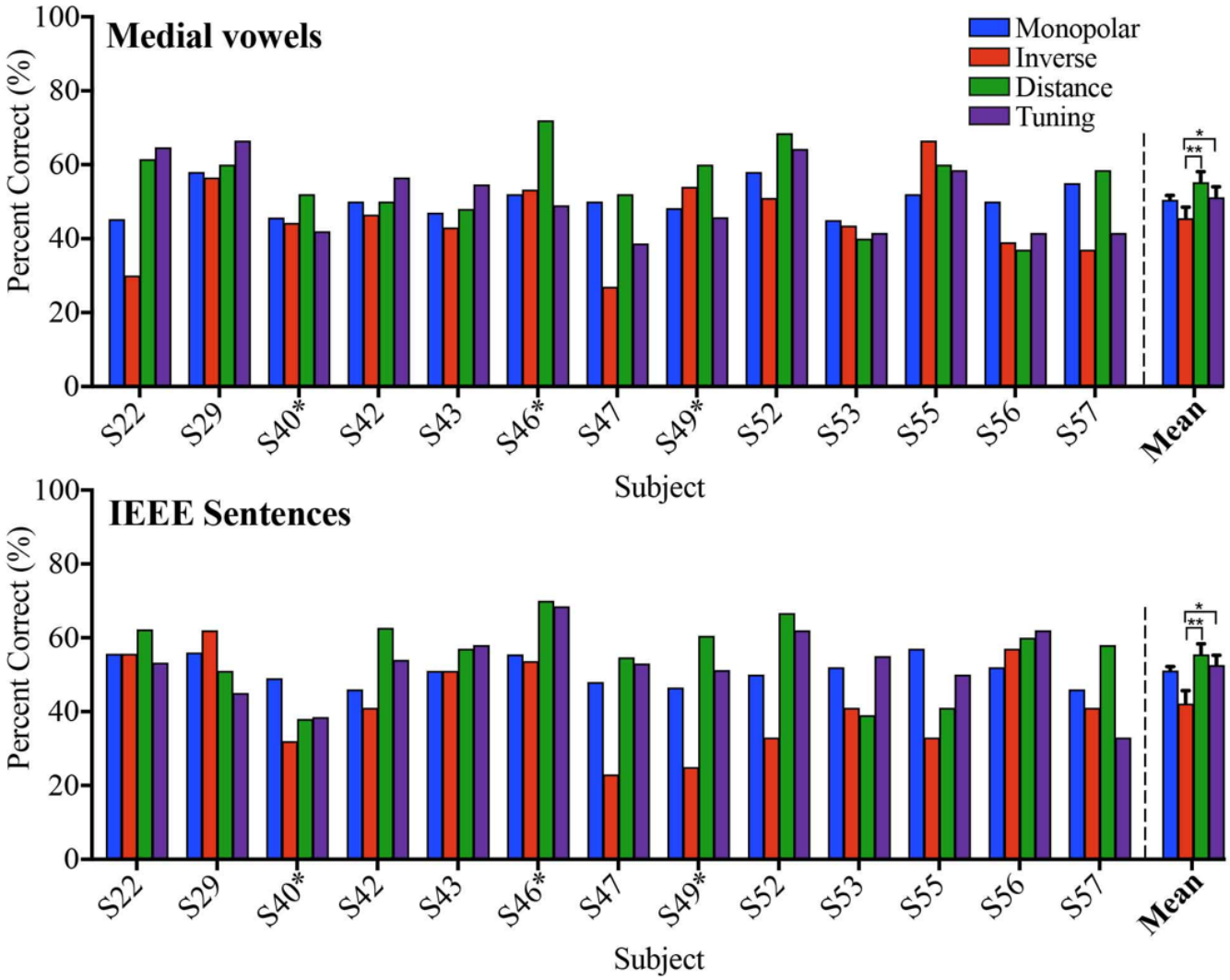

*Figure 4-5: **A**: Raw scores (percent correct) on the medial vowel identification task, within (left of dashed line) and across subjects (right of dashed line). Scores are presented for Monopolar-Control (blue), Inverse-Control (red), Distance (green), and Tuning (purple) programs. Brackets with asterisks indicate significance differences between programs. **B:** Raw scores (percent correct) on the sentence recognition task. All subjects used IEEE sentences except S40, S46, and S49, which are marked with an asterisk. All other conventions are the same as the top panel.*

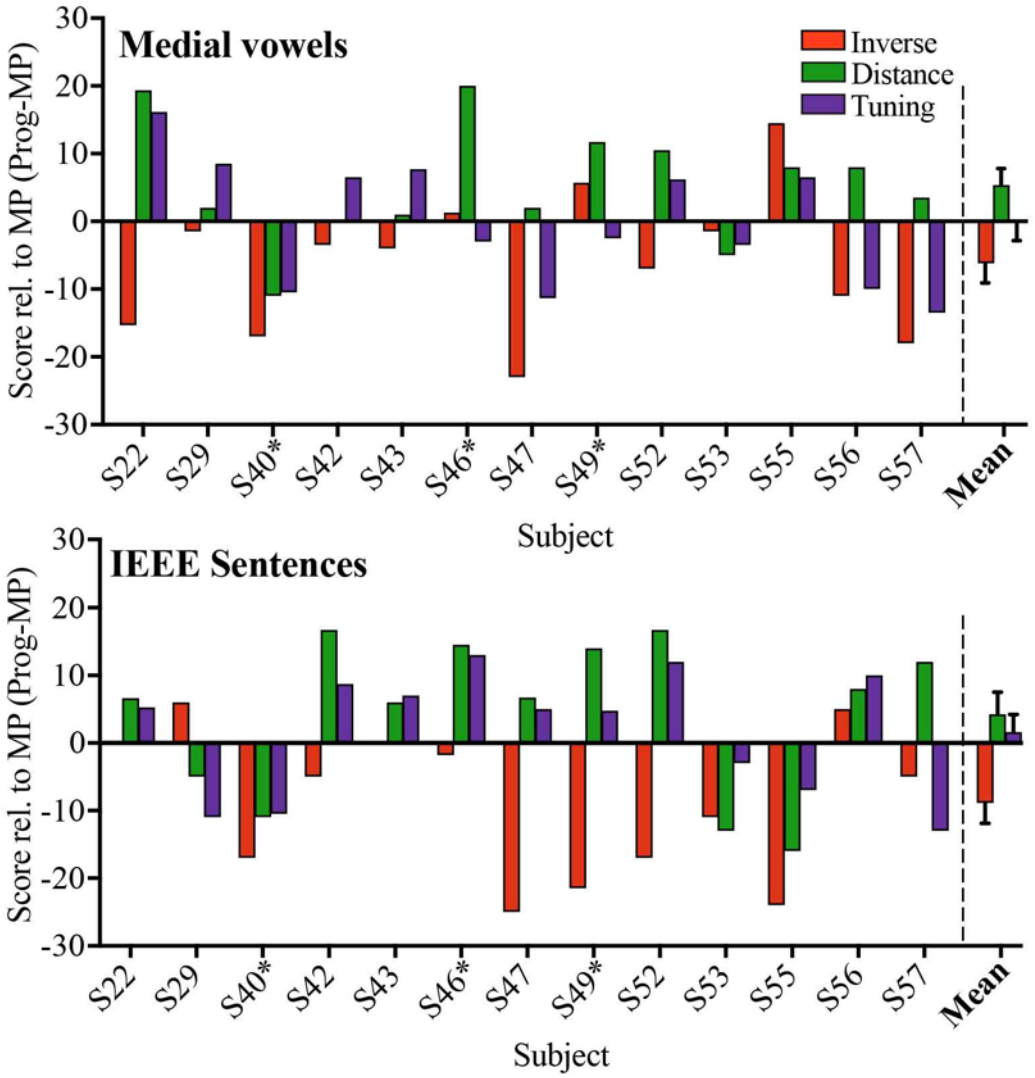

Figure 4-6: ***A:*** *Performance relative to the Monopolar-Control program (percent correct) on the medial vowel identification task, within (left of dashed line) and across subjects (right of dashed line). Scores are presented for Inverse-Control (red), Distance (green), and Tuning (purple) programs.* ***B:*** *Performance relative to the Monopolar-Control program (percent correct) on the sentence recognition task. All subjects used IEEE sentences except S40, S46, and S49, which are marked with an asterisk. All other conventions are the same as the top panel.*

PTC ERB_{DR} and electrode-to-modiolus distance correlation and no correlation groups

Subjects whose PTC ERB_{DR}s were well predicted by electrode-to-modiolus distance may receive a different benefit from the Distance and Tuning programs than those without this correlation (see Figure 4-4). For example, if a subject has broad PTC ERB_{DR}s that are poorly correlated with electrode-to-modiolus distance, there may be a neural health issue at the ENI. It was expected that those with this correlation will perform similarly with the Distance and Tuning programs, whereas those without this correlation were not expected to perform as well with the Tuning

program as compared to the Distance program. Figure 4-7 displays average performance on all programs for both the sentence recognition and medial vowel identification tasks, split between ERB_{DR}-Distance correlation and ERB_{DR}-Distance no correlation groups.

Results from the mixed model show a significant effect of program ($F(3,76.38) = 12.95$, $p < .0001$), across sentence recognition and medial vowel identification tests. There was no effect of duration of deafness ($F(1,30.21) = .16$, $p = .69$), no interaction between program and ERB_{DR}-Distance correlation/no correlation groups ($F(3,76.38) = .58$, $p = .63$), and no interaction between test administered and ERB_{DR}-Distance correlation/no correlation groups ($F(8,80.55) = .51$, $p = .60$).

After Bonferroni correction, for sentence recognition, subjects with the ERB_{DR} -Distance correlation performed better with the Distance program as compared to the Inverse-Control program ($p = .02$). There were no significant differences between any other programs. For medial vowel identification, subjects with the ERB_{DR} -Distance correlation performed better on

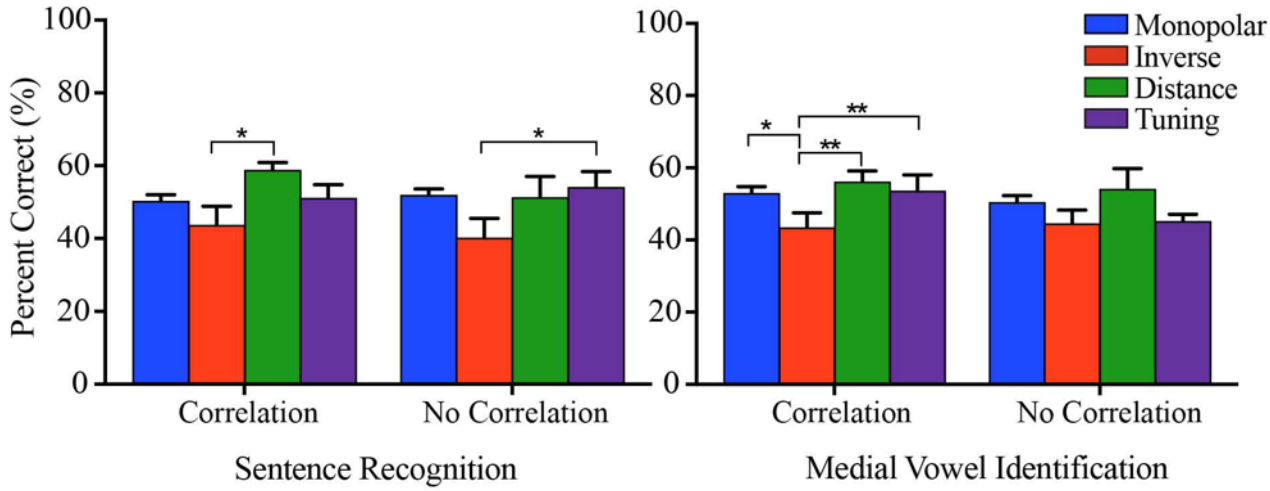

*Figure 4-7: **A:** Raw scores (percent correct) on the sentence recognition task for ERB_{DR}-Distance correlation (left) and no correlation groups (right). All subjects used IEEE sentences except S40, S46, and S49. All subjects were combined for ease of viewing. Scores are presented for Monopolar-Control (blue), Inverse-Control (red), Distance (green), and Tuning (purple) programs. Brackets with asterisks indicate significance differences between programs. **B**: Raw scores (percent correct) on the medial vowel identification task for ERB_{DR}-Distance correlation (left) and no correlation groups (right).*

Distance ($p < .001$), Tuning ($p = .003$), and Monopolar-Control ($p = .04$) programs as compared to the Inverse-Control program.

For the ERB_{DR}-Distance no correlation group, performance on the Tuning program was significantly *better* for sentence recognition than with the Inverse-Control program ($p = .02$), with no other differences between programs. There were no significant differences between programs on the medial vowel identification task for this group.

Figure 4-8 shows the distribution of CNC word scores with the subject's every day program, split between the ERB_{DR}-Distance correlation/no correlation groups. A univariate ANOVA shows a trend toward higher clinical CNC word scores for those in the ERB_{DR}-Distance correlation group ($F(1, 12) = 4.15$, $p = .07$).

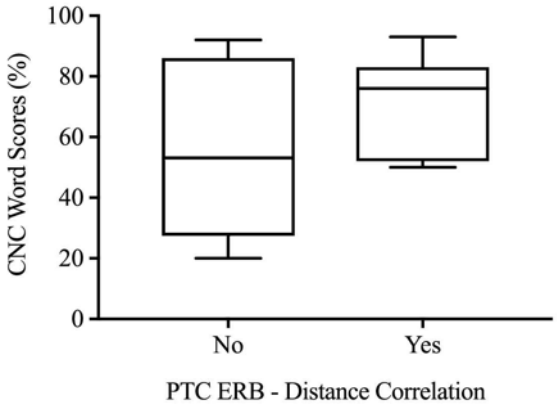

Figure 4-8: Boxplots showing the distribution of subjects CNC word scores with their everyday program (y-axis) for the ERB_{DR}-Distance no correlation (left) and correlation groups (right).

Sound quality ratings

A subjective questionnaire was administered for all programs, with a rating scale of 1 (worse than everyday program) to 10 (better than everyday program) on clarity in quiet, clarity in noise (where applicable), ease of listening, and naturalness. Figure 9 shows scatterplots of individual and across subject means for each aforementioned quality.

An RMANOVA with a Greenhouse-Geisser correction showed no significant differences in sound quality ratings within-subject and between programs for: clarity in quiet ($F(1.8, 19.5) = 1.66$, $p = .22$), clarity in noise ($F(2.27, 18.19) = 2.35$, $p = .12$), ease of listening ($F(2.52, 27.75) = .787$, $p = .49$), and naturalness ($F(2.51, 27.63) = 2.3$, $p = .11$). An additional correlational analysis was conducted to assess if a relationship existed between sound quality ratings and

performance. This analysis did not reach significance for both sentence recognition and medial vowel identification ($p > .05$), suggesting that better performance may not be indicative of subject acceptance of a given program.

However, some within-subject patterns were observable. For example, S43 (downward triangles) gave high ratings for all programs and qualities, perhaps indicating that he felt all the programs were equally suitable, or that he was not particularly sensitive to differences in sound quality. S46 (diamond) performed significantly higher with the Distance program but tended to rate it low compared to the other programs; perhaps his familiarity with monopolar stimulation was an overriding subjective factor. Listeners may have varying "profiles" in how they experience changes in device programming, though extended listener experience is needed to assess this.

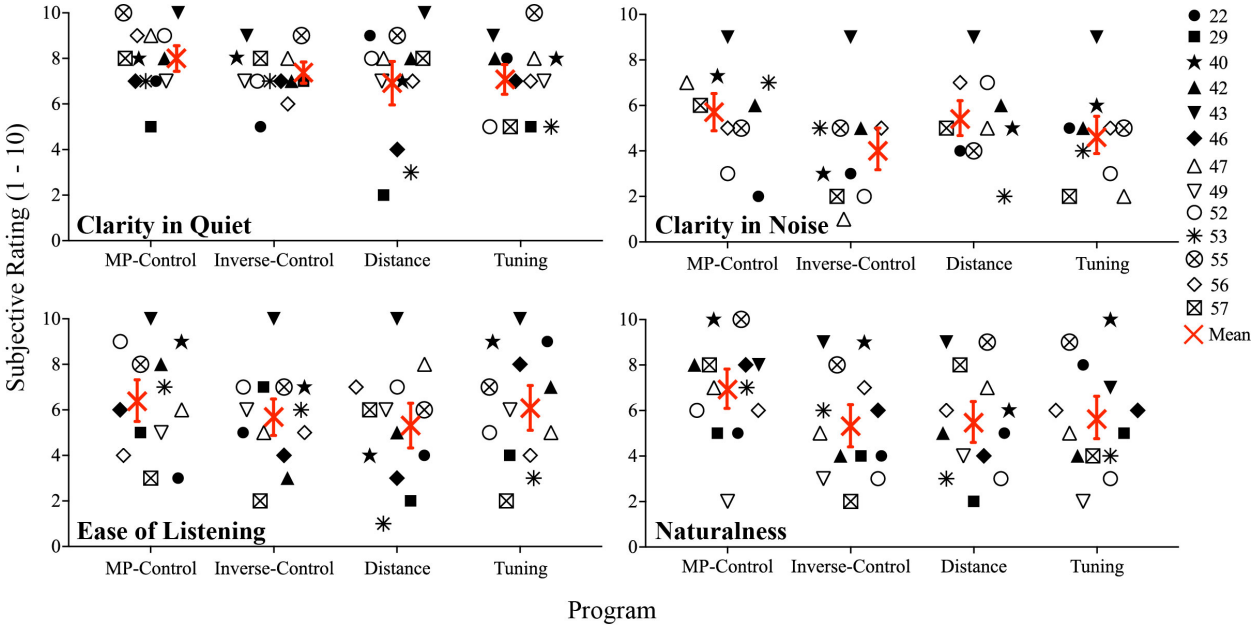

Figure 4-9: Scatterplots showing individual (black symbols) and mean (red symbol) sound quality ratings (y-axis) for clarity in quiet (top left), clarity in noise (top right), ease of listening (bottom left), and naturalness (bottom right) for each program tested (x-axis). Note that S49, S46, and S49 were not tested in noise and therefore did not assess clarity in noise.

D. Discussion

The present study had two aims: 1) to assess the within-subject relationship between electrode-to-modiolus distance and PTC bandwidths, and 2) to reduce channel interaction by creating listener programs that use focused stimulation on electrodes close to the modiolus or with broad PTC bandwidths. Across subjects, results showed that medial vowel identification and sentence recognition scores for channel interaction reduction strategies were similar to scores for a traditional Monopolar-Control program. Interestingly, when channels were focused for electrodes *close* to the modiolus (Inverse-Control), performance was significantly reduced across listeners. For those subjects whose electrode-to-modiolus distances correlated with their PTC bandwidths, the aforementioned results held for medial vowel identification, but not for sentence recognition, where only the Distance program resulted in significantly better performance than the Inverse-Control program. Subjects whose PTC bandwidths did not correlate with electrode-to-modiolus distance tended to perform better with the Tuning program on sentence recognition, with no other significant differences observed. Finally, no differences in subjective sound quality ratings were observed across subjects. These results suggest a potential differential benefit of channel interaction reduction strategies based on the relationship between spatial tuning and electrode position.

Within-subject PTC bandwidths and electrode-to-modiolus distance

Spatial tuning has been shown to vary along the electrode array within CI listeners. Broad tuning may result in increased channel interaction and reduced spectral resolution abilities (Bierer and Faulkner, 2010; Anderson et al., 2011; DeVries and Arenberg, in press), possibly due to regions of poor neural health and/or large electrode-to-modiolus distances. In the present study, PTC ERB_{DR}s were correlated with CT-estimated electrode-to-modiolus distance in 7 out of 13

listeners. This is consistent with previous studies that used electrophysiological (Brown et al., 1990; Cohen et al., 2003; Hughes and Abbas 2006b; DeVries et al., 2016) and modeling techniques (Briaire and Frijns, 2006) to correlate spread of neural excitation and electrode position.

Figure 4-8 demonstrated that the relationship between PTC ERB_{DR} and electrode-to-modiolus distance can have an effect on word recognition scores. While a larger sample size is needed to define this relationship, we speculate that subjects in the ERB_{DR}-Distance correlation group were more likely to have better clinical performance and to benefit from channel interaction reduction strategies because most of their channel interaction resulted from poor electrode position. Those subjects in the ERB_{DR}-Distance no correlation group may have received a smaller benefit from channel focusing, as their broader PTCs likely resulted from other aspects of the ENI, such as neural health. We are not aware of any studies that have evaluated PTC bandwidth and electrode position in relation to speech. Although, Long et al. (2014) found that subjects whose electrode-to-modiolus distances were well predicted by focused behavioral thresholds performed better on speech perception tasks. While electrode-to-modiolus distance alone may not be predictive of speech perception abilities (Long et al., 2014; van der Marel et al., 2015; DeVries et al., 2016; DeVries & Arenberg, in press), the relationship between psychophysical measures and electrode position may explain some of the variability observed in speech outcomes for CI listeners.

Speech perception: channel focusing

We applied focused stimulation to channels with large electrode-to-modiolus distances and broad PTCs in an effort to reduce channel interaction. The assumption is that narrower current spread will ameliorate the effects of excessive channel interaction and result in improved spectral

resolution abilities (e.g. Landsberger et al., 2012; Padilla and Landsberger, 2016). Other investigators have used focused stimulation on all channels to compare to traditional MP stimulation. Srinivasan et al. (2013) observed a consistent improvement in speech perception in noise with TP programs across listeners. Berenstein et al. (2008) found some listeners benefited from pTP, and others from MP + current steering. This is similar to Bierer and Litvak (2016), who found that poorer performing listeners tended to benefit more from the use of pTP stimulation on all channels, and with MP stimulation with high *or* low threshold channels deactivated; however, using pTP stimulation with high and low threshold channels deactivated was not beneficial for the same listeners. Finally, Arenberg and colleagues (2018) used dynamic focusing to improve vowel identification; this strategy uses pTP with a variable focusing coefficient depending on the input level (σ values ranging from 0.8 to 0.5 for low to high intensity inputs, respectively). Their results showed an improvement in noise, but no improvement under quiet conditions. These studies show that while results are mixed, channel focusing has the potential to improve speech perception, particularly in noise. However, methodological differences and small sample sizes make across-study interpretation difficult.

Our results show speech perception scores when focusing a subset of channels based on electrode-to-modiolus and PTC bandwidths are similar to traditional MP programs. When channels near the modiolus were focused (Inverse-Control), there was a significant *detriment* to performance for most listeners. It is possible that using focused stimulation near the modiolus obscures neural representation of spectral information at higher pulse rates, as suggested by Zhou and Pfingst (2016). Further, distant electrodes using monopolar stimulation are presumed to have excessive channel interaction, possibly contributing to the observed detriment in performance.

This may provide an explanation for why using focused stimulation on all channels does not benefit all listeners; perhaps these listeners consistently differ in an as-yet unknown manner.

Speech perception: electrode-to-modiolus distance and PTC bandwidths

Few studies have used electrode position to create listener strategies with a reduced number of channels. Noble and colleagues (2013; 2014; 2016) used a CT image-guided technique to identify and deactivate electrodes modeled to have a high degree of channel interaction in both adult and pediatric CI listeners. Subjects were tested in the bilateral condition, with the experimental strategy, and with the contralateral ear alone as a control condition on speech and spectral modulation detection tasks. Across subjects, they found a small but significant benefit of the experimental strategy and improved subjective quality of communication. It is unclear how the experimental strategy would compare to traditional programming in the same ear, as the contralateral ear was used as the control.

Though our results were similar to the Noble studies using focused stimulation, we found that performance with the Distance *and* Inverse-Control program was similar to the Monopolar-Control program across subjects (Figure 4-5). While the Inverse-Control program resulted in poorer performance in general, it was not statistically lower than the Monopolar-Control program. Performance with the Distance program was higher than with the Inverse-Control, indicating that single-channel manipulations can be detrimental to performance if the "wrong" channels are selected.

To our knowledge, there are no studies that have used PTCs to create channel interaction reduction strategies. In this study, performance with the Tuning program was significantly higher than the Inverse-Control program, and similar to the Distance and Monopolar-Control programs across subjects. These results suggest that focusing channels based on a behavioral measure of

channel interaction and CT-estimates of electrode-to-modiolus distance can result in slight benefits for speech perception, even when listeners have little to no experience listening to the test programs. Studies of chronic listening (> 1 month) with the reduced channel interaction programs may lead to even greater benefit.

When considering the ERB_{DR}-Distance correlation and no correlation groups, some interesting patterns emerge (Figure 4-7). For those in the ERB_{DR}-Distance correlation group, particularly for medial vowel identification, the aforementioned results hold. However, for the ERB_{DR}-Distance no correlation group, only the Tuning program was beneficial compared to the Inverse-Control program for the sentence recognition task. For this group, it may be when focusing channels with broad PTCs the most egregious areas of channel interaction were reduced, allowing these subjects to perform better than expected with the Tuning program. However, as this was not observed for the medial vowel identification task and is not significant when removing the subjects that used the HINT, this finding could be spurious. It may also be that traditional MP programs are more appropriate for some listeners, highlighting the need to identify why some listeners benefit from channel manipulations and others do not. Further, as the Monopolar-Control program was similar to the Distance and Tuning programs across subjects, it is difficult to conclude whether these experimental programs are beneficial enough to warrant long-term use. Several studies have shown that when given long-term exposure, listeners can adapt to new program settings (Fu et al., 2002; Fu and Galvin, 2007). Future studies will examine listening experience with these programs to ascertain whether benefits are obtainable above and beyond traditional MP programs.

Conclusions and Future Directions

In summary, the first and second experiments suggest that an objective and behavioral measure of channel interaction can predict CT-estimates of electrode position in some CI listeners. The third experiment shows that when using focused stimulation on electrodes with broad tuning curves or poor electrode position, some listeners can perform as well as or better than with traditional monopolar stimulation. An important finding was that when using focused stimulation on channels close to the modiolus, most listeners showed a detriment in performance. This indicates that when performing channel manipulations, there is a significant risk of reducing outcomes if the approach is not carefully considered. Further, performance with these novel strategies may depend on the cause of excessive channel interaction: electrode position or some other source, such as neural health or bone and tissue growth. It is possible that different CI listeners will benefit from different strategies. For example, if excessive channel interaction occurs due to poor neural health, it may be that channel deactivation and/or monopolar stimulation is a more appropriate approach than using focused stimulation.

Additional studies that evaluate different programming approaches for listeners with and without correlations between electrode position and broad PTCs will be conducted in the same subjects, if possible. For instance, selecting a predetermined number of broad PTCs and testing whether outcomes differ with deactivation or focused stimulation may point to key differences in the ENI between these groups. This could lead to more individualized programming based on channel interaction measures.

Future studies will evaluate whether these novel strategies are beneficial above and beyond traditional strategies by providing prolonged take-home listening experience. Examining vowel error patterns before and after chronic listening experience will provide additional

information about how these channel manipulations affect spectral resolution and vowel perception. Finally, channel manipulations performed at the ENI are likely to impact higher level processes, especially after long term experience. Effects of aging and cognitive factors such as attention and memory may be important when implementing unique listener strategies in CI listeners, and should be incorporated into future investigations.

References

Abbas PJ, Brown CJ, Shallop JK, Firszt JB, Hughes ML, Hong SH, & Staller SJ (1999) Summary of results using the nucleus CI24M implant to record the electrically evoked compound action potential. Ear Hear 20: 45-59.

Abbas PJ, Hughes ML, Brown CJ, et al (2004) Channel Interaction in Cochlear Implant Users Evaluated Using the Electrically Evoked Compound Action Potential. Audiol Neurotol 9:203–213.

Anderson ES, Nelson DA, Kreft H, et al (2011) Comparing spatial tuning curves, spectral ripple resolution, and speech perception in cochlear implant users. The Journal of the Acoustical Society of America 130:364–375.

Arenberg JG, Parkinson WS, Litvak L, et al (2018) A Dynamically Focusing Cochlear Implant Strategy Can Improve Vowel Identification in Noise. Ear Hear doi: 10.1097/AUD.0000000000000566.

Aschendorff A, Kromeier J, Klenzner T, Laszig R (2007) Quality control after insertion of the nucleus contour and contour advance electrode in adults. Ear Hear 28:75S–79S.

Baayen RH, Davidson DJ, Bates DM (2008) Mixed-effects modeling with crossed random effects for subjects and items. J Mem Lang 59:390–412.

Berenstein CK, Mens LH, Mulder JJ, Vanpoucke FJ (2008) Current steering and current focusing in cochlear implants: comparison of monopolar, tripolar, and virtual channel electrode configurations. Ear Hear 29:250–260.

Bierer J (2010) Probing the Electrode-Neuron Interface With Focused Cochlear Implant Stimulation. Trends in Amplif 14:84–95.

Bierer JA (2007) Threshold and channel interaction in cochlear implant users: Evaluation of the tripolar electrode configuration. J Acoust Soc Am 121:1642–1653.

Bierer JA, Bierer SM, Kreft HA, Oxenham AJ (2015) A Fast Method for Measuring Psychophysical Thresholds Across the Cochlear Implant Array. Trends Hear 19:1—12.

Bierer JA, Bierer SM, Middlebrooks JC (2010) Partial tripolar cochlear implant stimulation: Spread of excitation and forward masking in the inferior colliculus. Hear Res 270:134–142.

Bierer JA, Faulkner KF (2010) Identifying cochlear implant channels with poor electrode-neuron interface: partial tripolar, single-channel thresholds and psychophysical tuning curves. Ear Hear 31(2):247-58.

Bierer JA, Litvak L (2016) Reducing Channel Interaction Through Cochlear Implant Programming May Improve Speech Perception: Current Focusing and Channel Deactivation. Trends Hear 20:1-12.

Bierer, JA & Middlebrooks JC (2002) Auditory cortical images of cochlear-implant stimuli: Dependence on electrode configuration. J Neurophysiol 82: 478-492.

Bierer JA & Nye AD (2014) Comparisons between detection threshold and loudness perception for individual cochlear implant channels. Ear Hear 35: 641-651.

Boëx C, Kos MI, Pelizzone M (2003) Forwarding masking in different cochlear implant systems. J Acoust Soc Am 114: 2058-2065.

Blamey P, Artieres F, Baskent D, et al (2013) Factors Affecting Auditory Performance of Postlinguistically Deaf Adults Using Cochlear Implants: An Update with 2251 Patients. Audiol Neurotol 18:36–47.

Briaire JJ, Frijns JHM (2006) The consequences of neural degeneration regarding optimal cochlear implant position in scala tympani: A model approach. Hear Res 214:17–27.

Brown CJ, Abbas PJ, Gantz B (1990) Electrically evoked whole-nerve action potentials: data from human cochlear implant users. J Acoust Soc Am 88:1385–1391.

Cohen LT (2009) Practical model description of peripheral neural excitation in cochlear implant recipients: 1. Growth of loudness and ECAP amplitude with current. Hear Res 247:87–99.

Cohen LT, Richardson LM, Saunders E, Cowan RS. (2003) Spatial spread of neural excitation in cochlear implant recipients: comparison of improved ECAP method and psychophysical forward masking. Hear Res 179:72–87.

Cohen LT, Saunders E, Clark GM (2001) Psychophysics of a prototype peri-modiolar cochlear implant electrode array. Hear Res155:63–81.

Crew JD, Galvin JJ, & Fu QJ (2012) Channel interaction limits melodic pitch perception in stimulated cochlear implants. J Acoust Soc Am 132: 429-435.

DeVries L, Scheperle R, Bierer JA (2016) Assessing the Electrode-Neuron Interface with the Electrically Evoked Compound Action Potential, Electrode Position, and Behavioral Thresholds. J Assoc Res Otolaryngol :237–252.

Dillier N, Lai WK, Almqvist B, Frohne C, Muller-Deile J, Stecker M & Von Wallenberg E (2002) Measurement of the electrically evoked compound action potential via a neural response telemetry system. Ann Otol Rhinol Laryngol 111: 407-414.

Finley CC, Holden TA, Holden LK, et al (2008) Role of electrode placement as a contributor to variability in cochlear implant outcomes. Otol Neurotol 29:920–928.

Frijns JH, de Snoo SL, Schoonhoven R (1995) Potential distributions and neural excitation patterns in a rotationally symmetric model of the electrically stimulated cochlea. Hear Res 87:170–186.

Frijns JH, de Snoo SL, ten Kate JH (1996) Spatial selectivity in a rotationally symmetric model of the electrically stimulated cochlea. Hear Res 95:33–48.

Fu Q-J, Galvin JJ (2007) Perceptual Learning and Auditory Training in Cochlear Implant Recipients. Trends Amp 11:193–205.

Fu Q-J, Shannon RV, Galvin JJ (2002) Perceptual learning following changes in the frequency-to-electrode assignment with the Nucleus-22 cochlear implant. J Acoust Soc Am 112:1664–1674.

Garadat SN, Zwolan TA, Pfingst BE (2013) Using Temporal Modulation Sensitivity to Select Stimulation Sites for Processor MAPs in Cochlear Implant Listeners. Audiol Neurotol18:247–260.

Goldwyn JH, Bierer SM, Bierer JA (2010) Modeling the electrode–neuron interface of cochlear implants: Effects of neural survival, electrode placement, and the partial tripolar configuration. Hear Res 268:93–104.

Gordon KA & Papsin BC (2013) From Nucleus 24 to 513: Changing Cochlear Implant Design Affects Auditory Response Thresholds. Otol Neurotol 34: 436-442.

Grolman W, Maat A, Verdam F, Simis Y, Carelsen B, Freling N & Tange R (2009) Spread of excitation measurements for the detection of electrode array foldovers: a prospective study comparing 3-dimensional rotational x-ray and intraoperative spread of excitation measurements. Otol Neurotol 30: 27-33.

Hall RD (1990) Estimation of surviving spiral ganglion cells in the deaf rat using the electrically evoked auditory brainstem response. Hear Res 49:155–168.

Henshall KR, McKay CM (2001) Optimizing electrode and filter selection in cochlear implant speech processor maps. Am J Audiol 12:478–489.

Hinojosa R, Lindsay JR (1980) Profound deafness. Associated sensory and neural degeneration. Arch Otolaryngol 106:193–209.

Holden LK, Finley CC, Firszt JB, et al (2013) Factors affecting open-set word recognition in adults with cochlear implants. Ear Hear 34:342–360.

Hughes ML & Abbas PJ (2006a) The relation between electrophysiologic channel interaction and pitch ranking in cochlear implant recipients. Acoust Soc Am 119(3): 1527-1537.

Hughes ML & Abbas PJ (2006b) Electrophysiologic channel interaction, electrode pitch ranking, and behavioral threshold in straight versus perimodiolar cochlear implant electrode arrays. J Acoust Soc Am 119(3): 1538-1547.

Hughes ML (2008) A re-evaluation of the relation between physiological channel interaction and electrode pitch ranking in cochlear implants. Acoust Soc Am 124(5): 2711-2714.

Hughes ML (2013) Electrically evoked compound action potential *In Objective Measures in Cochlear Implants.* Eds. Zwolan, T. & Wolfe, J. Plural Publishing, Inc., San Diego, CA.

Hughes ML, Stille LJ (2008) Psychophysical Versus Physiological Spatial Forward Masking and the Relation to Speech Perception in Cochlear Implants: Ear Hear 29:435–452.

Hughes ML & Stille LJ (2010) Effect of stimulus and recording parameters on spatial spread of excitation and masking patterns obtained with the electrically evoked compound action potential in cochlear implants. Ear Hear 31: 679-692.

Jolly CN, Spelman FA, Clopton BM (1996) Quadrupolar stimulation for cochlear prostheses: modeling and experimental data. IEEE 43:857–865.

Jeon EK, Brown CJ, Etler CP, O'Brien S, Chiou L, & Abbas PJ (2010) Comparison of Electrically Evoked Compound Action Potential Thresholds and Loudness Estimates for the Stimuli Used to Program the Advanced Bionics Cochlear Implant. J Am Acad Audiol 21(1): 16-27.

Jones GL, Ho Won J, Drennan WR, Rubinstein JT (2013) Relationship between channel interaction and spectral-ripple discrimination in cochlear implant users a. J Acoust Soc Am 133:425–433.

Kalkman RK, Briaire JJ, Dekker DMT, Frijns JHM (2014) Place pitch versus electrode location in a realistic computational model of the implanted human cochlea. Hear Res 315:10–24.

Kawano A, Seldon HL, Clar GM (1998) Intracochlear Factors Contributing to Psychophysical Percepts Following Cochlear Implantation. Acta Oto-Laryngologica 118:313–326.

Khan AM, Handzel O, Damian D, et al (2005) Effect of cochlear implantation on residual spiral ganglion cell count as determined by comparison with the contralateral nonimplanted inner ear in humans. Ann Otol Rhinol Laryngol 114:381–385.

Kim JR, Abbas PJ, Brown CJ, Elter CP, O'Brien S & Kim L (2010) The Relationship Between Electrically Evoked Compound Action Potential and Speech Perception: A Study in Cochlear Implant Users with Short Electrode Array. Otol Neurotol 31: 1041-1048.

Koch DB, Osberger MJ, Segel P, Kessler D (2004) HiResolution™ and Conventional Sound Processing in the HiResolution™ Bionic Ear: Using Appropriate Outcome Measures to Assess Speech Recognition Ability. Audiol Neurotol 9:214–223.

Lai WK & Dillier N (2000) A simple two-component model of the electrically evoked compound action potential in the human cochlea. Audio Neurotol 5: 333-345.

Landsberger DM, Padilla M, Srinivasan AG (2012) Reducing current spread using current focusing in cochlear implant users. Hear Res 284:16–24.

Landsberger DM, Srinivasan AG (2009) Virtual channel discrimination is improved by current focusing in cochlear implant recipients. Hear Res 254:34–41.

Levitt H (1971) Transformed up-down methods in psychoacoustics. J Acoust Soc Am 49: 467–477.

Linthicum FH, Fayad J, Otto SR, et al (1991) Cochlear implant histopathology. Am J Otol 12:245–311.

Litvak LM, Spahr AJ & Emadi G (2007) Loudness growth observed under partially tripolar stimulation: Model and data from cochlear implant listeners. J Acoust Soc Am 122: 967-981.

Litvak LM, Spahr AJ, Saoji AA, Fridman GY (2007) Relationship between perception of spectral ripple and speech recognition in cochlear implant and vocoder listeners. J Acoust Soc Am 122:982–991.

Long CJ, Holden TA, McClelland GH, et al (2014) Examining the Electro-Neural Interface of Cochlear Implant Users Using Psychophysics, CT Scans, and Speech Understanding. J Assoc Res Otolaryngol 15:293–304.

Mens LHM (2007) Advances in cochlear implant telemetry: Evoked neural responses, electrical field imaging, and technical integrity. Trends Amplif 11: 143-159.

McKay CM (2012) Forward masking as a method of measuring place specificity of neural excitation in cochlear implants: a review of methods and interpretation. J Acoust Soc Am 131:2209–2224.

McKay CM, Chandan K, Akhoun I, Siciliano C & Kluk K (2013) Can ECAP Measures Be Used for Totally Objective Programming of Cochlear Implants? J Assoc Res Otolayngol 14: 879-890.

Miller CA, Abbas PJ & Robinson BK (1994) The use of long-duration current pulses to assess neural survival. Hear Res: 78: 11-26.

Miller CA, Brown CJ, Abbas PJ & Sui-Ling C (2008) The clinical application of potentials evoked from the peripheral auditory system. Hear Res 242: 184-197.

Nadol JB (1997) Patterns of neural degeneration in the human cochlea and auditory nerve: implications for cochlear implantation. Otolaryng Head Neck 117:220–228.

Nadol JB, Young YS, Glynn RJ (1989) Survival of spiral ganglion cells in profound sensorineural hearing loss: implications for cochlear implantation. Ann Otol Rhinol Laryngol 98:411–6.

Nelson DA, Donaldson GS, Kreft H (2008) Forward-masked spatial tuning curves in cochlear implant users. J Acoust Soc Am 123:1522–1543.

Nelson DA, Kreft HA, Anderson ES, Donaldson GS (2011) Spatial tuning curves from apical, middle, and basal electrodes in cochlear implant users. J Acoust Soc Am 129:3916–3933.

Nilsson M, Soli SD, Sullivan JA (1994) Development of the Hearing in Noise Test for the measurement of speech reception thresholds in quiet and in noise. J Acoust Soc Am 95:1085–1099.

Noble JH, Gifford RH, Hedley-Williams AJ, et al (2014) Clinical Evaluation of an Image-Guided Cochlear Implant Programming Strategy. Audiol Neurotol 19:400–411.

Noble JH, Labadie RF, Gifford RH, Dawant BM (2013) Image-guidance enables new methods for customizing cochlear implant stimulation strategies. IEEE T Neur Sys Reh 21:820–829.

Padilla M, Landsberger DM (2016) Reduction in spread of excitation from current focusing at multiple cochlear locations in cochlear implant users. Hear Res 333:98–107.

Pfingst BE, Bowling SA, Colesa DJ, et al (2011) Cochlear infrastructure for electrical hearing. Hear Res 281:65–73.

Pfingst BE, Xu L (2004) Across-Site Variation in Detection Thresholds and Maximum Comfortable Loudness Levels for Cochlear Implants. J Assoc Res Otolayngol 5:11–24.

Pfingst BE, Xu L, Thompson CS (2004) Across-Site Threshold Variation in Cochlear Implants: Relation to Speech Recognition. Audiol Neurotol 9:341–352.

Saleh SM, Saeed SR, Meerton L, et al (2013) Clinical use of electrode differentiation to enhance programming of cochlear implants. Cochlear Implants Int 14 Suppl 4:S16-18.

Ramekers D, Versnel H, Strahl SB, et al (2014) Auditory-Nerve Responses to Varied Inter-Phase Gap and Phase Duration of the Electric Pulse Stimulus as Predictors for Neuronal Degeneration. J Assoc Res Otolaryngol 15:187–202.

Scheperle RA, Abbas PJ (2015) Relationships among peripheral and central electrophysiological measures of spatial and spectral selectivity and speech perception in cochlear implant users. Ear Hear 36:441.

Sęk A, Alcántara J, Moore BCJ, et al (2005) Development of a fast method for determining psychophysical tuning curves. Int J Audiol 44:408–420.

Shannon R, Fu Q-J, Galvin Iii J (2004) The number of spectral channels required for speech recognition depends on the difficulty of the listening situation. Acta Oto-Laryngologica 124:50–54.

Shepherd RK, Hatsushika S, Clark GM (1993) Electrical stimulation of the auditory nerve: the effect of electrode position on neural excitation. Hear Res 66:108–120.

Shepherd RK, Javel E (1997) Electrical stimulation of the auditory nerve. I. Correlation of physiological responses with cochlear status. Hear Res 108:112–144.

Skinner MW, Holden TA, Whiting BR, et al (2007) In vivo estimates of the position of advanced bionics electrode arrays in the human cochlea. Ann Oto Rhinol Laryn 116:2–24.

Skinner MW, Ketten DR, Holden LK, et al (2002) CT-Derived Estimation of Cochlear Morphology and Electrode Array Position in Relation to Word Recognition in Nucleus-22 Recipients. J Assoc Res Otolaryngol 3:332–350.

Smith L, Simmons FB (1983) Estimating eighth nerve survival by electrical stimulation. Ann Otol Rhinol Laryngol 92:19–23.

Snel-Bongers J, Briaire JJ, Vanpoucke FJ, & Frijns JHM (2012) Spread of excitation and channel interaction in single and dual-electrode cochlear implant stimulation. Ear Hear 33: 367-376.

Snyder RL, Bierer JA, Middlebrooks JC (2004) Topographic Spread of Inferior Colliculus Activation in Response to Acoustic and Intracochlear Electric Stimulation. J Assoc Res Otolaryngol 5:305–322.

Spahr AJ, Dorman MF, Litvak LM, et al (2012) Development and Validation of the AzBio Sentence Lists: Ear Hear 33:112–117.

Srinivasan AG, Landsberger DM, Shannon RV (2010) Current focusing sharpens local peaks of excitation in cochlear implant stimulation. Hear Res 270:89–100.

Srinivasan AG, Padilla M, Shannon RV, Landsberger DM (2013) Improving speech perception in noise with current focusing in cochlear implant users. Hear Res 299:29–36.

Teymouri J, Hullar TE, Holden TA, Chole RA (2011) Verification of computed tomographic estimates of cochlear implant array position: a micro-CT and histologic analysis. Otol Neurotol 32:980–986.

Throckmorton CS, Collins LM (1999) Investigation of the effects of temporal and spatial interactions on speech-recognition skills in cochlear-implant subjects. J Acoust Soc Am 105:861–873.

van der Marel KS, Briaire JJ, Verbist BM, et al (2015) The Influence of Cochlear Implant Electrode Position on Performance. Audiol Neurotol 20:202–211.

Verbist BM, Frijns JH, Geleijns J, Van Buchem MA (2005) Multisection CT as a valuable tool in the postoperative assessment of cochlear implant patients. Am J of Neuroradiol 26:424–429.

Vickers D, Degun A, Canas A, et al (2016) Deactivating Cochlear Implant Electrodes Based on Pitch Information for Users of the ACE Strategy. In: van Dijk P, Başkent D, Gaudrain E, et al. (eds) Physiology, Psychoacoustics and Cognition in Normal and Impaired Hearing. Springer International Publishing, Cham, pp 115–123.

Won JH, Drennan WR, Rubinstein JT (2007) Spectral-Ripple Resolution Correlates with Speech Reception in Noise in Cochlear Implant Users. J Assoc Res Otolaryngol 8:384–392.

Wright R, Souza P (2012) Comparing Identification of Standardized and Regionally Valid Vowels. J Speech Lang Hear R 55:182–193.

Zhou N, Pfingst BE (2012) Psychophysically based site selection coupled with dichotic stimulation improves speech recognition in noise with bilateral cochlear implants. J Acoust Soc Am 132:994–1008.

Zwolan TA, Collins LM, Wakefield GH (1997) Electrode discrimination and speech recognition in postlingually deafened adult cochlear implant subjects. J Acoust Soc Am 102:3673–3685.

Zhou N, Pfingst BE (2016b) Evaluating multipulse integration as a neural-health correlate in human cochlear-implant users: Relationship to spatial selectivity. J Acoust Soc Am 140:1537–1547.

Zhou N, Kraft CT, Colesa DJ, Pfingst BE (2015) Integration of Pulse Trains in Humans and Guinea Pigs with Cochlear Implants. J Assoc Res Otolaryngol 16:523–534.

Zhou N, Dong L, Hang M (2018) Evaluating Multipulse Integration as a Neural-Health Correlate in Human Cochlear Implant Users: Effects of Stimulation Mode. J Assoc Res Otolaryngol 19:99–111.